THE HYDROPHOBIC HANDOFF
BETWEEN NPC2 AND THE N-TERMINAL DOMAIN OF NPC1
IN THE EXPORT OF CHOLESTEROL FROM LYSOSOMES

APPROVED BY COMMITTEE

Michael S. Brown, M.D. (Mentor) _____

Joseph L. Goldstein, M.D. (Mentor) _____

Philip Thomas, Ph.D. (Chair) _____

Michael Roth, Ph.D. _____

Sandra Hofmann, M.D., Ph.D. _____

Guosheng Liang, Ph.D. _____

DEDICATION

This is dedicated to my wife, Angie.

THE HYDROPHOBIC HANDOFF BETWEEN NPC2 AND THE N-TERMINAL DOMAIN OF NPC1 IN THE EXPORT OF CHOLESTEROL FROM LYSOSOMES

by

MICHAEL LEECHUN WANG

DISSERTATION

Presented to the Faculty of the Graduate School of Biomedical Sciences

The University of Texas Southwestern Medical Center at Dallas

In Partial Fulfillment of the Requirements

For the Degree of

DOCTOR OF PHILOSOPHY

The University of Texas Southwestern Medical Center at Dallas

Dallas, Texas

August, 2010

THE HYDROPHOBIC HANDOFF
BETWEEN NPC2 AND THE N-TERMINAL DOMAIN OF NPC1
IN THE EXPORT OF CHOLESTEROL FROM LYSOSOMES

Publication No._____

Michael Leechun Wang, Ph.D.

The University of Texas Southwestern Medical Center at Dallas, 2010

Supervising Professors: Michael S. Brown, M.D. and Joseph L. Goldstein, M.D.

Low density lipoproteins (LDL) and related plasma lipoproteins deliver cholesterol to cells by receptor-mediated endocytosis. The lipoprotein is degraded in late endosomes and lysosomes where its cholesterol is released. Egress of cholesterol from late endosomes and lysosomes (hereafter referred to as lysosomes) requires two proteins: Niemann-Pick C2 (NPC2), a soluble protein of 132 amino acids; and NPC1, an intrinsic membrane protein of 1278 amino acids and 13 postulated membrane-spanning helices that span the lysosomal membrane. Recessive loss-of-function mutations in either NPC2 or NPC1 produce NPC disease, which causes death in childhood owing to cholesterol accumulation in lysosomes of liver, brain, and lung.

Consistent with their cholesterol export role, NPC2 and NPC1 both bind cholesterol. The cholesterol binding site on NPC1 is located in the NH_2-terminal domain (NTD), which projects into the lysosomal lumen. This domain, designated NPC1(NTD), can be expressed *in vitro* as a soluble protein of 240 amino acids that retains cholesterol binding activity. This thesis studies NPC2 and NPC1(NTD) in detail as summarized below.

Two major differences exist between the cholesterol binding of NPC2 and NPC1(NTD). 1) Competitive binding studies and crystal structures indicate that the two proteins bind cholesterol in opposite orientations. NPC2 binds the iso-octyl side chain, leaving the 3ß-hydroxyl exposed, whereas NPC1 binds the 3ß-hydroxyl, leaving the side chain partially exposed. 2) Kinetic studies of cholesterol binding reveal that NPC2 binds and releases cholesterol rapidly (half-time < 2 min at 4^oC), while NPC1(NTD) binds cholesterol very slowly (half-time > 2 hr at 4^oC).

Its rapid cholesterol binding allows NPC2 to transfer cholesterol to and from liposomes. Unlike NPC2, NPC1(NTD) cannot rapidly transfer its bound cholesterol to liposomes. However, NPC1(NTD) can accomplish this delivery when NPC2 is present. Furthermore, cholesterol binding to NPC1(NTD) is accelerated by >15-fold when the sterol is first bound to NPC2 and then transferred to NPC1(NTD). These data led us to advance a model in which NPC2 can mediate bi-directional transfer of cholesterol to or from NPC1(NTD). In cells, we envision that NPC2 accepts cholesterol in the lysosomal lumen and transports it to membrane-bound NPC1, thus accounting for the requirement for both proteins for lysosomal cholesterol export.

Amino acid residues important or binding or transfer of cholesterol on NPC2 and NPC1(NTD) were identified through alanine scan mutagenesis. For both NPC2 and NPC1(NTD), residues that decreased binding mapped to areas surrounding the binding pockets

on the crystal structures; residues that decreased transfer, but not binding, mapped to discrete surface patches near the opening of the binding pockets. These surface patches may be sites where the two proteins interact to transfer cholesterol. The most severe mutations disrupting binding were P120S for NPC2 and P202A/F203A for NPC1(NTD); and those that disrupted transfer were V81D for NPC2 and L175Q/L176Q for NPC1(NTD). Furthermore, the functional significance of both the binding and transfer of cholesterol by NPC2 and NPC1(NTD) in the egress of cholesterol from lysosomes was confirmed. The above binding- or transfer-defective mutants of NPC2 and NPC1 were unable to rescue LDL-stimulated cholesteryl ester synthesis in NPC2 or NPC1-deficient cells, respectively, in contrast to wild-type NPC2 and NPC1.

With these data, we envision that NPC2 binds cholesterol the instant that it is released from LDL, either as the free sterol or after cleavage of lipoprotein-derived cholesteryl esters by lysosomal acid lipase. This binding would prevent cholesterol from crystallizing in the lysosomal lumen. According to the model, NPC2 can transfer its bound cholesterol to NPC1(NTD) directly, thus avoiding the necessity for the insoluble cholesterol to transit the water phase. This transfer of cholesterol from NPC2 to NPC1(NTD) has a special functional relevance in light of the near-absolute insolubility of cholesterol in water, and we have named this process a “hydrophobic handoff.”

ACKNOWLEDGEMENTS

I thank my mentors, Dr. Michael Brown and Dr. Joseph Goldstein, for their support and guidance. I am grateful for the time and money they have invested in me, and the education that I have received.

I also thank my thesis committee members Drs. Philip Thomas, Michael Roth, Sandra Hofmann, and Guosheng Liang for their suggestions regarding my project and encouragement along the way.

In addition, I acknowledge former and current members of the Brown and Goldstein lab for their help – Rodney Infante, Massoud Motamed, Lina Abi-Mosleh, Tongjin Zhao, Yukio Ikeda, and Arun Radhakrishnan. Also, none of this work would have been possible without the great technical assistance from the tissue culture staff – Lisa Beatty, Shomanike Head, Ije Onweneme, and Angela Carrol. Last but not least, thanks to Debbie Morgan and Dorothy Williams for their technical assistance.

Finally, I thank my family. Specifically, my parents and sister for their encouragement and guidance throughout my life; and my wife Angie Wang for her loving support, technical expertise, helpful suggestions, and her pure awesomeness that made everything alright throughout this process.

TABLE OF CONTENTS

PRIOR PUBLICATIONS

Suh JM, Zeve D, McKay R, Seo J, Salo Z, Li R, **Wang M**, Graff JM. Adipose is a conserved dosage-sensitive antiobesity gene. Cell Metab. 2007 Sep;6(3):195-207.

Infante RE, Radhakrishnan A, Abi-Mosleh L, Kinch LN, **Wang ML**, Grishin NV, Goldstein JL, Brown MS. Purified NPC1 protein: II. Localization of sterol binding to a 240-amino acid soluble luminal loop. J Biol Chem. 2008 Jan 11;283(2):1064-75.

Infante RE, **Wang ML**, Radhakrishnan A, Kwon HJ, Brown MS, Goldstein JL. NPC2 facilitates bidirectional transfer of cholesterol between NPC1 and lipid bilayers, a step in cholesterol egress from lysosomes. Proc Natl Acad Sci U S A. 2008 Oct 7;105(40):15287-92.

Lee YC, Block G, Chen H, Folch-Puy E, Foronjy R, Jalili R, Jendresen CB, Kimura M, Kraft E, Lindemose S, Lu J, McLain T, Nutt L, Ramon-Garcia S, Smith J, Spivak A, **Wang ML**, Zanic M, Lin SH. One-step isolation of plasma membrane proteins using magnetic beads with immobilized concanavalin A. Protein Expr Purif. 2008 Dec;62(2):223-9.

Kwon HJ , Abi-Mosleh L ,**Wang ML**, Deisenhofer J, Goldstein JL, Brown MS, Goldstein JL, Infante RE. Structure of the N-terminal domain of NPC1 suggests transfer mechanism for exit of LDL-Cholesterol from lysosomes. Cell. 2009 Jun 26;137(7):1213-24.

Wang ML, Motamed M, Infante RE, Abi-Mosleh L, Kwon HJ, Brown MS, Goldstein JL. Identification of Surface Residues on Niemann-Pick C2 (NPC2) Essential for Hydrophobic Handoff of Cholesterol to NPC1 in Lysosomes. Cell Metab. 2010 Aug 4;12(2):166-73.

LIST OF FIGURES

CHAPTER 1

CHAPTER 2

CHAPTER 3

CHAPTER 4

CHAPTER 5

CHAPTER 6

LIST OF ABBREVIATIONS

ACAT, acyl-CoA:cholesterol acyl-transferase

ALLN, N-acetyl-Leu-Leu norleucinal

BMP, bis(monooleoylglycero)phosphate

BSA, bovine serum albumin

CHO, Chinese hamster ovary

CMC, critical micellar concentration

CMV, cytomegalovirus

DMEM, Dulbecco's modified Eagle's medium

Endo H, endogylcosidase H

ER, endoplasmic reticulum

FCS, fetal calf serum

HMG-CoA, 3-hydroxy-3-methylglutaryl-coenzyme A

HSV, herpes simplex virus

LDL, low density lipoprotein

LPDS, lipoprotein-deficient serum

Ni-NTA, nickel-nitrilotriacetic acid

NP-40, nonidet P-40

NPC, Niemann-Pick Type C

NPC1, Niemann-Pick Type C1 disease protein

NPC1(NTD), N-terminal domain of NPC1 (amino acids 23-264)

NPC2, Niemann-Pick Type C2 disease protein

NTD, N-terminal domain

PBS, phosphate-buffered saline

PC, egg yolk L-α-phosphatidylcholine

PNGase F, Peptide: N-Glycosidase F

SCAP, SREBP cleavage-activating protein

SREBP, sterol regulatory element-binding protein

Texas Red dye, Texas Red 1,2,-dihexadecanoyl-sn-glycero-3-phosphoethanolamine

TK, thymidine kinase

WT, wild-type

25-HC, 25-hydroxycholesterol

β-VLDL, β-migrating very low density lipoprotein

CHAPTER ONE

INTRODUCTION TO INTRACELLULAR CHOLESTEROL TRANSPORT AND THE NPC PROTEINS

CHOLESTEROL TRANSPORT AND HOMEOSTASIS IN CELLS

Disorders of cholesterol metabolism are the leading causes of death in the Western world. Elevations in plasma cholesterol-carrying lipoproteins are the underlying causes of heart attacks and strokes. Despite its dangers, cholesterol is also required for the growth and survival of mammalian cells, and it plays important structural and regulatory roles in the plasma membrane and endoplasmic reticulum. Also, its metabolites such as bile acids, oxysterols, and steroid hormones are very important for physiologic functions (Chang et al., 2006).

There are two main sources of cholesterol: 1) endogenous biosynthesis, and 2) the diet. The de novo synthesis of endogenous cholesterol occurs at the ER, while exogenous cholesterol from the diet is mainly acquired by mammalian cells through the low density lipoprotein (LDL) receptor pathway (Brown and Goldstein, 1986). LDL, the main carrier of cholesterol (in the form of cholesteryl esters) in blood, binds to the LDL receptor, internalizes, and enters the endocytic compartment. Here the cholesteryl esters are hydrolyzed by lysosomal acid lipase to cholesterol and fatty acids, where the free cholesterol then appears in the late endosomes/lysosomes (Chang et al., 2005). The cholesterol, either synthesized or acquired, is then distributed among the membranes of the cell (Chang et al., 2006).

The regulatory system of cellular cholesterol homeostatis in mammalian cells is found in the ER. Cells respond to low membrane cholesterol levels by increasing cholesterol synthesis and uptake. When membrane cholesterol accumulates, these processes are downregulated

accordingly. Two ER proteins play key roles in this regulatory system: sterol regulatory element binding protein (SREBP) (Brown and Goldstein, 1997), and acyl-CoA:cholesterol acyltransferase (ACAT). SREBP is synthesized as an ER membrane bound transcription factor, while ACAT is a cholesterol esterification enzyme. In response to low membrane cholesterol, SREBP is transported to the Golgi where it undergoes two successive proteolytic cleavages, resulting in the active transcription factor that localizes to the nucleus to activate transcription of genes encoding proteins such as HMG-CoA reductase and the LDL-receptor to increase endogenous synthesis and uptake of cholesterol, respectively. In addition, ACAT activity is decreased. In high membrane cholesterol conditions, ACAT is activated, increasing the esterification of excess cholesterol for storage in lipid droplets in the cytoplasm. This process is important because it prevents the toxic accumulation of free cholesterol in various cell membrane fractions and allows the cells to use cholesterol esters within lipid droplets as a source of free cholesterol when the cholesterol levels decrease (Chang et al., 1997). Furthermore, high membrane cholesterol inhibits SREBP processing.

The way in which LDL particles containing cholesterol esters are internalized through receptor-mediated endocytosis and how this cholesterol exerts its regulatory effects once at the ER are well understood. However, for the cell to regulate its cholesterol content through the ER, LDL-derived cholesterol must be transported from lysosomes to the ER, and this transport process remains poorly understood.

NIEMANN-PICK TYPE C DISEASE

A clue to how LDL-derived cholesterol is transported to the ER comes from Niemann-Pick Type C (NPC) disease. NPC disease is a rare autosomal recessive lysosomal storage disease characterized by progressive central nervous system neurodegeneration, motor skill deficiencies,

hepatosplenomegaly, and pulmonary complications (Vanier and Millat, 2003). The disease is eventually fatal, with most patients dying before adulthood (Chang et al., 2005). Currently, there is no cure. Cells from these patients exhibit accumulation of unesterified cholesterol, sphingolipids, and other lipids within lysosomes (Chang et al., 2006).

NPC disease can be caused by homozygous mutations in either the NPC1 or NPC2 genes. Mutations in NPC1 account for 90% of the patients (Carstea et al., 1993; Greer et al., 1999; Park et al., 2003; Vanier et al., 1996), while mutations in NPC2 account for 4% (Millat et al., 2001; Naureckiene et al., 2000). NPC1 and NPC2 are likely to work in the same pathway, since homozygous mutations in either one of the proteins results in the same NPC phenotype (Sleat et al., 2004). As NPC1 and NPC2 are important in the intracellular transport of exogenous cholesterol from lysosomes to cellular membranes such as the PM and ER, deciphering their functions will have a positive impact on our understanding of and ability to treat Niemann-Pick Type C disease.

NPC1 AND NPC2

Human NPC1 (1278 amino acids) is predominantly located within the late endosomal membrane. It contains 13 transmembrane helices, an N-terminal signal peptide, a NPC1 domain (highly conserved among species), a sterol-sensing domain, and a C-terminal lysosomal targeting sequence (Loftus et al., 1997). NPC2 (132 amino acids) is a soluble lysosomal protein that can be secreted and uses the mannose-6-phosphate marker for targeting to late endosomes (Chang et al., 2005). In keeping with their cholesterol export role, NPC2 and NPC1 both bind cholesterol (Infante et al., 2008a; Xu et al., 2007). The cholesterol binding site on NPC1 is located in the NH_2-terminal domain (NTD), which projects into the lysosomal lumen. This domain, designated

NPC1(NTD), can be expressed *in vitro* as a soluble protein of 240 amino acids that retains cholesterol binding activity (Infante et al., 2008b). To advance our understanding of how NPC2 and NPC1 work together in the egress of cholesterol from lysosomes, this thesis contributes by studying NPC1(NTD) and NPC2 in detail, as summarized below.

FIGURE 1-1

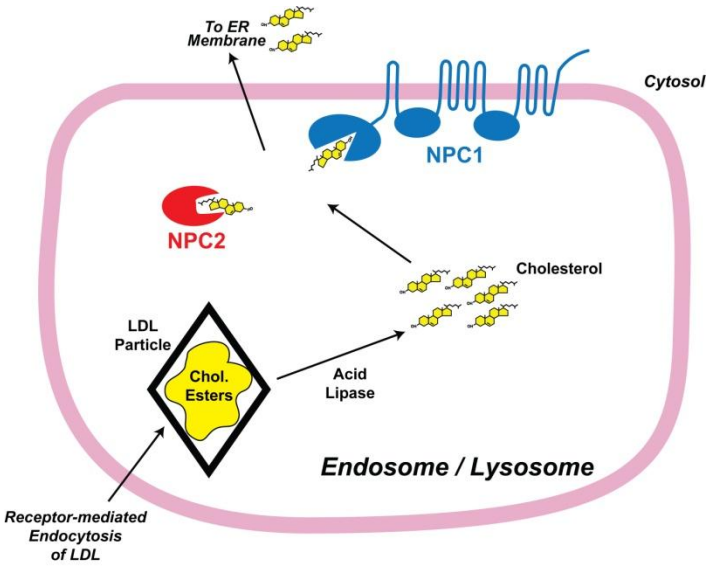

FIGURE 1-1. The Requirement of NPC1 and NPC2 in the Egress of LDL-derived Cholesterol from Lysosomes.

We first compared the cholesterol binding of the two proteins. Through competitive binding studies (Infante et al., 2008b) we show that NPC2 and NPC1(NTD) bind cholesterol in opposite orientations. This is also supported by crystal structures (Kwon et al., 2009; Xu et al., 2007). NPC2 binds the iso-octyl side chain, leaving the 3ß-hydroxyl exposed, whereas NPC1(NTD) binds the 3ß-hydroxyl, leaving the side chain partially exposed. Another important difference between NPC2 and NPC1(NTD) lies in the kinetics of sterol binding. NPC2 binds and releases cholesterol rapidly at 4°C (half-time < 2 min) (Infante et al., 2008c). In contrast, at 4°C NPC1(NTD) binds cholesterol very slowly (half-time > 2 hr) (Infante et al., 2008c).

The differences in cholesterol binding between NPC1(NTD) and NPC2 led us to explore the possibility of a transfer of bound cholesterol between the proteins. Its rapid binding of cholesterol enables NPC2 to transfer cholesterol to and from liposomes. Unlike NPC2, NPC1(NTD) cannot rapidly transfer its bound cholesterol to liposomes. However, NPC1(NTD) can accomplish this delivery when NPC2 is present (Infante et al., 2008c). Also, cholesterol binding to NPC1(NTD) is accelerated by >15-fold when the sterol is first bound to NPC2 and then transferred to NPC1(NTD). This led to the hypothesis that NPC2 can mediate bi-directional transfer of cholesterol to and from NPC1(NTD).

We then identified the amino acid residues important for binding or transfer of cholesterol on NPC2 and NPC1(NTD) through alanine scan mutagenesis. For both NPC2 and NPC1(NTD), residues that decreased binding mapped to areas surrounding the binding pockets on the crystal structures; residues that decreased transfer, but not binding, mapped to discrete surface patches near the opening of the binding pockets (Kwon et al., 2009; Wang et al., 2010). Furthermore, the functional significance of both the binding and transfer of cholesterol by NPC2 and NPC1(NTD) in the egress of cholesterol from lysosomes was confirmed by the inability of these mutants in NPC2 and NPC1 to rescue LDL-stimulated cholesteryl ester synthesis in NPC2 or NPC1-deficient cells, respectively, in contrast to wild-type NPC2 and NPC1 (Kwon et al., 2009; Wang et al., 2010).

In cells, we hypothesize that NPC2 accepts cholesterol in the lysosomal lumen and transports it to membrane-bound NPC1(NTD), which then inserts the cholesterol into lysosomal membranes, from which it is transferred to the ER. In this case, membrane insertion is likely mediated by the complex membranous domain of NPC1. This would account for the requirement for both proteins for lysosomal cholesterol export (Infante et al., 2008c; Kwon et al., 2009).

CHAPTER TWO

STEROL BINDING OF NPC2 AND THE N-TERMINAL DOMAIN OF NPC1

SUMMARY

Defects in Niemann-Pick, Type C-1 protein (NPC1) cause cholesterol, sphingolipids, phospholipids, and glycolipids to accumulate in lysosomes of liver, spleen, and brain. In cultured fibroblasts, NPC1 deficiency causes lysosomal retention of lipoprotein-derived cholesterol after uptake by receptor-mediated endocytosis. NPC1 contains 1278 amino acids that form 13 membrane-spanning helices and three large loops that project into the lumen of lysosomes, and has been shown to bind cholesterol and oxysterols. Here we localize the binding site to the N-terminal domain (NTD), a 242-amino acid domain with 18 cysteines. When produced in cultured cells, NPC1(NTD) was secreted as a soluble protein, and bound [^{3}H]cholesterol (*Kd*, 130 nM) and [^{3}H]25-hydroxycholesterol (25-HC, *Kd*, 10 nM). Binding of both sterols was competed by oxysterols (24-, 25-, and 27-HC). Unlabeled cholesterol competed strongly for binding of [^{3}H]cholesterol, but weakly for [^{3}H]25-HC binding. Clinical mutations found in NPC1(NTD) did not alter sterol binding. Glutamine 79 in NPC1(NTD) is important for sterol binding; a Q79A mutation abolished binding of [^{3}H]cholesterol and [^{3}H]25-HC to full-length NPC1. Nevertheless, the Q79A mutant restored cholesterol transport to NPC1-deficient CHO cells. We also studied NPC2, a soluble protein whose deficiency causes a similar disease phenotype. NPC2 bound cholesterol, but not oxysterols. Epicholesterol and cholesteryl sulfate competed for [^{3}H]cholesterol binding to NPC2, but not NPC1(NTD).

INTRODUCTION

Through studies of humans with inborn errors of metabolism, scientists have uncovered many aspects of lipid biochemistry (Brady, 1978; Goldstein and Brown, 2001; Kolter and Sandhoff, 2006). One disorder that remains puzzling is the complex disease known as Niemann-Pick Type C, which is caused by loss-of-function mutations in one of two different genes, *NPC1* (Vanier and Millat, 2003) and *NPC2* (Pentchev, 1995).

Evidence indicates that NPC1 is a polytopic membrane protein with 13 membrane-spanning helices (Davies and Ioannou, 2000). The protein has a cleaved N-terminal signal sequence, which targets the protein for insertion into membranes, three large luminal loops, and a cytoplasmic C-terminal segment that includes a dileucine sequence, which targets the protein to lysosomes (Watari et al., 1999). In previous studies it was shown that recombinant human NPC1 bound cholesterol as well as oxysterols, and the binding site was localized to its N-terminal domain (NTD) (Infante et al., 2008a).

In contrast, NPC2 is a soluble protein that is partially sequestered in lysosomes, and partially secreted by cells (Naureckiene et al., 2000). Cultured cells from subjects with NPC2 deficiency have the same defect in release of lysosomal cholesterol as do cells with an NPC1 mutation (Frolov et al., 2003). NPC2 has been demonstrated to bind cholesterol (Cheruku et al., 2006; Friedland et al., 2003; Ko et al., 2003; Okamura et al., 1999), and a crystal structure of NPC2 with bound cholesterol sulfate has been solved (Xu et al., 2007). The similarity in phenotypes between NPC1 and NPC2 mutations strongly suggests that the two proteins function sequentially in a pathway that releases cholesterol from lysosomes, but the order of their actions has not been determined (Sleat et al., 2004).

In these studies we prepared NPC1(NTD) as a soluble protein of 242 amino acids that is secreted by cells. Purified NPC1(NTD) binds oxysterols and cholesterol with high affinity. We characterize this binding reaction and provide evidence that the NTD contains the majority, if not all, of the cholesterol-binding activity of NPC1. We also purified NPC2, and compared its cholesterol binding activity with that of NPC1(NTD). Even though both NPC proteins bound cholesterol with similar affinity, their cholesterol binding activities showed a striking difference in specificity.

EXPERIMENTAL PROCEDURES

Materials – We obtained [1,2,6,7-^{3}H]cholesterol (60 Ci/mmol) from American Radiolabeled Chemicals; all other sterols from Steraloids; bovine serum albumin (BSA) from Pierce (Cat. No. 23210); glycosidase Endo H and PNGase F from New England Biolabs; Coomassie Brilliant Blue R-250 stain from Bio-Rad; Nonidet P-40 (NP-40) and FuGENE 6 from Roche Applied Sciences; Ni-NTA-agarose Beads from Qiagen; and Superdex 200 10/300 GL columns from GE Healthcare Biosciences. Reagents and lipoproteins for assays of cholesterol esterification and SREBP-2 processing were as previously described (Goldstein et al., 1983; Infante et al., 2008a).

Buffers and Media – Buffer A contains 50 mM Tris-chloride at pH 7.4, 150 mM NaCl. Buffer B contains 50 mM Tris-chloride at pH 7.4, 50mM KCl, 10% (v/v) glycerol, 5 mM dithiothreitol (DTT), 1 mM sodium EDTA, and protease inhibitor mixture (1 μg/ml pepstatin A, 2 μg/ml aprotinin, 10 μg/ml leupeptin, 200 μM phenylmethylsulfonyl fluoride, and 25 μg/ml of *N*-acetyl-Leu-Leu-norleucinal). Buffer C contains 50mM Tris-chloride at pH 7.4, 1% NP-40, 1 mM EDTA, and 0.1 mM DTT. Buffer D contained 50 mM Tris-chloride at pH 7.4, 100 mM KCl,

and 1% NP-40. Medium A contains a 1:1 mixture of Ham's F-12 medium and Dulbecco's Modified Eagle's medium, 100 units/ml penicillin, and 100 µg/ml streptomycin sulfate.

Plasmid Constructions – All plasmids are under the control of the CMV promoter unless otherwise stated, and were constructed by site-directed mutagenesis (QuikChange II XL kit, Stratagene) from pCMV-NPC1 or pCMV-NPC2 (Origene Technologies). pCMV-NPC1(1-264)-LVPRGS-His8-FLAG encodes the N-terminal domain of WT human NPC1 (amino acids 1-264) followed sequentially by 8 histidines and a FLAG tag. pCMV-NPC1-His8-FLAG encodes WT human NPC1 (amino acids 1-1278) followed sequentially by 8 histidines and a FLAG tag. pCMV-NPC2-His8 encodes WT human NPC2 (amino acids 1-151) followed sequentially by 8 histidines. pTKHSV-BP-2 encodes WT herpes simplex virus (HSV)-tagged human SREBP-2 under control of the thymidine kinase promoter (Hua et al., 1996b). Mutations in the above plasmid constructs were generated by site-directed mutagenesis. The coding regions of all plasmids were sequenced to ensure integrity of each construct.

Transfection of CHO Cells – Stock cultures of CHO-K1 cells were grown in monolayer at 37°C in an atmosphere of 8–9% CO_2 and maintained in medium A containing 5% (v/v) fetal calf serum (FCS). On day 0, CHO-K1 cells were set up for experiments in medium A containing 5% FCS at $6x10^5$ cells/100-mm dish. On day 2, each dish was transfected with one of the following plasmids: 5 µg of pCMV-NPC1-His8-FLAG, 5 µg of pCMV-NPC1(NTD)-His8-FLAG (WT or the indicated mutant versions), or 5 µg of pCMV-NPC2-His8, using FuGENE 6 reagent as described (Naureckiene et al., 2000). After 16 h, the transfected cells were used for purification of NPC1 proteins as described below. Mutant CHO 4-4-19 cells, defective in NPC1 (Dahl et al., 1992), were obtained from Laura Liscum (Tufts University School of Medicine, Boston, MA). The defective NPC1 in 4-4-19 cells results from an amino acid substitution (Gly-

660 to Arg). On day 0, 4-4-19 cells were set up in medium A containing 5% fetal calf serum at $2x10^5$ cells/60-mm dish. On day 2, each dish was transfected in OPTI-MEM (Invitrogen) with the indicated plasmid, using Lipofectamine 2000 according to the manufacturer's directions. After 5 h, the medium was switched to medium A containing 5% newborn calf LPDS. After 16 h, the cells were used for assays of ACAT and SREBP-2 processing.

Purification of Epitope-Tagged Full-length NPC1 from Transfected CHO Cells – CHO-K1 cells were set up on day 0 and transfected on day 2 as described above. After incubation for 24 h at 37°C, the cells were harvested, washed, and resuspended in ice-cold buffer B. Cells were homogenized with a 15-ml or 40-ml Dounce homogenizer and then subjected to 100,000 x *g* centrifugation for 30 min at 4 °C. The membrane pellet was resuspended by Dounce homogenization in buffer C containing the protease inhibitor mixture (4 dishes of cells per 1 ml of buffer), incubated overnight at 4°C to solubilize membrane proteins, and centrifuged at 100,000 x *g* for 30 min. The resulting 100,000 x *g* supernatant (containing detergent-solubilized membranes) was dialyzed against buffer D for 6–12 h at 4 °C, after which imidazole was added at a final concentration of 20 mM. This material was then loaded onto a 1-ml His Trap HP nickel column pre-equilibrated with buffer D. The column was washed sequentially with 10 column volumes of buffer D, 10 column volumes of buffer G plus 25 mM imidazole, and 20 column volumes of buffer D plus 50 mM imidazole. Bound protein was eluted in 1.5-ml fractions with buffer D plus 200 mM imidazole. The eluted fractions containing anti-FLAG (NPC1) immunoblot reactivity were then loaded onto a column containing 1-ml anti-FLAG M2-agarose beads (Sigma), which had been preequilibrated with buffer D. The column was washed with 6 column volumes of buffer A with 0.004% NP-40. Bound protein was eluted with 0.1 mg/ml of FLAG peptide in 9 column volumes of buffer A with 0.004% NP-40. Protein concentration of

purified NPC1 was estimated by silver staining and densitometric scanning of an 8% SDS-PAGE gel in which known amounts (50 to 400 ng) of bovine serum albumin (Pierce) was used as a reference.

Purification of Epitope-Tagged NPC1(NTD) and NPC2 from Medium of Transiently Transfected CHO Cells – CHO-K1 cells were set up on day 0 and transfected on day 2 as described above. On day 3, the medium (7 ml per dish) was switched to medium A containing 1% (v/v) Cellgro ITS (Fisher Scientific). After 24 h, the medium was collected, and fresh medium A containing 1% ITS was added. This cycle of collection/replenishment of medium was repeated for three consecutive days. All subsequent operations were carried out at 4°C. The medium from each daily collection was centrifuged at 1,800 x *g* for 5 min, filtered through an Express Plus 0.22-μM filter, and stored at 4°C for up to 2 weeks. The media was then loaded onto a 30-ml column (Bio-Rad) filled with 20-ml slurry of Ni-NTA-agarose beads (Qiagen) for purification of NPC1(NTD)-His8-FLAG or NPC2-His8. Each column was preequilibrated with 4 column volumes of buffer A. A total of 1 liter of medium was applied to each column (flow rate of ~1 ml/min over ~16 h). Each column was then washed sequentially with 5 column volumes of buffer A containing 20 mM imidazole and then with 5 column volumes of buffer A containing 40 mM imidazole. Bound protein was eluted with 5 column volumes of buffer A containing 250 mM imidazole. The elution containing each protein was concentrated to 0.5 ml in a spin concentrator using an Amicon Ultracel 10K filter device (Millipore). The concentrated material was then subjected to gel-filtration chromatography on a 24-ml Superdex-200 10/300 column preequilibrated with buffer A. Fractions containing peak A280 activity (between elution volumes of 13.5 and 16.5 ml for NPC1(NTD) and 15.5 and 18.5 ml for NPC2) were pooled, and their protein content was quantified with the BCA assay (Smith et al., 1985). Pooled proteins were

subjected to 8 or 13% SDS-PAGE for NPC1(NTD) and NPC2, respectively, followed by Coomassie staining to determine purity.

Ni-NTA Agarose Assay for ^{3}H-Sterol Binding – Incubation conditions are detailed in figure legends. After incubation for the indicated time at 4°C, each reaction was loaded onto a 2-ml Bio-Spin column (Bio-Rad) packed with 0.3 ml of Ni-NTA-agarose beads that had been preequilibrated with buffer A containing 0.004% NP-40. The beads were washed with either 5 ml buffer A with 1% NP-40 for NPC1(NTD) or 6 ml buffer A with 0.004% NP-40 for NPC2 (and for NPC1(NTD) if in the same experiment with NPC2). Protein-bound [^{3}H]cholesterol was eluted with 1 ml buffer A containing 250 mM imidazole and 1 or 0.5% NP-40 for NPC1(NTD) and NPC2, respectively, and quantified by scintillation counting.

Glycosidase Treatments – Each reaction, in a final volume of 42 µl, was carried out according to the manufacturer's directions (New England Biolabs) for 16 h at 37°C with the indicated amount of purified protein in the presence or absence of 4000 units of Endo H or 5000 units of PNGase F.

SREBP-2 Processing in Cultured Cells – Mutant CHO 4-4-19 cells (defective in NPC1) were transfected as described above. On day 3, the medium was switched to medium A containing 5% newborn calf LPDS, 5 µM compactin, and 50 µM sodium mevalonate. On day 4, the cells received fresh medium A supplemented with 5% newborn calf LPDS, 50 µM compactin, 50 µM sodium mevalonate, and various concentrations of β-VLDL or 25-HC. After incubation at 37°C for 5 h, cells were treated with 25µg/ml of *N*-acetyl-Leu-Leu-norleucinal for 1 h and then harvested. Duplicate dishes were pooled for preparation of nuclear extract and 100,000 x *g* membrane fractions, which were then analyzed by immunoblotting for SREBP-2 (described below).

Immunoblot Analysis – Samples were subjected to 8% or 13% SDS-PAGE, after which the proteins were transferred to nitrocellulose filters. The immunoblots were performed at room temperature using the following primary antibodies: 1 μg/ml of a rabbit polyclonal antibody against human NPC1 (Novus); 5 μg/ml of a mouse monoclonal antibody against the FLAG epitope (IgG fraction; Sigma); 10 μg/ml of a rabbit polyclonal antibody (IgG-1819) directed against amino acids 1–100 of human SREBP-2 (raised by injecting rabbits with a His8-tagged recombinant version of the antigen), and 0.2 μg/ml of a mouse monoclonal antibody against the glycoprotein D epitope of HSV (Novagen, Inc). Bound antibodies were visualized by chemiluminescence (SuperSignal Substrate, Pierce) using a 1:5000 dilution of anti-mouse IgG (Jackson ImmunoResearch Laboratories, Inc.) or a 1:2000 dilution of anti-rabbit IgG conjugated to horseradish peroxidase (Amersham Biosciences). The filters were exposed to Kodak X-Omat Blue XB-1 film at room temperature.

ACAT Assay – The rate of incorporation of [^{14}C]oleate into cholesterol [^{14}C]oleate and [^{14}C]triglycerides by intact cell monolayers was measured as previously described (Goldstein et al., 1983).

RESULTS

NPC1, NPC1(NTD), and NPC2 Proteins – Fig. 2-1A shows a diagram of the postulated domain structure of human NPC1, as well as the soluble secreted N-terminal domain of NPC1. The full-length protein is believed to contain 13 putative transmembrane helices (Davies and Ioannou, 2000) that divide the protein into the following structural domains: 1) a cleaved signal sequence (amino acids 1–24) (Carstea et al., 1997); 2) luminal loop-1 (amino acids 23–264); 3) luminal loop-2 (amino acids 371–621); 4) a putative sterol-sensing domain (transmembrane

helices 3–7, amino acids 616–791) (Millard et al., 2005; Nohturfft et al., 1998); 5) luminal loop-3 (amino acids 855–1098); and 6) a lysosomal targeting signal (LLNF) at the C terminus (amino acids 1275–1278) (Watari et al., 1999). This N-terminal domain of NPC1, designated NPC1(NTD), contains the signal sequence and NTD as shown in Fig. 2-1A. The calculated molecular mass for the protein component of the epitope-tagged NPC1(NTD) is 28.7 kDa. However, the secreted protein migrated on SDS-PAGE as a diffuse band slightly above the 50-kDa marker (Fig. 2-1B). Treatment of the secreted protein with the glycosidase PNGase F under denaturing conditions caused the recombinant protein to migrate as a compact band close to the 30-kDa marker (data not shown). Thus, the diffuse migration is attributable to glycosylation of some or all of the five potential *N*-linked glycosylation sites on the NTD (Fig. 2-1B). Upon gel filtration in the absence of detergents, this protein eluted as a single symmetrical peak corresponding to ~100 kDa (Fig. 2-3B). When the protein was analyzed by CD (Fig. 2-3C), it showed a spectrum characteristic of high α-helical content with minima at 207 and 222 nm (Chen et al., 1974). Fig. 2-1C shows a diagram of the soluble secreted NPC2. The calculated molecular mass of the secreted protein component of NPC2-His8 is 15.7 kDa. However, purified NPC2-His8 migrated on SDS-PAGE as three distinct bands (23, 21, and 18 kDa) as visualized by Coomassie staining (Fig. 2-1D). Previous studies showed that NPC2 contains two *N*-linked carbohydrate chains that contain mannose 6-phosphate (Chikh et al., 2004). Treatment of purified NPC2-His8 with the glycosidase Endo H (which removes only high mannose chains) reduced the molecular mass of band 2 from 21 to 19 kDa and band 3 from 18 to 16 kDa (Fig. 2-1D), whereas treatment with PNGase F (which removes all *N*-linked chains) reduced all three bands to the predicted protein molecular mass of 16 kDa (Fig. 2-1D). Gel-filtration studies of the

recombinant NPC2 showed that it eluted as a single symmetrical peak corresponding to ~20 kDa (data not shown).

Binding Specificity of NPC1(NTD) – To measure the binding of ^{3}H-labeled sterols to purified NPC1(NTD)-His8-FLAG, we used an assay in which the protein was trapped on a nickel-agarose column, and bound [^{3}H]sterols were quantified by scintillation counting (Infante et al., 2008a; Radhakrishnan et al., 2007). The binding reactions were conducted in a low concentration of NP-40 (0.004%), which is slightly higher than the critical micellar concentration (CMC), which is 0.0015% (discussed below). Fig. 2-2A shows binding of [^{3}H]25-HC to NPC1(NTD)-His8-FLAG in the absence and presence of an excess of unlabeled 25-HC. Binding of [^{3}H]25-HC was saturable with an apparent *Kd* of 10 nM (average of seven experiments). At saturation, we estimated that 1 molecule of [^{3}H]25-HC bound to 1 dimer of NPC1(NTD)-His8-FLAG. Binding of [^{3}H]25-HC was inhibited by an excess of unlabeled 25-HC (Fig. 2-2A) and by similar concentrations of unlabeled 24-HC and 27-HC (see Fig. 2-5F). We then tested the ability of NPC1(NTD) to bind [^{3}H]cholesterol. As shown in Fig. 2-2B, this protein fragment bound [^{3}H]cholesterol with an apparent *Kd* of 130 nM (average of seven experiments). At saturation, we estimated that 1 molecule of [^{3}H]cholesterol bound to 1 dimer of NPC1(NTD)-His8-FLAG, a similar binding stoichiometry to that of [^{3}H]25-HC. The binding of [^{3}H]cholesterol was inhibited by an excess of unlabeled cholesterol. [^{3}H]Progesterone did not show saturable binding to NPC1(NTD)-His8-FLAG when tested at concentrations from 1–400 nM (data not shown). In studies not shown, we found that the maximal binding of [^{3}H]cholesterol or [^{3}H]25-HC to NPC1(NTD)-His8-FLAG was similar over a pH range of 4–8. Moreover, binding of [^{3}H]25-HC or [^{3}H]cholesterol was not affected by the presence of EDTA up to 10 mM, but both binding activities were markedly decreased in the presence of 10 mM dithiothreitol, a reducing agent that

would be expected to disrupt the multiple disulfide bonds that are postulated based on the cysteine rich amino acid sequence of NPC1(NTD). To examine in more detail the binding of [^{3}H]25-HC and [^{3}H]cholesterol to NPC1(NTD), we carried out competitive binding studies, as shown in Fig. 2-2, C and D. When [^{3}H]25-HC was present at a concentration near its *Kd* (10 nM), unlabeled 25-HC competed with an IC50 value of ~10 nM, whereas unlabeled cholesterol did not effectively compete except at concentrations of 3 μM (Fig. 2-4C). When [^{3}H]cholesterol was present at a concentration near its *Kd* (130 nM), unlabeled cholesterol competed with an IC50 of ~100 nM, whereas unlabeled 25-HC inhibited with an IC50 ~5 nM (Fig. 2-2C). Thus, by two different assays (direct binding and competition), NPC1(NTD) showed a 13- to 20-fold higher affinity for 25-HC than cholesterol. Epicholesterol showed no ability to compete for binding of either [^{3}H]25-HC or [^{3}H]cholesterol (Fig. 2-2, C and D). Moreover, 19-hydroxycholesterol, a cholesterol analogue with a hydroxyl group on the sterol nucleus, did not compete for the binding of [^{3}H]25-HC when tested at concentrations up to 3 μM (data not shown).

Mutational Analysis of NPC1(NTD) – We subjected NPC1(NTD)-His8-FLAG to mutational analysis to pinpoint amino acids crucial for sterol binding. We focused on five residues (Gln-79, Asn-103, Gln-117, Phe-120, and Tyr-157) that are conserved in 12 vertebrate NPC1 orthologs and that exhibit >75% identity among homologs of NPC1 found in 76 eukaryotic species (data not shown). These residues were also chosen for their hydrogen-bonding potential (Gln-79, Asn-103, and Gln-117) or for their ability to form ring-stacking interactions (Phe-120 and Tyr-157). Each of these residues was mutated to alanine. The two hydrophobic residues, Phe-120 and Tyr-157, were also mutated to methionine. In addition to these novel mutations, we reproduced six "clinical" mutations corresponding to substitutions in NPC1(NTD) observed in patients with NPC1 disease (Q92R, T137M, P166S, N222S, D242H, and G248V)

(Scott and Ioannou, 2004). Plasmids encoding each mutant version of NPC1(NTD) were expressed in CHO cells, and the recombinant proteins were purified from the medium in a similar manner to the WT version. All mutant proteins were secreted, and they all showed a normal behavior on gel filtration and SDS-PAGE. The data for the Q79A mutant is shown in Fig. 2-3, E-F. Of the 14 mutant proteins, only two of the novel mutants, Q79A and Q117A, showed an abnormality in sterol binding. The most striking abnormality was observed with the Q79A mutant, which showed no detectable binding of [^{3}H]25-HC (Fig. 2-3A) and a 40% decrease in maximal binding of [^{3}H]cholesterol (Fig. 2-3B). Similar results were obtained in four additional experiments involving three different preparations of purified NPC1(NTD). CD spectra of the Q79A protein was identical to that of the WT protein, showing a spectrum characteristic of high α-helical content with minima at 207 and 222 nm, indicating no major structural changes (Fig. 2-3G). Mutant Q117A also showed a 40% decrease in binding of [^{3}H]cholesterol (Fig. 2-3B) but only a slight decrease in [^{3}H]25-HC binding (Fig. 2-3A). Fig. 2-3, C and D shows the binding data for two of the clinical mutants, Q92R and T137M, both of which showed normal binding for both [^{3}H]25-HC and [^{3}H]cholesterol.

Sterol Binding Properties of Full-length Mutant NPC1 (Q79A) – To determine whether the point mutation Q79A that disrupts 25-HC binding in NPC1(NTD) also affects the binding properties of the full-length NPC1 molecule, we expressed and purified the Q79A mutant version of full-length NPC1-His8-FLAG in 0.004% NP-40 in the same manner as the WT protein. As shown in the binding curves in Fig. 2-4A, [^{3}H]25-HC did not bind to the Q79A mutant protein. The Q79A mutant protein also bound very little [^{3}H]cholesterol as compared with the WT version (Fig. 2-4B).

Full-length Mutant NPC1 (Q79A) Restores NPC1 Function to CHO 4-4-19 Cells – The availability of a point mutation in the full-length NPC1 protein that abolishes its 25-HC-binding activity provided the opportunity to determine whether oxysterol binding to WT NPC1 influences the transport of lipoprotein-derived cholesterol from endosomes/lysosomes to the ER. To test this hypothesis, we transfected WT and mutant versions of NPC1-His8-FLAG into CHO 4-4-19 cells, a mutant line of CHO cells deficient in NPC1 function. In these cells, LDL and β-VLDL have a reduced ability to stimulate ACAT activity as measured by cholesteryl [^{14}C]oleate formation in intact cells (Dahl et al., 1992). On the other hand, 25-HC activates ACAT normally in these cells (Dahl et al., 1992). Fig. 2-4C shows an immunoblot of membrane extracts from CHO 4-4-19 cells that were transfected with cDNAs encoding WT and Q79A mutant versions of NPC1-His8-FLAG. As a result of this transient transfection, these cells expressed high levels of both versions of NPC1 as compared with the mock-transfected cells. When the transfected CHO4-4-19 cells were incubated with β-VLDL, a cholesterol-rich lipoprotein that binds to LDL receptors with high affinity and delivers cholesterol to lysosomes (van Driel et al., 1987), the cholesterol from β-VLDL reached the ER and markedly stimulated cholesteryl [^{14}C]oleate formation in the cells expressing either the WT or the Q79A mutant version of NPC1, but not in the cells transfected with a control mock plasmid (Fig. 2-4D). In WT cells, when cholesterol derived from β-VLDL reaches the ER, it prevents the exit of SREBP-2, thereby blocking its proteolytic processing (Goldstein et al., 2006). In mock transfected CHO 4-4-19 cells, high concentrations of β-VLDL (30 μg of protein/ml) did not block SREBP-2 processing (Fig. 2-4E, *lane 2*). In contrast, when the CHO 4-4-19 cells were transfected with cDNAs encoding either WT NPC1 or its Q79A mutant version, β-VLDL blocked SREBP-2 processing at concentrations as low as 1 μg of protein/ml (Fig. 2-4F, lanes 4 and 11). All three transfected CHO 4-4-19 cells

(mock, NPC1 WT, and NPC1 Q79A mutant) responded to 25-HC (Fig. 2-4E, lane 3; Fig. 2-4F, lanes 8 and 15).

Sterol Binding Properties of Recombinant NPC2 and NPC1(NTD) – About 4% of patients with Niemann-Pick Type C disease harbor mutations in NPC2, a soluble 132-amino acid protein that is secreted into plasma and also resides within the cell, primarily in lysosomes (Naureckiene et al., 2000). Previous studies have shown that NPC2 binds cholesterol with measured *Kd* values that range from 50 nM to 5 μM in different laboratories (Friedland et al., 2003; Ko et al., 2003; Okamura et al., 1999). To compare the sterol binding properties of NPC1 and NPC2, we prepared a plasmid encoding pCMV-NPC2-His8, expressed it in CHO cells, and purified the secreted NPC2 using the same procedure as described for NPC1(NTD). When incubated with [^{3}H]cholesterol, NPC2-His8 showed saturable binding with an apparent *Kd* of ~150 nM (Fig. 2-5B). The protein did not bind [^{3}H]25-HC (Fig. 2-5A). This all-or-none difference in binding of [^{3}H]cholesterol *versus* [^{3}H]25-HC is in contrast to that of NPC1(NTD), which binds both [^{3}H]cholesterol (Fig. 2-5B) and [^{3}H]25-HC (Fig. 2-5A). Competitive binding studies confirmed that NPC2-His8 binds cholesterol, but not 25-HC (Fig. 2-5C) or two other iso-octyl oxysterols, 24-HC and 27-HC (Fig. 2-5E). The difference in sterol-binding properties of NPC1 and NPC2 was further supported by the competition experiments in which epicholesterol and cholesteryl sulfate competed efficiently for [^{3}H]cholesterol binding to NPC2 (Fig. 2-5, C and E), but not to NPC1(NTD) (Fig. 2-7, D and F). Moreover, androstenol, a cholesterol analogue that lacks the iso-octyl side chain, did not compete for [^{3}H]cholesterol binding to either NPC1(NTD) or NPC2 when tested at concentrations up to 3 μM (data not shown). These results are consistent with the recent studies of Liou *et al.* (Liou et al., 2006), who assessed the sterol-binding specificity of NPC2 with a competition assay in which the labeled ligand was a

fluorescent plant sterol (*i.e.* dehydroergosterol), and the competitor unlabeled sterols were each tested at a single concentration. The most effective competitor was cholesteryl sulfate (100% inhibition), whereas the iso-octyl oxysterols showed either no competitive inhibition (25-HC) or a partial inhibition of ~35% (24-HC and 27-HC).

FIGURE 2-1. Purified NPC1(NTD) and NPC2 Proteins.

(A), Diagrammatic illustration of NPC1 with predicted topology and of NPC1(NTD)-His8-FLAG, showing the secreted soluble domain after cleavage of signal peptide (amino acids 23-264). (B) Purified recombinant human NPC1(NTD)-His8-FLAG (5ug) was subjected to 8% SDS-PAGE, then visualized with Coomassie Brilliant Blue R-250 stain. (C) Diagrammatic illustration of NPC2-His8 as a secreted soluble protein after cleavage of signal peptide (amino acids 20-151). (D) Purified recombinant human NPC2-His8 (7.6μg) was treated with or without Endo H or PNGase F, subjected to 15% SDS-PAGE, then visualized with Coomassie Brilliant Blue R-250 stain. *Asterisks* denote the migration of Endo H (*lane 2*) and PNGase F (*lane 3*). *Bands 1–3* denote different glycosylated forms of purified NPC2-His8.

FIGURE 2-1

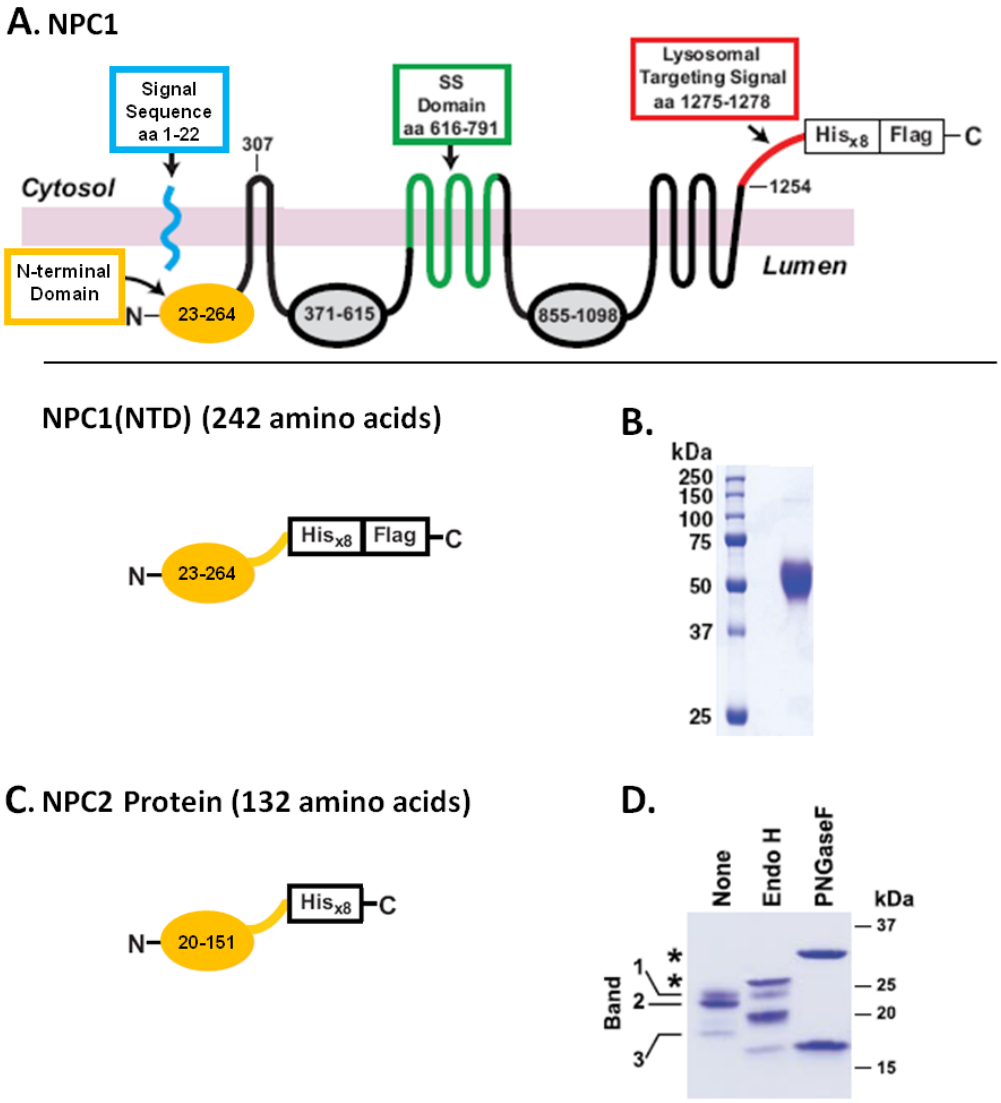
A. NPC1
Signal Sequence aa 1-22
SS Domain aa 616-791
Lysosomal Targeting Signal aa 1275-1278
307
Cytosol
1254
Lumen
N-terminal Domain
N
23-264
371-615
855-1098
His x8
Flag
C
NPC1(NTD) (242 amino acids)
N
23-264
His x8
Flag
C
B.
kDa
250
150
100
75
50
37
25
C. NPC2 Protein (132 amino acids)
N
20-151
His x8
C
D.
None
Endo H
PNGaseF
kDa
37
25
20
15
Band
1
2
3
*
*

FIGURE 2-2. [^{3}H]25-HC and [^{3}H]Cholesterol Binding Activities of Purified NPC1(NTD).

(A and B) *S*aturation curves for NPC1(NTD) binding of [^{3}H]25-HC and [^{3}H]cholesterol. Each reaction, in a final volume of 80 µl of buffer A with 0.004% NP-40, contained 100 ng of purified human NPC1(NTD)-His8-FLAG, 1 µg of BSA, and 10–300 nM of either [^{3}H]25-HC (A) or [^{3}H]cholesterol (B), both delivered in ethanol, in the absence (*black*) or presence of 3 µM unlabeled 25-HC (*blue*) or cholesterol (*red*) as indicated. After incubation for 4 h at 4 °C, bound [^{3}H]25-HC (A) or [^{3}H]cholesterol (B) was measured using the Ni-NTA-agarose binding assay. Each value is the average of duplicate assays and represents total binding without subtraction of blank values. (C and D) Competitive binding of [^{3}H]25-HC (C) and [^{3}H]cholesterol (D) to NPC1(NTD). Each reaction, in a final volume of 80 µl of buffer A with 0.004% NP-40, contained 100 ng of NPC1(NTD)-His8-FLAG, 1 µg of BSA, either 10 nM [^{3}H]25-HC (C) or 130 nM [^{3}H]cholesterol (D), and varying concentrations of the indicated unlabeled sterol. After incubation at 4 °C for 16 h, bound [^{3}H]25-HC (C) or [^{3}H]cholesterol (D) was measured. Each value is the average of duplicate assays and represents the amount of [^{3}H]sterol bound relative to that in the control tube, which contained no unlabeled sterol. The 100% of control values were 340 fmol/tube (C) and 580 fmol/tube (D). Blank values of 3 fmol/tube (C) and 68 fmol/tube (D) were subtracted from these values.

FIGURE 2-2

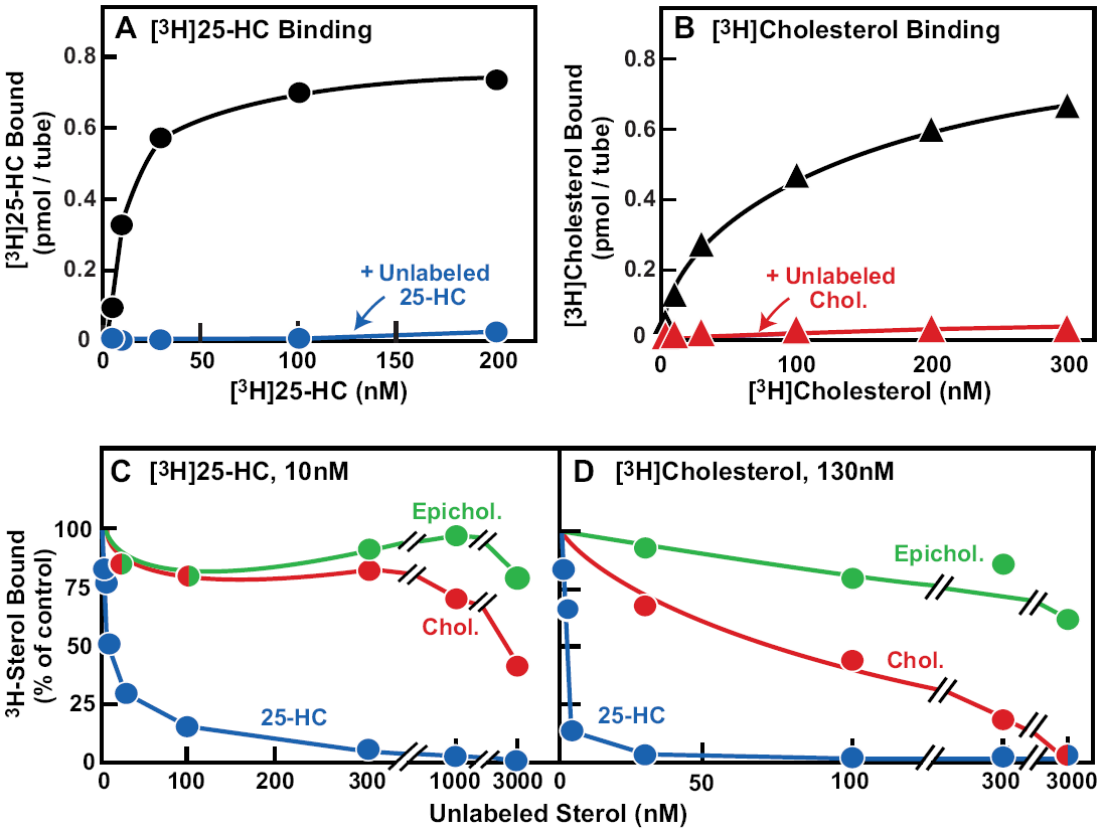
A [3H]25-HC Binding
[3H]25-HC Bound (pmol / tube)
0.8
0.6
0.4
0.2
0
0
50
100
150
200
[3H]25-HC (nM)
+ Unlabeled 25-HC
B [3H]Cholesterol Binding
[3H]Cholesterol Bound (pmol / tube)
0.8
0.6
0.4
0.2
0
0
100
200
300
[3H]Cholesterol (nM)
+ Unlabeled Chol.
C [3H]25-HC, 10nM
3H-Sterol Bound (% of control)
100
75
50
25
0
0
100
200
300
1000
3000
Epichol.
Chol.
25-HC
D [3H]Cholesterol, 130nM
0
50
100
300
3000
Epichol.
Chol.
25-HC
Unlabeled Sterol (nM)

FIGURE 2-3. [^{3}H]25-HC and [^{3}H]Cholesterol Binding to Versions of NPC1(NTD) Corresponding to Novel Mutations in Conserved Residues and Clinical Mutations found in Patients with NPC1.

(A–D) *S*aturation curves for [^{3}H]sterol binding to WT and mutant NPC1(NTD) proteins. Each reaction, in a final volume of 80 µl of buffer A with 0.004% NP-40, contained 100 ng of purified WT or the indicated mutant version of NPC1(NTD)-His8-FLAG, 1 µg of BSA, and 10–300 nM of either [^{3}H]25-HC (A and C) or [^{3}H]cholesterol (B and D), both delivered in ethanol. After incubation for 4 h at 4°C, bound [^{3}H]sterol was measured using the Ni-NTA-agarose binding assay. Each value is the average of duplicate assays and represents total binding without subtraction of blank values. (E) Coomassie staining. Aliquots (5µg) of purified WT and the Q79A mutant version of NPC1(NTD)-His8-FLAG were subjected to 8% SDS-PAGE, then visualized with Coomassie stain. Molecular masses of protein standards are indicated. (F) Gel-filtration chromatography of purified proteins. Buffer A (0.5 ml) containing 60 µg of either WT or the Q79A mutant version of NPC1(NTD)-His8-FLAG was loaded onto a Superdex200 10/300 GL column and chromatographed at a flow rate of 0.5 ml/min. Absorbance at 280 nm was monitored continuously to identify the indicated NPC1(NTD) protein. Standard molecular mass markers (thyroglobulin, 670 kDa; bovine γ-globulin, 158 kDa; chicken ovalbumin, 44 kDa; equine myoglobin, 17 kDa; and vitamin B12, 1.35 kDa) were chromatographed on the same column (*arrows*). The apparent molecular mass of NPC1(NTD)-His8-FLAG is ~100 kDa. (G) CD of 200 µg of WT or the Q79A mutant version of NPC1(NTD)-His8-FLAG in buffer A was measured on an Aviv 62DS spectrometer using a 2-mm path length cuvette. The data shown represent the averaged values from 9 spectra.

FIGURE 2-3

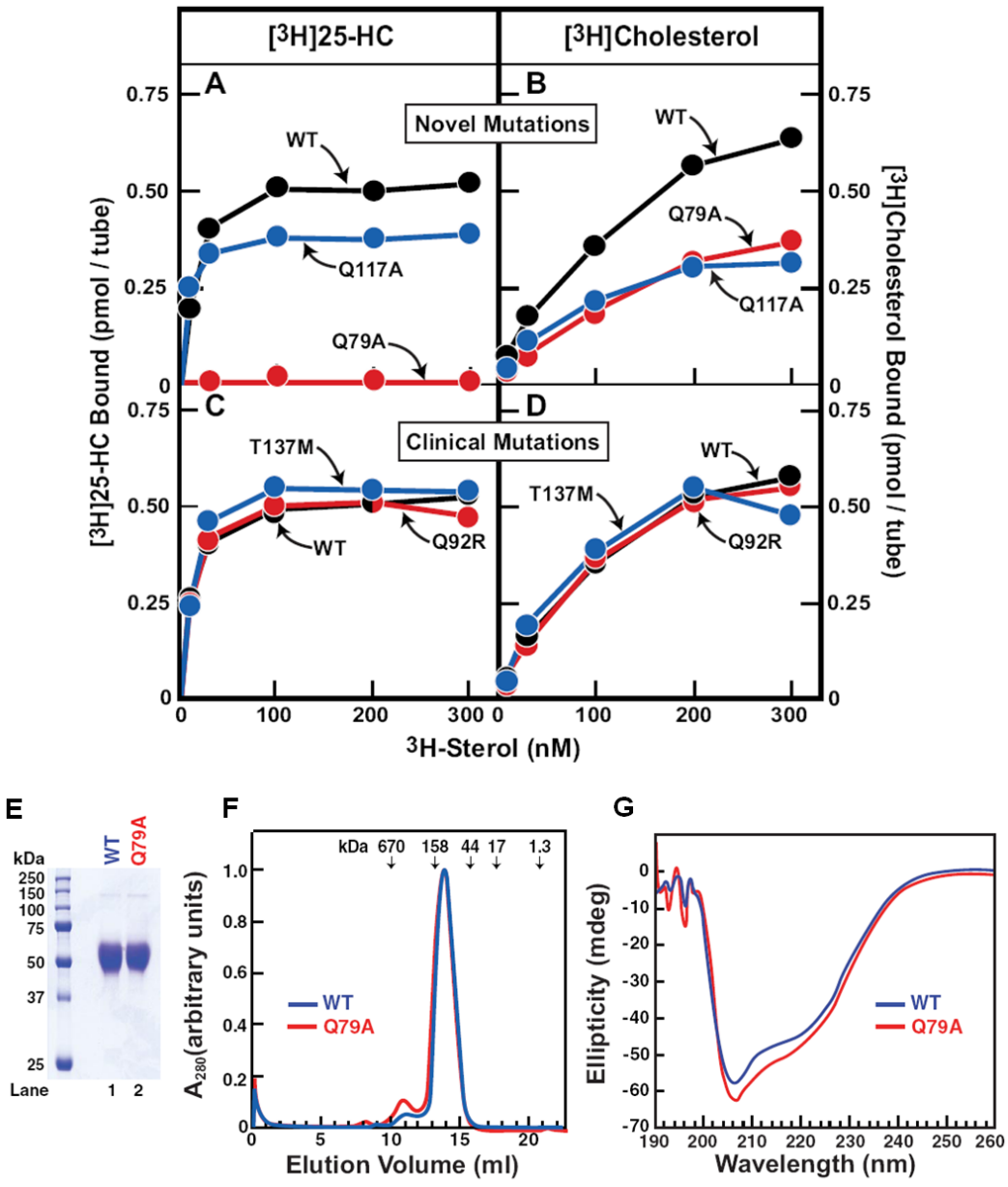
[3H]25-HC
[3H]Cholesterol
A
B
C
D
Novel Mutations
Clinical Mutations
WT
Q117A
Q79A
T137M
Q92R
[3H]25-HC Bound (pmol / tube)
[3H]Cholesterol Bound (pmol / tube)
3H-Sterol (nM)
E
kDa
250
150
100
75
50
37
25
Lane 1 2
F
kDa 670 158 44 17 1.3
A280(arbitrary units)
Elution Volume (ml)
G
Ellipticity (mdeg)
Wavelength (nm)

FIGURE 2-4. ^{3}H-Sterol Binding Activities and of WT and Mutant Q79A Versions of Full-length NPC1 and their Abilities to Rescue NPC1-defective Cells.

(A and B) Sterol Binding. Each reaction, in a final volume of 80 µl of buffer A, contained ~50 ng of WT or Q79A human NPC1-His8-FLAG purified in 0.004% NP-40, 1 µg of BSA, and 10–300 nM of either [^{3}H]25-HC (A) or [^{3}H]cholesterol (B), both delivered in ethanol. The final concentration of NP-40 was ~0.0008%. After incubation for 16 h at 4°C, bound [^{3}H]sterol was measured. Each value is the average of duplicate assays and represents total binding without subtraction of blank values. (C–F) On day 0, mutant CHO 4-4-19 cells were set up in medium A containing 5% fetal calf serum. (C) Immunoblot analysis of NPC1 proteins. On day 2, the cells were transfected with 2 µg of pcDNA3.1 (mock, *M*) or 2 µg of WT or mutant Q79A version of pCMV-NPC1-His8-FLAG. On day 3, the cells were harvested, and whole cell extracts were prepared (Adams et al., 2004) and processed for immunoblot analysis of the indicated proteins. (D) Cholesterol esterification assay in mutant CHO cells. On day 2, the cells were transfected as described in C. On day 3, the medium was switched to medium A containing 5% newborn calf LPDS, 5 µM compactin, and 50 µM sodium mevalonate. On day 4, the medium was switched to medium A supplemented with 5% newborn calf LPDS, 50 µM compactin, 50 µM sodium mevalonate, and the indicated concentration of β-VLDL. After incubation for 5 h at 37°C, each monolayer was pulse-labeled for 2 h with 0.2 mM sodium [^{14}C]oleate (6446 dpm/pmol). The cells were then harvested for measurement of their content of cholesteryl [^{14}C]oleate and [^{14}C]triglycerides. Each value is the average of duplicate incubations. The cellular content of [^{14}C]triglycerides (data not shown in the figure) for mock, WT NPC, or Q79A NPC1-transfected cells incubated with 10 µg of protein/ml of β-VLDL were 209, 184, and 194 nmol/h/mg, respectively. (E) Immunoblot analysis of SREBP-2 in mutant CHO cells overexpressing SREBP-

2. On day 2, the cells were transfected with 3 μg of pTK-HSV-BP2. (F) Immunoblot analysis of SREBP-2 cleavage in mutant CHO cells overexpressing full-length NPC1 (WT or Q79A). On day 2, the cells were either mock-transfected with pcDNA3.1 (*M*) or co-transfected with 3 μg of pTK-HSV-BP-2 together with 2 μg of either WT or mutant Q79A version of pCMV-NPC1-FLAG. (E and F) On day 3, the medium was switched to medium A supplemented with 5% newborn calf LPDS, 5 μM compactin, and 50 μM sodium mevalonate. On day 4, the medium was switched to medium A supplemented with 5% newborn calf LPDS with the indicated concentration of β-VLDL or 1 μg/ml of 25-HC. After incubation for 6 h, the cells were harvested and processed for immunoblot analysis of the indicated proteins. (C and E) All filters were exposed on x-ray film for 5–10 s except for the nuclear SREBP-2 filter, which was exposed for 20 s.

FIGURE 2-4

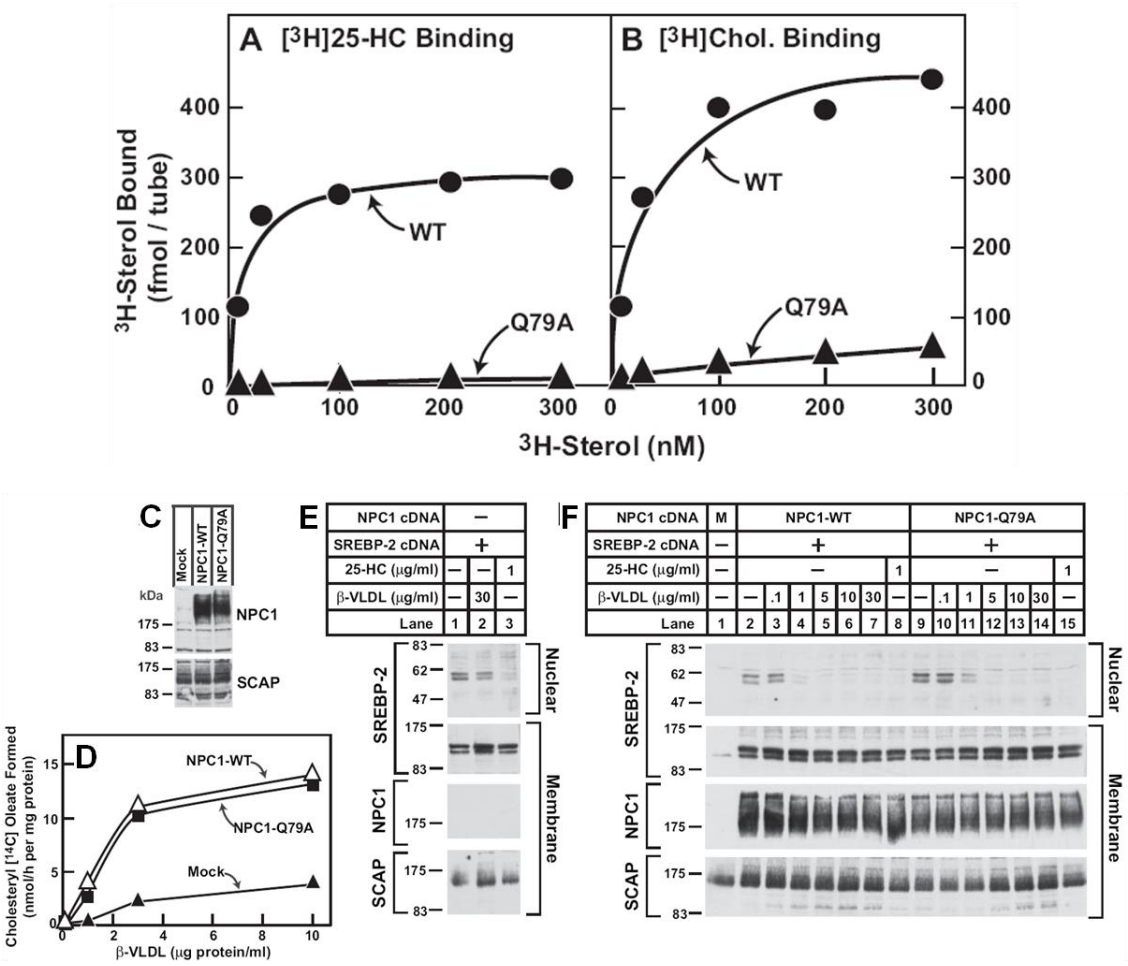

(Data for C-F from Lina Abi-Mosleh)

FIGURE 2-5. ^{3}H-Sterol Binding Specificities of Purified NPC1(NTD) and NPC2.

(A and B) Saturation curves for binding of [^{3}H]sterols to NPC1(NTD) and NPC2. Each reaction, in a final volume of 80 µl of buffer A with 0.004% NP-40, contained either 290 ng of purified human NPC2 or 200 ng of purified human NPC1(NTD)-His8-FLAG, 1 µg of BSA, and 0–400 nM [^{3}H]25-HC (A) or [^{3}H]cholesterol (B), both delivered in ethanol. After incubation for 16 h at 4°C, bound [^{3}H]sterols were measured. Each value is the average of duplicate assays and represents total binding without subtraction of blank values. (C-F) Competitive binding of [^{3}H]cholesterol to NPC2 and NPC1(NTD). Each reaction, in a final volume of 80 ul of buffer A with 0.004% NP-40, contained 200 ng NPC2 or 150 ng NPC1(NTD), 1 µg BSA, 200nM [^{3}H]cholesterol, and the indicated concentrations of various unlabeled sterols. After incubation for 4 h at 4^{o}C, bound [^{3}H]cholesterol was measured. Each value is the average of duplicate assays and represents the amount of [^{3}H]cholesterol bound relative to that in the control tube, which contained no unlabeled sterol. The 100% of control values were 1.61 (C), 6.9 (D), 1.56 (E), and 7.4 (F) pmol/tube. Blank values of 0.03-0.07 pmol/tube were subtracted.

FIGURE 2-5

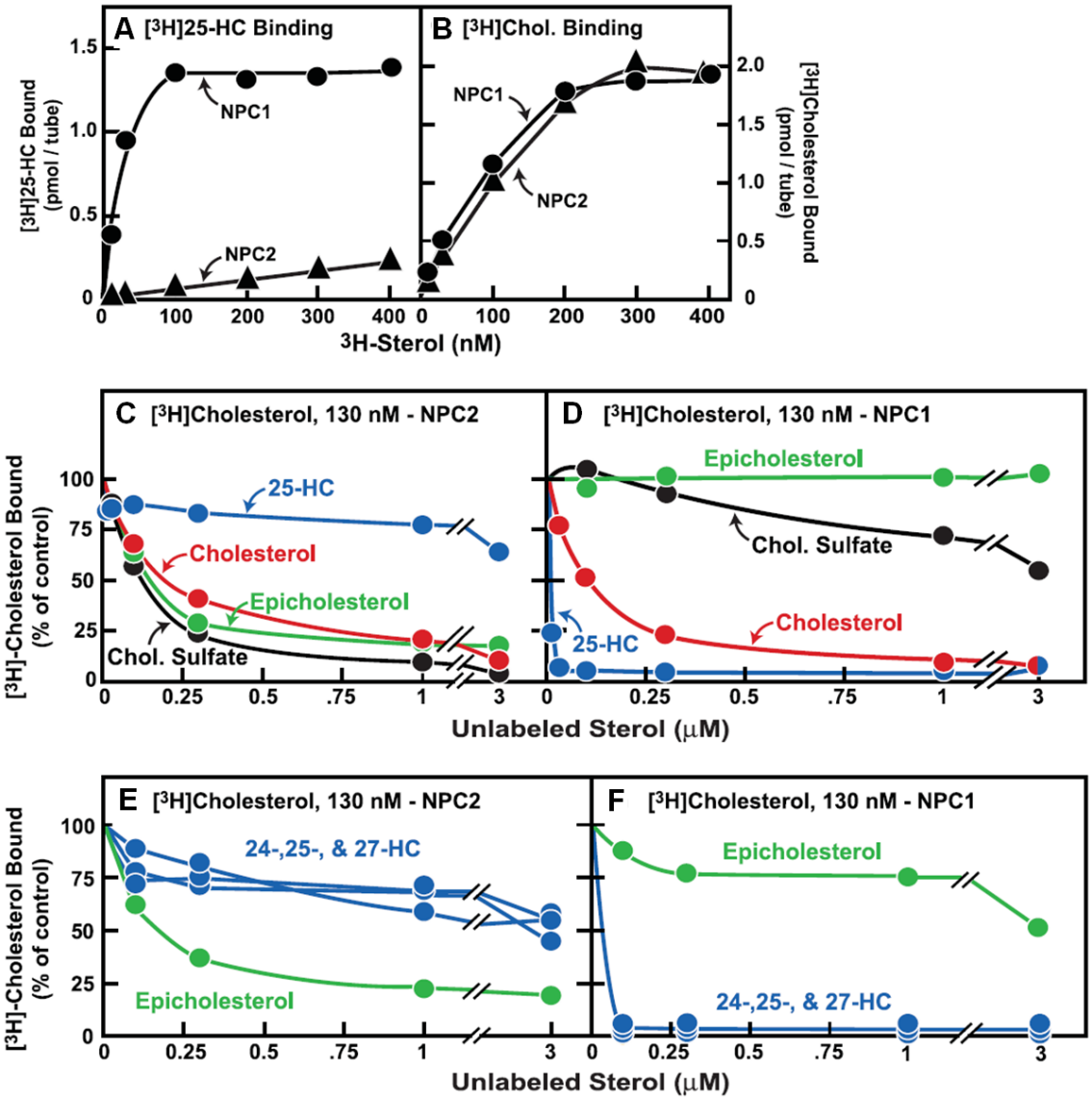
A [3H]25-HC Binding
B [3H]Chol. Binding
[3H]25-HC Bound (pmol / tube)
[3H]Cholesterol Bound (pmol / tube)
NPC1
NPC2
3H-Sterol (nM)
C [3H]Cholesterol, 130 nM - NPC2
D [3H]Cholesterol, 130 nM - NPC1
[3H]-Cholesterol Bound (% of control)
25-HC
Cholesterol
Epicholesterol
Chol. Sulfate
Unlabeled Sterol (μM)
E [3H]Cholesterol, 130 nM - NPC2
F [3H]Cholesterol, 130 nM - NPC1
24-,25-, & 27-HC

DISCUSSION

The current data reveal a saturable sterol binding site on the N-terminal domain human NPC1. The importance of this 242-amino acid domain is revealed by its strong sequence conservation in all vertebrate orthologs of NPC1 and in related proteins from eukaryotes as remote as yeast. When isolated as a soluble, secreted protein, its affinity for 25-HC (*Kd*, 10 nM) was 13-fold higher than the affinity for [^{3}H]cholesterol (*Kd*, 130 nM). Consistent with this difference, 25-HC was an effective competitor of cholesterol binding, whereas cholesterol was a poor competitor for 25-HC binding.

In the only previous study of cholesterol binding to NPC1, a photoactivated analog of cholesterol (7,7-azocholestanol) was used (Ohgami et al., 2004). They added a radiolabeled version of this compound to intact cells and observed cross-linking to NPC1. There was a marked reduction in cross-linking when the cells expressed a loss-of-function mutant of NPC1 with a substitution in the sterol-sensing domain (P692S). Whether this crosslinking was caused by direct binding to the sterol-sensing domain, or whether this domain played a permissive role, could not be determined from these studies. The sterol specificity of the cross-linking in terms of whether or not the cholesterol interaction was competed by oxysterols was also not determined. In the current studies, we found evidence that NPC1(NTD) is the sole oxysterol binding site on NPC1, at least under the conditions of our *in vitro* assays. Thus, a point mutation in the NTD (Q79A) abolished binding of 25-HC to the soluble NPC1(NTD) (Fig. 2-3A), and it also abolished binding to full-length recombinant NPC1 (Fig. 2-4A). The situation with regard to cholesterol binding is less clear. When produced as soluble NPC1(NTD), the Q79A mutation reduced binding of [^{3}H]cholesterol by ~40% (Fig. 2-3B), yet this mutation in full-length NPC1 abolished binding of [^{3}H]cholesterol completely (Fig. 2-4B). This difference could be

attributable to the sensitivity of the cholesterol binding reaction to the presence of detergents. It is possible that the Q79A mutation impairs cholesterol binding to the extent that it becomes more sensitive to the presence of even small amounts of detergent, and that the full-length protein has more detergent bound to it than does the soluble protein. The important question of whether NPC1(NTD) is the sole cholesterol binding site on NPC1 will not be resolved until *in vitro* assays can be performed with NPC1 in a more normal environment, either *in situ* in isolated membranes or after reconstitution in liposomes. The difference in the specificity of sterol binding between NPC1 and NPC2 suggests major differences in the sterol binding pocket of the two proteins. Whereas NPC1(NTD) and NPC2 both bound [^{3}H]cholesterol with similar affinities, only NPC1 bound [^{3}H]25-HC (Fig. 2-5A). Moreover, binding of [^{3}H]cholesterol to NPC2 was inhibited by epicholesterol and cholesteryl sulfate, whereas binding to NPC1(NTD) was not inhibited. The crystal structure of cholesteryl sulfate bound to NPC2 provides an explanation for the specificity of the binding reaction of NPC2 (Xu et al., 2007). The cholesterol moiety binds with its hydrophobic side chain deeply embedded in a hydrophobic pocket that molds itself to accommodate the side chain and thus would not be expected to tolerate the presence of a polar hydroxyl, a finding consistent with our experimental data showing that 24-HC, 25-HC, and 27-HC do not bind NPC2 (Fig. 2-5E). On the other hand, the 3-hydroxyl of cholesterol is fully exposed to solvent, and therefore the binding would not be disrupted by the α-orientation of this hydroxyl in epicholesterol. The sterol binding site on NPC1(NTD) must be quite different. This site must be able to accommodate polar groups on the side chain since the addition of a 25-hydroxyl group increases the affinity of binding by 13-fold. The site must also recognize the 3-hydroxyl on the other end of the cholesterol molecule, because binding strongly prefers the β-orientation. It should be possible to define the sterol binding site crystallographically, because it

is possible to produce large amounts of soluble, secreted NPC1(NTD). The major challenge for the future is to define the functional role, if any, of the sterol binding site on NPC1(NTD). Sterol binding to this site does not seem to be important for the known function of NPC1 in fibroblasts. Thus, in NPC1-deficient cells 25-HC blocks SREBP cleavage (Infante et al., 2008a), accelerates the degradation of 3-hydroxy-3-methlglutyl CoA reductase,7 and activates ACAT in a normal manner (Infante et al., 2008a; Liscum and Faust, 1987). Moreover, the Q79A mutant of NPC1, which does not bind sterols *in vitro*, nevertheless restored the ability of cholesterol-carrying β-VLDL to activate ACAT and block SREBP-2 processing in mutant CHO cells that lack NPC1 function (Fig. 2-4). It should be noted that these latter studies all involved marked overexpression of the Q79A mutant using a strong CMV promoter and thus could be obscuring a sterol-dependent regulatory role for NPC1(NTD). Future studies will need to be done in stably transfected cells expressing WT and mutant NPC1 under control of a weak promoter.

It is likely that the sterol binding site in NPC1(NTD) is essential for some function of NPC1 that is required *in vivo*, but is not reflected in cultured fibroblasts. As noted in the introduction, the lipid storage abnormalities and the functional deficits in organs of NPC1-deficient humans and animals are complex and cannot be explained solely by the single cholesterol transport defect observed in fibroblasts. *In vivo* the affected cells are primarily hepatocytes, macrophages, neurons, and glia. Major accumulations of gangliosides and other phospholipids often outweigh the accumulations of unesterified cholesterol. It seems likely that in specific cell types NPC1 performs a regulatory role involving phospholipid and glycolipid metabolism and that the sterol binding site on NPC1(NTD) may influence this role. This hypothesis is currently under exploration.

Material from Chapter 2 was originally published in the Journal of Biological Chemistry. Infante RE, Radhakrishnan A, Abi-Mosleh L, Kinch LN, Wang ML, Grishin NV, Goldstein JL, Brown MS. Purified NPC1 protein: II. Localization of sterol binding to a 240-amino acid soluble luminal loop. *J Biol Chem.* 2008 Jan 11;283(2):1064-75.

CHAPTER THREE

TRANSFER OF CHOLESTEROL BETWEEN NPC2 AND THE N-TERMINAL DOMAIN OF NPC1

SUMMARY

Egress of lipoprotein-derived cholesterol from lysosomes requires two lysosomal proteins, polytopic membrane-bound Niemann–Pick C1 (NPC1) and soluble Niemann–Pick C2 (NPC2). The reason for this dual requirement is unknown. Previously, we showed that the soluble luminal N-terminal domain (NTD) of NPC1 (amino acids 23–264) binds cholesterol. This NTD is designated NPC1(NTD). We and others showed that soluble NPC2 also binds cholesterol. Here, we establish an *in vitro* assay to measure transfer of [^{3}H]cholesterol between these two proteins and phosphatidylcholine liposomes. Whereas NPC2 rapidly donates or accepts cholesterol from liposomes, NPC1(NTD) acts much more slowly. Bidirectional transfer of cholesterol between NPC1(NTD) and liposomes is accelerated >100-fold by NPC2. A naturally occurring human mutant of NPC2 (Pro120Ser) fails to bind cholesterol and fails to stimulate cholesterol transfer from NPC1(NTD) to liposomes. NPC2 may be essential to deliver or remove cholesterol from NPC1, an interaction that links both proteins to the cholesterol egress process from lysosomes. These findings may explain how mutations in either protein can produce a similar clinical phenotype.

INTRODUCTION

Although much has been learned about the regulation of cellular cholesterol metabolism, a major question remains: How does lipoprotein-derived cholesterol transfer from its entry point in endosomes/lysosomes to the endoplasmic reticulum (ER), where it performs regulatory functions, or to the plasma membrane, where it plays a crucial structural role? A major source of cellular cholesterol comes from plasma low-density lipoproteins (LDL), which enter cells by receptor-mediated endocytosis after binding to cell-surface LDL receptors (Brown and Goldstein, 1986). After internalization in coated pits and vesicles, LDL particles are delivered to endosomes and lysosomes. On average, each LDL particle contains 1,500 molecules of cholesteryl esters. The esters are hydrolyzed in lysosomes by lysosomal acid lipase (Goldstein et al., 1975), and the resulting free cholesterol somehow leaves the lysosome and arrives at the ER, plasma membrane, and other membranes.

A major clue to the mechanism of cholesterol exit from lysosomes was supplied by discoveries in cells from patients with autosomal recessive Niemann–Pick Type C (NPC) disease (Pentchev, 1995). In affected individuals, unesterified cholesterol, sphingomyelin, and other lipids accumulate in endosomes and lysosomes of many organs, including the brain. Lysosomal cholesterol accumulation can be reproduced in patients' cells *in vitro* by incubating the cells with LDL (Li et al., 1988; Pentchev, 2004).

The defect in NPC disease has been traced to mutations in either of two genes, both of whose products are required for cholesterol export from lysosomes. One gene, *NPC1*, encodes a polytopic membrane protein of 1,278 aa that is located in membranes of late endosomes and lysosomes (Carstea et al., 1997). The second gene, *NPC2*, encodes a soluble protein of 132 aa that is concentrated in lysosomes and is also excreted in seminal fluid and milk (Naureckiene et

al., 2000). Homozygous loss-of-function mutations in either gene produce the same NPC phenotype, suggesting that both genes function in the same pathway for lysosomal cholesterol export (Pentchev, 2004).

Of the two NPC proteins, NPC2 is the more well studied. NPC2 has been shown to bind cholesterol and derivatives such as cholesterol sulfate (Friedland et al., 2003; Infante et al., 2008b; Ko et al., 2003). X-ray crystallography reveals that cholesterol sulfate binds in such a manner that the iso-octyl side chain of the sterol is deeply buried in a hydrophobic pocket and the sulfate on the 3 position of the A ring is exposed to solvent (Xu et al., 2007). Introduction of a hydrophilic moiety, such as a hydroxyl group, on the cholesterol side chain prevents binding (Infante et al., 2008b). On the other hand, changing the configuration of the 3-hydroxyl group, as with cholesterol sulfate or epicholesterol, does not reduce binding (Infante et al., 2008b). Because of its ability to bind cholesterol, NPC2 can transfer cholesterol from one liposome to another (Babalola et al., 2007). This transfer is accelerated in the presence of anionic phospholipids such as bis(monooleoylglycero)phosphate (BMP) and phosphatidyl inositol, which are found in lysosomes (Babalola et al., 2007; Cheruku et al., 2006).

Recently, the NPC1 protein has come under study as a result of its purification from rabbit liver membranes (Infante et al., 2008a). The 1,254 aa of the mature protein (after removal of its signal peptide) are organized into 13 putative membrane-spanning helices separated by 12 cytosolic or luminal loops (Davies and Ioannou, 2000). A noteworthy feature is the presence of three large luminal domains. The first luminal domain consists of the N-terminal 242 aa (residues 23–264) whose N terminus lies free in the lumen after cleavage by signal peptidase. We designate this sequence as the N-terminal domain (NTD), i.e., NPC1(NTD), which is the most highly conserved sequence in the full-length protein (Carstea et al., 1997). The second and

third luminal domains are loops that connect transmembrane helices 2/3 and 8/9, respectively. Full-length NPC1 was shown to bind cholesterol with saturation kinetics (Infante et al., 2008a), and the binding site was localized to the NPC1(NTD) (Infante et al., 2008b). NPC1(NTD) was prepared as a soluble secreted protein by transfecting cells with a cDNA encoding the signal sequence (amino acids 1–22), followed by amino acids 23–264, followed by an epitope tag (Infante et al., 2008b). In direct contrast to the findings with NPC2, sterol binding to NPC1(NTD) was not blocked by addition of hydroxyl groups to the 24, 25, or 27 positions on the iso-octyl side chain (Infante et al., 2008b). Indeed, these modifications increased the apparent affinity for the protein. On the other hand, binding was abolished when the 3-hydroxyl was switched from the β to the α orientation. These findings led to the suggestion that NPC1(NTD) binds primarily to the A ring, whereas NPC2 binds to the opposite end of the sterol, namely the iso-octyl side chain (Infante et al., 2008b).

The current study addresses the question of how NPC1(NTD) and NPC2 interact in the transfer of cholesterol. In agreement with previous findings (Babalola et al., 2007; Cheruku et al., 2006), we show that the on-rate and off-rate of cholesterol from NPC2 is rapid. In sharp contrast, the on- and off-rates of cholesterol from NPC1(NTD) are slow, even in the presence of liposomal membranes. NPC2 accelerates both the binding and release of cholesterol by NPC1(NTD). These findings suggest that NPC2 functions to transfer cholesterol to and/or from NPC1, thereby explaining the requirement for both proteins in the exit of LDL-cholesterol from lysosomes.

EXPERIMENTAL PROCEDURES

Materials – We obtained [1,2,6,7-3H]cholesterol (60 Ci/mmol) from American Radiolabeled Chemicals; anti-FLAG M2-agarose affinity beads and monoclonal anti-FLAG M2 antibody from Sigma; QuikChange II XL Site-Directed Mutagenesis kit from Stratagene; Texas red 1,2-dihexadecanoyl-*sn*-glycero-3-phosphoethanolamine from Invitrogen; egg yolk L-α-phosphatidylcholine (chicken) from Avanti Polar Lipids, Inc.; FuGENE 6 and Nonidet P-40 from Roche Applied Sciences; and Hybond-C Extra nitrocellulose filters and all chromatography products (unless otherwise stated) from GE Healthcare Biosciences.

Buffers – Buffer A contained 50 mM Tris-chloride (pH 7.4) and 150 mM NaCl. Buffer B contained 50 mM Mes-chloride (pH 5.5 or pH 6.5) and 150 mM NaCl. Buffer C contained 25 mM Tris-chloride (pH 7.5), 150 mM NaCl, and 0.01% (wt/vol) sodium azide. Buffer D contained 25mMTris-chloride (pH 7.5), 50 mM NaCl, and 0.01% sodium azide. Buffer E contained 50 mM sodium citrate (pH 4.5) and 150 mM NaCl.

Plasmid Construction – pCMV-NPC2-His-10 encodes human NPC2, followed sequentially by 10 histidines under control of the cytomegalovirus (CMV) promoter. pCMV-NPC2-FLAG encodes human NPC2, followed sequentially by the FLAG sequence DYKDDDDK. Both plasmids were constructed from pCMV-NPC2 (Origene Technologies) by site-directed mutagenesis (QuikChange II XL kit). The P120S mutant version of NPC2 was produced by site-directed mutagenesis of pCMV-NPC2-His-10. pCMV-NPC1 (1–264)-LVPRGS-His-8-FLAG encodes human NPC1(1–264), followed by sequentially a 6-amino acid thrombin cleavage site, eight histidines, and a FLAG tag under control of the CMV promoter. This plasmid was constructed from pCMV-NPC1(1–264)-His8-FLAG (Infante et al., 2008b) by site-directed mutagenesis using the 5'-oligonucleotide, 5'-CCT GCT CCC TGG ACG ATC CTT GGC TTA GTC CCC CGA GGC AGC CAT CAC CAT CAC CAT CAC CAT CAC GAC TAT

AAA- 3'; and the 3'-oligonucleotide 5'-TTT ATA GTC GTG ATG GTG ATG GTG ATG GTG ATG GCT GCC TCG GGG GAC TAA GCC AAG GAT CGT CCA GGG AGC AGG-3'. The coding region of each plasmid was sequenced to ensure integrity of the construct. When this plasmid is expressed in CHO-KI cells, the resulting protein (after signal peptide cleavage) consists of the N-terminal domain (NTD) of NPC1 (amino acids 23–264). This protein is hereafter referred to as NPC1(NTD).

Purification of Epitope-Tagged NPC2 from Medium of Transiently Transfected CHO Cells – CHO-K1 cells were set up on day 0 at 6 x 10^5 cells per 100-mm dish in medium A (1:1 mixture of Ham's F-12 medium and Dulbecco's modified Eagle's medium, 100 units/ml penicillin, and 100 µg/ml streptomycin sulfate) containing 5% (v/v) FCS, grown in monolayer at 37°C in 8–9% CO2, and transfected on day 2 with 5 µg of wild-type or mutant pCMV-NPC2-His10 or 5 µg of pCMV-NPC2-FLAG as described (Rawson et al., 1999). On day 3, the medium (7 ml per dish) was switched to medium A containing 1% (v/v) Cellgro ITS (Fisher Scientific). After 24 h, the medium was collected, and fresh medium A containing 1% ITS was added. This cycle of collection/replenishment of medium was repeated for three consecutive days. All subsequent operations were carried out at 4°C. The medium from each daily collection was centrifuged at 1,800 x *g* for 5 min, filtered through an Express Plus 0.22-µM filter apparatus (Millipore), stored at 4°C for up to 7 days, and then loaded onto a 30-ml column (Bio-Rad) filled with 20-ml slurry of Ni-NTA-agarose beads (Qiagen) for purification of wild-type or mutant versions of NPC2-His10 or a 5-ml bed of anti-FLAG M2-agarose affinity beads for purification of NPC2-FLAG. Each column was preequilibrated with 4 column volumes of buffer A. A total of 1 liter of medium was applied to each column (flow rate of ~1 ml/min over ~16 h). Each column was then washed sequentially with 5 column volumes of buffer A with 20 mM imidazole

and then with 40 mM. Bound protein was eluted with buffer A supplemented either with 250 mM imidazole for Ni-NTA-agarose beads or with 0.1 mg/ml FLAG peptide for anti-FLAG beads. Eluted fractions containing wild-type or mutant versions of NPC2-His10 or NPC2-FLAG were each concentrated to 0.5 ml in a spin concentrator using an Amicon Ultracel 10K filter device (Millipore). The concentrated material was then subjected to gel-filtration chromatography on a 24-ml Superdex-200 column preequilibrated with buffer A. Fractions containing the peak A280 activity, (between elution volume 15.5 and 18.5 ml) were pooled, and their protein content was quantified with the BCA kit (Pierce). Pooled proteins were subjected to 13% SDS-PAGE, followed by Coomassie staining to determine purity.

Stably Transfected CHO Cells Expressing NPC1(NTD) – CHO-K1 cells were grown in monolayer at 37°C in 8–9% CO2. On day 0, cells were plated at a density of 6 x 10^6 cells per 100-mm dish in medium A containing 5% FCS. On day 3, the cells were cotransfected with 0.3 µg of pcDNA3.1 and 2.0 µg of pCMV-NPC1(1–264)-LVPRGS-His8-FLAG using FuGENE 6 as described (Rawson et al., 1999). Twenty-four hours after transfection, the medium was switched to medium A containing 5% FCS and 700 µg/ml G418 to select for cells expressing the *neo*-containing plasmid. Fresh medium was added every 2–3 days until colonies formed at ~14 days. Individual colonies were isolated with cloning cylinders and subcloned by dilution plating. Expression of NPC1(NTD)-LVPRGS-His8-FLAG was assessed by immunoblot analysis. Once a stably transfected cell line was established, it was grown in roller bottles as described below.

Purification of NPC1(NTD) from Medium of Stably Transfected CHO Cells – The above stably transfected CHO cell line expressing NPC1(NTD)-LVPRGS-His8-FLAG was set up for experiments on day 0 in 850-cm^2 roller bottles (Falcon) containing 100 ml of medium A supplemented with 5% FCS and 500 µg/ml G418. The cells were cultured at 37°C at a CO_2

concentration of 8%. On day 4, the medium was switched to 100 ml of medium A containing 5% FCS and 1% ITS. After 3–4 days, the medium was collected, and fresh medium A containing 5% FCS and 1% ITS was added. This 3–4-day cycle of collecting/replenishing the medium was done over a 3-week period. After each collection, the medium was centrifuged at 2,500 rpm for 5 min at 4°C, filtered through an Express Plus 0.22-μM filter apparatus, and stored at 4°C for up to 2 weeks. All subsequent operations were carried out at 4°C. One liter of filtered medium was concentrated, exchanged into buffer C to a final volume of 150 ml by using a 10-kDa Pellicon 2 Ultrafiltration Module (Millipore), loaded onto a 10-ml Ni-NTA agarose column, and washed sequentially with 100 ml of buffer C and 100 ml of buffer C containing 25 mM imidazole. Bound protein was eluted with buffer C containing 250 mM imidazole and buffer-exchanged into buffer D by successive concentration/dilution using a 10K Amicon Ultracel Centrifugal Filter device (Millipore). The concentrated protein was loaded onto a 7-ml MonoQ column, washed with 70 ml of buffer D, and eluted by using a linear gradient from 50–500 mM NaCl. Fractions containing NPC1(NTD)-LVPRGS-His8-FLAG were concentrated and subjected to size-exclusion chromatography using a 24-ml Superdex 200 column equilibrated with buffer C. Fractions containing NPC1(NTD)-LVPRGS-His8-Flag were pooled and concentrated. In some cases, the His8 and FLAG epitope tags of the NPC1(NTD) protein were removed by incubation with 5 units of thrombin (Cat. No. T6634; Sigma) for 1 h at 25°C, followed by 11 h at 4°C. The digest was passed through a Ni-NTA column equilibrated with buffer C to separate cleaved and uncleaved forms of NPC1(NTD). The flow-through was diluted to 50 mM NaCl and purified by MonoQ and Superdex 200 chromatography as described above. The resulting purified protein is referred to as NPC1(NTD)-LVPR.

Isolation of Complexes of [^{3}H]Cholesterol-NPC1(NTD) and [^{3}H]Cholesterol-NPC2 – Each reaction contained, in a final volume of 300 µl of buffer B (pH 5.5), 500 nM [^{3}H]cholesterol (132 x 10^3 dpm/pmol; delivered in ethanol at final concentration of 3%) and one of the following NPC proteins: 30 µg of NPC2-His10, 30 µg of NPC2-FLAG, 60 µg of NPC1(NTD)-LVPRGS-His8- FLAG, or 60 µg of NPC1(NTD)-LVPR, each delivered in 3–30 µl of buffer A. The final pH of the reaction was 5.5. After incubation for 24–48 h at 4°C, the mixture was passed through a 24-ml Superdex-200 column preequilibrated with buffer B (pH 5.5). Protein-bound [^{3}H]cholesterol emerged between 15.5 and 18.5 ml for NPC2 and between 13.5 and 16.5 ml for NPC1(NTD). The respective pooled fractions were used for the [^{3}H]cholesterol transfer assays described below.

Preparation of Liposomes – Liposomes were generated by using a standard sonication procedure (Lasch, 2003). Briefly, a chloroform solution (1 ml) containing 9.8–10 mg of egg yolk L-α-phosphatidylcholine (PC) and 10 µg of Texas Red dye in the absence or presence of 0.2 mg of [^{3}H]cholesterol (930 dpm/pmol; ~4 mole%) was added to a round-bottom flask. The solvent was evaporated under a stream of nitrogen, leaving behind a thin uniform film of lipid. The flask was placed under vacuum for at least 24 h to remove any trace of organic solvent, sealed, and stored at ~20°C until use. The dry lipid film was hydrated by the addition of 2 ml of buffer A. After incubation at room temperature for 30 min, the large multilamellar vesicle suspension was disrupted with a Branson tip-sonicator until the suspension cleared. Metal particles from the sonicator tip and undisrupted lipid aggregates were removed by centrifugation at 100,000 x *g* for 30 min at 4°C. The resulting hazy supernatant, composed primarily of small unilamellar vesicles, was stored at 4°C for a maximum of 5 days before use. The concentration of liposome solutions was determined by a malachite green colorimetric assay of inorganic phosphate released from

phospholipids after acidic digestion (Li et al., 1988). The location of liposomes in column fractions during nickel agarose chromatography was tracked by measuring the fluorescence of Texas Red dye (excitation/emission wavelengths: 595/615 nm).

Immunoblot Analysis – After SDS-PAGE on 13% gels, proteins were transferred to Hybond-C Extra nitrocellulose filters. The filters were incubated at room temperature with one of the following primary antibodies: 1.0 μg/ml monoclonal anti-FLAG M2 antibody and 1:1,000 dilution of polyclonal antibodies against human NPC1(NTD)-His8-FLAG and NPC2-His-10 (see below). Bound antibodies were visualized by chemiluminescence (Super Signal Substrate; Pierce) by using a 1:5,000 dilution of donkey anti-mouse IgG (Jackson ImmunoResearch) or a 1:2,000 dilution of anti-rabbit IgG (Amersham) conjugated to horseradish peroxidase. Filters were exposed to Phoenix Blue X-Ray Film (F-BX810; Phoenix Research Products) at room temperature for 1–60 s. Polyclonal antibodies directed against recombinant human NPC1(NTD)-His8-FLAG (purified as previously described (Infante et al., 2008b)) and NPC2-His10 (purified as described above) were produced by immunizing each rabbit s.c. with 500 μg of the recombinant protein in incomplete Freud's adjuvant, followed by alternating s.c. booster injections every 2 weeks of 250 μg of the protein.

RESULTS

Purified NPC1(NTD) and NPC2 – The current studies take advantage of the fact that NPC1(NTD) as well as NPC2 are water-soluble proteins, and therefore transfer assays can be carried out in the absence or presence of very low concentrations of detergents, i.e., 0.004% NP-40. For this purpose, we isolated recombinant NPC1(NTD) and NPC2 from the culture medium of CHO cells that were transfected with plasmids encoding the proteins with or without C-terminal His or FLAG tags. After purification as described in *Methods*, NPC1(NTD) gave a single diffuse Coomassie-stained band on SDS-PAGE; while NPC2 gave multiple bands (data not shown), owing to differing degrees of N-linked glycosylation (Chikh et al., 2004; Infante et al., 2008b).

Cholesterol Binding to NPC1(NTD) and NPC2 – To measure cholesterol binding, we incubated the His-tagged proteins with [^{3}H]cholesterol at either 4°C or 37°C in the presence of 0.004% NP-40. Protein-bound [^{3}H]cholesterol was isolated by nickel chromatography and quantitated by scintillation counting (Fig. 3-1). To measure dissociation rates, we first incubated the proteins with [^{3}H]cholesterol at 4°C and then isolated the cholesterol–protein complexes by gel filtration as described in *Methods*. The proteins were then bound to nickel agarose beads, and dissociation was measured by release of [^{3}H]cholesterol into the supernatant. The rates of association and dissociation of [^{3}H]cholesterol to and from NPC1(NTD) were strongly influenced by temperature (Fig. 3-1, A and C). At 4°C, binding was extremely slow (Fig. 3-1A), and dissociation was so slow as to be unmeasurable, even after 2 h (Fig. 3-1C). Both processes were accelerated dramatically at 37°C. In comparison with NPC1(NTD), NPC2 bound and released [^{3}H]cholesterol relatively rapidly at 4°C as well as at 37°C (Fig. 3-1, B and D). To measure saturation binding at equilibrium for NPC1(NTD), we carried out incubations for 45

min at 37°C and for 20 h at 4°C (Fig. 3-1E). The calculated *K*d for [^{3}H]cholesterol binding was 50 nM at 4°C and 90 nM at 37°C; maximal binding was slightly higher at 37°C. For NPC2, saturation binding at equilibrium was done for 45 min at both 4°C and 37°C (Fig. 3-1F). The calculated *K*d was 90 nM at 4°C and 130 nM at 37°C. The binding of [^{3}H]cholesterol to both proteins was unaffected when the pH was varied from 5.5 to 7.4 at either 4°C or 37°C (data not shown).

Cholesterol Transfer between NPC1(NTD) and NPC2 – Next, we conducted protein-to-protein cholesterol transfer assays in which [^{3}H]cholesterol was transferred from a donor NPC protein that lacks a His tag to an acceptor NPC protein that possesses a His tag. To prepare the donors, we incubated NPC1(NTD) or NPC2 with [^{3}H]cholesterol at 4°C and isolated each sterol-protein complex by gel filtration (data not shown). The transfer reactions were conducted either at 4°C or at 37°C (Fig. 3-2). After incubation, the reaction mixture was subjected to nickel agarose chromatography, and the amount of [^{3}H]cholesterol transferred to the indicated His-tagged NPC protein was measured by scintillation counting of the imidazole-eluted fraction. No donor protein was detected in the eluted fraction as determined by immunoblot analysis (data not shown). At 4°C, untagged NPC1(NTD) rapidly transferred [^{3}H]cholesterol to His-tagged NPC2 (Fig. 3-2A, filled circles). The measured values are probably an underestimate of true transfer because of the relatively long time required to process the sample, i.e., ~8–10 min. Remarkably, at 4°C, untagged NPC1(NTD) did not transfer [^{3}H]cholesterol to His-tagged NPC1(NTD) (Fig. 3-2A, open circles). On the other hand, even at 4°C, untagged NPC2 rapidly transferred [^{3}H]cholesterol to tagged versions of both NPC1(NTD) and NPC2 (Fig. 3-2B). The differences between NPC1(NTD) and NPC2 persisted when the concentrations of the acceptor protein were varied (Fig. 3-2, E and F). At 4°C, transfer of [^{3}H]cholesterol from NPC1(NTD) to NPC2

showed a maximum at pH 5.5, which reflects the pH of endosomes/lysosomes (Fig. 3-2G, filled circles). NPC1(NTD) did not transfer to itself at any pH (Fig. 3-2G, open circles). When NPC2 was the donor, the transfer rates were relatively constant over the pH range of 5.5 to 8.5 (Fig. 3-2H). At 37°C, NPC1(NTD) was able to transfer [^{3}H]cholesterol to the His-tagged version of itself (Fig. 3-2C, open circles), but even at this temperature the transfer to NPC2 was much faster (Fig. 3-2C, filled circles). Again, NPC2 transferred its [^{3}H]cholesterol rapidly either to NPC1(NTD) or NPC2 at 37°C (Fig. 3-2D).

Cholesterol Transfer from NPC Proteins to Liposomes – To measure protein-to-liposome transfer, we prepared unilamellar phosphatidylcholine (PC) liposomes by sonication as described in *Methods*. The donors were His-tagged NPC1(NTD) or NPC2 that had been complexed with [^{3}H]cholesterol and isolated by gel filtration. After incubation with liposomes, the reaction mixture was applied to a nickel agarose column. The liposomes (labeled with Texas Red dye) appeared in the flow-through fractions, whereas the His-tagged NPC proteins appeared in the imidazole-eluted fractions (data not shown). We measured the amount of [^{3}H]cholesterol transferred from donor NPC proteins to liposomes by scintillation counting of the flow-through fraction. To assure that transfer of [^{3}H]cholesterol was liposome dependent, we conducted parallel incubations in the absence of liposomes, and the amount of [^{3}H]cholesterol in the flow-through was measured. These values were subtracted from those in the liposome-containing incubations to measure liposome-dependent transfer. At 4°C, NPC1(NTD) failed to transfer [^{3}H]cholesterol to liposomes (Fig. 3-3A, open circles). Transfer to liposomes was enhanced dramatically (~100-fold) when NPC2 was included in the incubation (Fig. 3-3A, filled circles). As the temperature was increased from 4°C to 22°C to 37°C, there was a progressive increase in the ability of NPC1(NTD) to transfer [^{3}H]cholesterol to liposomes (data not shown). This rate

was enhanced dramatically when NPC2 was present (Fig. 3-3, A and C). When NPC2 was the donor, [^{3}H]cholesterol was transferred rapidly to liposomes at all temperatures, and the addition of NPC1(NTD) had no significant effect (Fig. 3-3, B and D). To confirm that the [^{3}H]cholesterol in the nickel agarose flowthrough had indeed been transferred to liposomes, we isolated the liposomes by flotation through a discontinuous sucrose gradient in an ultracentrifuge. All of the [^{3}H]cholesterol co-migrated with the Texas red dye-labeled liposomes (data not shown). Fig. 3-3E shows the transfer of [^{3}H]cholesterol from NPC1(NTD) to liposomes as a function of the concentration of liposomes. Transfer required the presence of NPC2 at all liposome concentrations, whereas transfer from NPC2 to liposomes did not require NPC1(NTD) (Fig. 3-3F). The transfer reactions showed only minor effects of pH in the range of 4.5–8.5 (Fig. 3-3, G and H).

Failure of NPC2 Mutant to Bind or Transfer Cholesterol – To confirm that the transfer activity of NPC2 required cholesterol binding, we exploited a naturally occurring missense mutation in NPC2(P120S). Homozygosity for this mutation was observed in a patient with NPC2 disease (Verot et al., 2007). Immunofluorescence of the patient's fibroblasts showed that the mutant protein reaches lysosomes, suggesting that the protein folds sufficiently to escape the quality-control system of the ER. However, the mutant protein is unable to carry out its function in facilitating cholesterol egress from lysosomes (Verot et al., 2007). To study NPC2(P120S), we prepared a cDNA encoding the mutant protein and introduced it into CHO cells by transfection. The protein was purified from the culture medium like native NPC2. SDS-PAGE, gel filtration, and circular dichroism spectroscopy (wavelength scan at 4°C) showed that the mutant protein behaved similarly to the wild type (Fig. 3-4A *Inset* and data not shown). The human P120S mutation replaces a residue that lies at the edge of the hydrophobic cholesterol-binding pocket as

indicated by the crystal structure of the bovine NPC2 (Xu et al., 2007). Indeed, as shown in Fig. 3-4A, the P120S mutant failed to bind [^{3}H]cholesterol under our assay conditions. The mutant NPC2 was also severely defective in facilitating the transfer of [^{3}H]cholesterol from NPC1(NTD) to liposomes (Fig. 3-4B). These data suggest that NPC2 must bind cholesterol to facilitate transfer of cholesterol from NPC1(NTD) to liposomes.

Cholesterol Transfer from Liposomes to NPC Proteins – Fig. 3-5 shows the results of the reciprocal assay, namely, the transfer of [^{3}H]cholesterol from PC liposomes to NPC1(NTD) or NPC2. At 4°C, there was little transfer to NPC1(NTD), and transfer was stimulated markedly by NPC2 (Fig. 3-5A). As the temperature was increased from 4°C to 22°C to 37°C, there was a progressive increase in the ability of NPC1(NTD) to accept [^{3}H]cholesterol from liposomes (data not shown). This rate was enhanced markedly at 4°C and 37°C when NPC2 was added (Fig. 3-5, A and C). Here again, NPC2 showed no requirement for NPC1(NTD). NPC2 rapidly accepted [^{3}H]cholesterol from liposomes at all temperatures, and there was no effect of adding NPC1(NTD) (Fig. 3-5, B and D). Fig. 3-5E shows the transfer of [^{3}H]cholesterol from PC liposomes to NPC1(NTD) as a function of increasing concentrations of NPC1(NTD) in the absence or presence of NPC2. As seen with the protein-to-liposome transfer, little transfer occurred unless NPC2 was present. Similarly, when the acceptor was NPC2, it alone effected transfer of [^{3}H]cholesterol from liposomes to itself, and this transfer was not influenced by NPC1(NTD) (Fig. 3-5F). Interestingly, the liposome-to-protein assay was pH dependent at 4°C. In the presence of NPC2, NPC1(NTD) accepted cholesterol optimally at pH 5.5 (Fig. 3-5G). NPC2 accepted cholesterol optimally at pH 4.5 (Fig. 3-5H).

FIGURE 3-1. Kinetics of [^{3}H]Cholesterol Binding to Purified NPC Proteins.

(A and B) Time course at different temperatures. Each reaction, in a final volume of 80 µl of buffer B (pH 6.5) with 0.004% NP-40, contained 4 pmol of NPC1(NTD)-LVPRGS-His8-FLAG (A) or 8 pmol of NPC2-His10 (B) and 100 nM [^{3}H]cholesterol (132 x 10^3 dpm/pmol). After incubation for indicated time at 4°C or 37°C, the amount of bound [^{3}H]cholesterol was measured with the Ni-NTA-agarose binding assay. Each value is the average of duplicate assays and represents total binding after subtraction of a blank value (0.01–0.02 pmol per tube). (C and D) Dissociation of previously bound [^{3}H]cholesterol from NPC proteins at different temperatures. [^{3}H]Cholesterol complexed to NPC1(NTD)-LVPRGS-His8-FLAG (C) or NPC2-His10 (D) at 4°C was isolated by gel filtration. Fractions containing NPC1 or NPC2 complexed to [^{3}H]cholesterol were pooled (3 ml), diluted 7-fold with buffer B (pH 6.5) containing 0.004% NP-40 and 10 µM unlabeled cholesterol, and incubated at 4°C or 37°C. At the indicated time, a 1-ml-aliquot of the pooled 21-ml sample was transferred to a tube containing 600 µl of Ni-NTA-agarose beads. After incubation for 3 min at 4°C, the beads were centrifuged at 600 x *g* for 1 min, after which the supernatant was assayed for radioactivity. Each value is the average of duplicate assays and represents the percentage of [^{3}H]cholesterol remaining bound to the beads relative to zero-time value. The ‘‘100% initial binding’’ values at zero time for NPC1(NTD) and NPC2 were 1.6 and 0.24 pmol per tube, respectively. (E and F) Saturation curves for equilibrium binding at different temperatures. This experiment was carried out as in *A* and *B* except that [^{3}H]cholesterol concentration varied as indicated, and incubation time at 4°C was 20 h for NPC1(NTD) and 45 min for NPC2 and at 37°C, 45 min for both proteins.

FIGURE 3-1

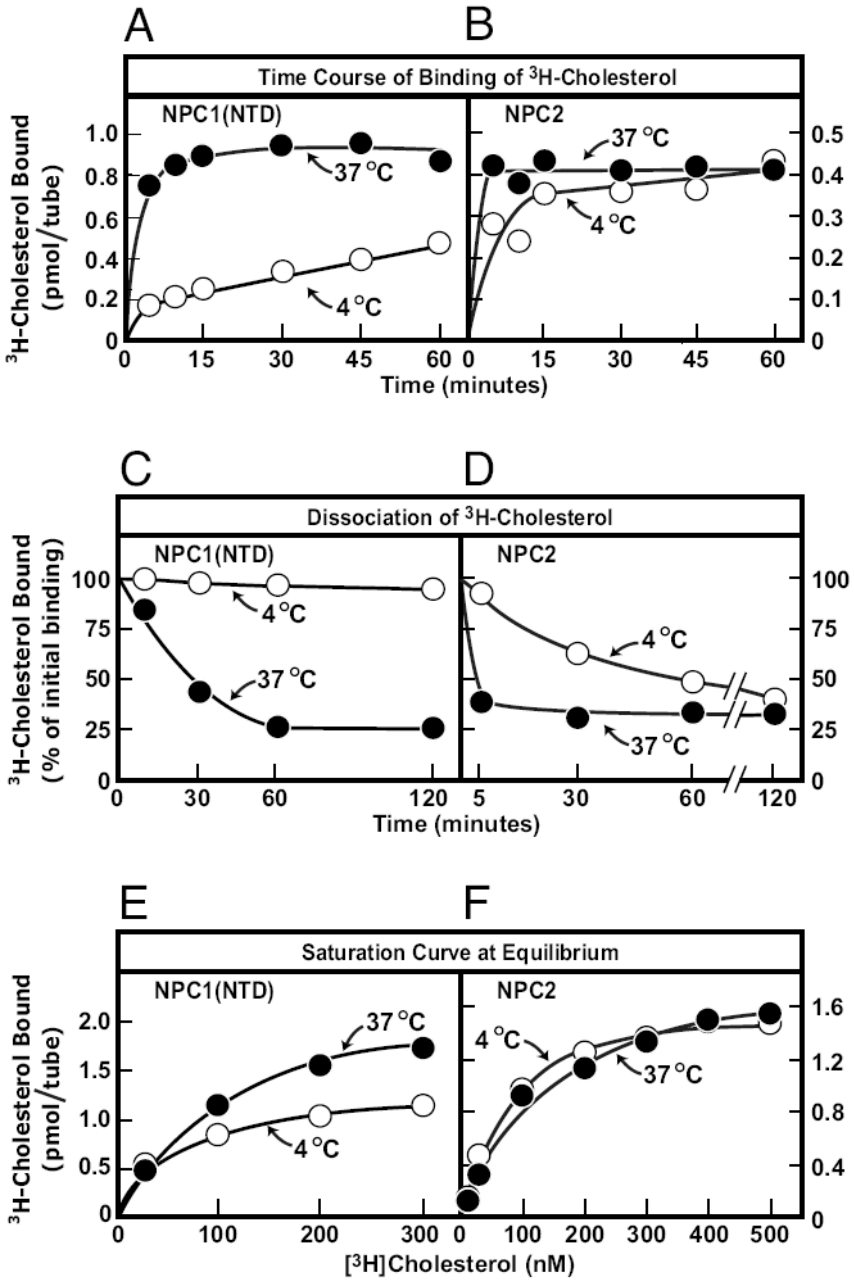
A
B
Time Course of Binding of ^{3}H-Cholesterol
NPC1(NTD)
NPC2
37 °C
4 °C
^{3}H-Cholesterol Bound (pmol/tube)
Time (minutes)
C
D
Dissociation of ^{3}H-Cholesterol
NPC1(NTD)
NPC2
4 °C
37 °C
^{3}H-Cholesterol Bound (% of initial binding)
Time (minutes)
E
F
Saturation Curve at Equilibrium
NPC1(NTD)
NPC2
37 °C
4 °C
^{3}H-Cholesterol Bound (pmol/tube)
[^{3}H]Cholesterol (nM)

FIGURE 3-2. Transfer of [^{3}H]Cholesterol from Donor NPC Protein to Acceptor NPC Protein.

Schematic diagrams of the two transfer assays are shown at the top of each column. (A–D) Time course at different temperatures. Each reaction, in a final volume of 100 µl of buffer B (pH 5.5) with 0.004% NP-40, contained ~40 pmol of NPC1(NTD)-LVPR (A and C) or NPC2-FLAG (B and D) each complexed to [^{3}H]cholesterol (1.3–1.9 pmol; 132 x 10^3 dpm/pmol) and 200 pmol of NPC1(NTD)-LVPRGS-His8-FLAG or NPC2-His10. After incubation for indicated time at 4°C (A and B) or 37°C (C and D), the amount of [^{3}H]cholesterol transferred to the indicated acceptor His-tagged NPC protein was measured with the Ni-NTA-agarose cholesterol transfer assay. Each value represents the percentage of [^{3}H]cholesterol transferred. The 100% values for transfer from donor were 1.9 pmol (A), 1.5 (B and C), and 1.3 (D). (E and F) Transfer at 4°C as a function of the amount of acceptor NPC protein. This experiment was carried out as in A–D except that the amount of acceptor NPC protein varied as indicated and time of incubation at 4°C was 30 min. The 100% values for transfer of [^{3}H]cholesterol from NPC1(NTD) and NPC2 were 2.0 and 1.2 pmol, respectively. (G and H) Transfer at 4°C as a function of pH. Each reaction in a final volume of 300 µl of buffer A, B, or E with 0.004% NP-40 at the indicated pH, contained ~30 pmol of NPC1(NTD)-LVPR (G) or NPC2-FLAG (H) each complexed to [^{3}H]cholesterol (1.6 and 1.0 pmol, respectively) and 200 pmol of either NPC1(NTD)-LVPRGS-His8-FLAG or NPC2-His10. After incubation for 30 min at 4°C, the amount of [^{3}H]cholesterol transferred to the indicated acceptor His-tagged NPC was measured as described above except samples were diluted with 1.1 ml of buffer A with 0.004% NP-40. Each value is the average of duplicate assays and represents the percentage of [^{3}H]cholesterol transferred. The 100% values for transfer from NPC1(NTD) and NPC2 were 1.6 and 1.0 pmol, respectively.

FIGURE 3-2

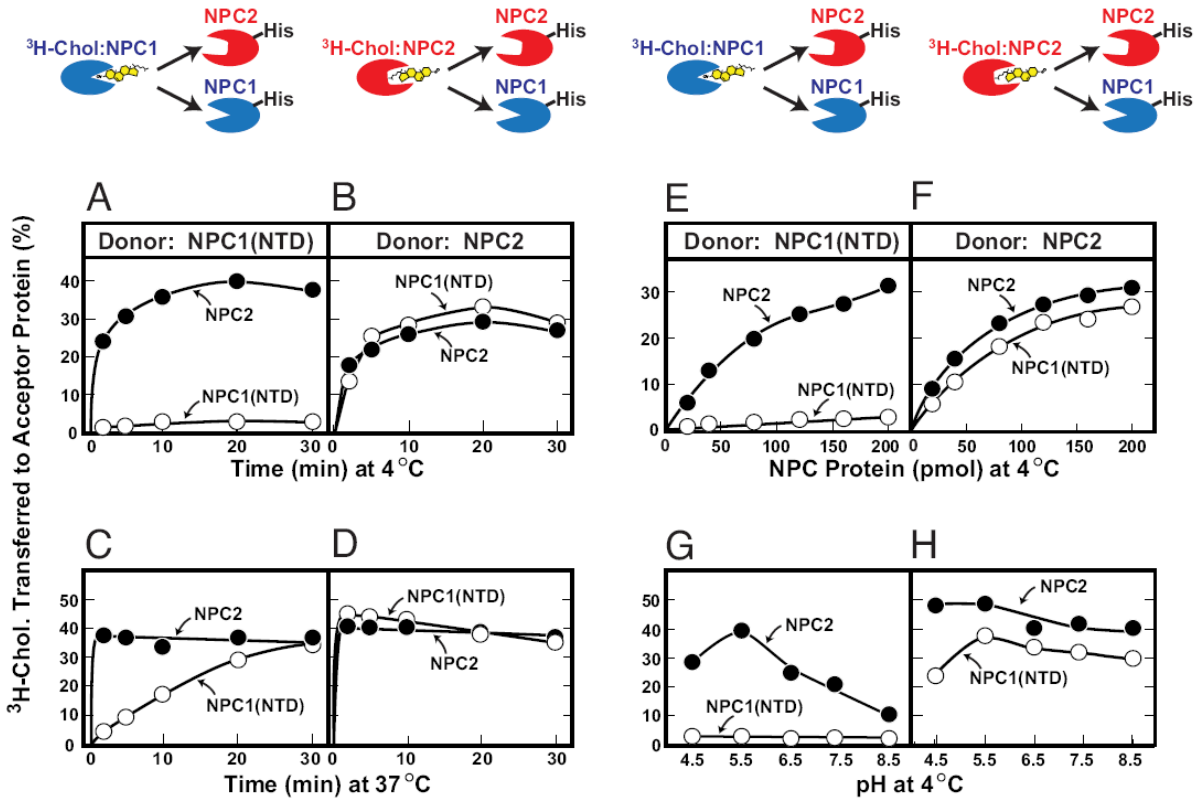
^{3}H-Chol:NPC1
NPC2 His
NPC1 His
^{3}H-Chol:NPC2
NPC2 His
NPC1 His
^{3}H-Chol:NPC1
NPC2 His
NPC1 His
^{3}H-Chol:NPC2
NPC2 His
NPC1 His
A
B
Donor: NPC1(NTD)
Donor: NPC2
NPC2
NPC1(NTD)
NPC1(NTD)
NPC2
^{3}H-Chol. Transferred to Acceptor Protein (%)
Time (min) at 4 °C
E
F
Donor: NPC1(NTD)
Donor: NPC2
NPC2
NPC1(NTD)
NPC2
NPC1(NTD)
NPC Protein (pmol) at 4 °C
C
D
NPC2
NPC1(NTD)
NPC1(NTD)
NPC2
Time (min) at 37 °C
G
H
NPC2
NPC1(NTD)
NPC2
NPC1(NTD)
pH at 4 °C

FIGURE 3-3. Transfer of [^{3}H]Cholesterol from Donor NPC Protein to Acceptor PC Liposomes.

Schematic diagrams of the two transfer assays are shown at the top of each column. (A–D) Time course at different temperatures. Each reaction, in a final volume of 200 µl of buffer B (pH 5.5), contained ~30 pmol of NPC1(NTD)-LVPRGS-His8-FLAG (A and C) or NPC2-His10 (B and D) each complexed to [^{3}H]cholesterol (1.0 and 0.3 pmol, respectively; 132 x 10^3 dpm/pmol) and 60 µg of PC liposomes labeled with Texas Red dye in the absence or presence of 100 pmol NPC2-His10 (A and C) or NPC1(NTD)-LVPRGS-His8-FLAG (B and D). After incubation for the indicated time at 4°C (A and B) or 37°C (C and D), the amount of [^{3}H]cholesterol transferred to liposomes was measured in the Ni-NTA-agarose cholesterol transfer assay. Each value is the average of duplicate assays and represents the percentage of [^{3}H]cholesterol transferred to liposomes. The 100% values for transfer from NPC1(NTD) and NPC2 were 1.0 and 0.3 pmol, respectively. Blank values in the absence of liposomes (1–4%) were subtracted. (E and F) Transfer at 4°C as a function of the amount of liposomes. This experiment was carried out as in A–D except that the amount of liposomes varied as indicated, and the time of incubation at 4°C was 30 min. The 100% values for transfer of [^{3}H]cholesterol from NPC1(NTD) and NPC2 were 0.4 and 1.7 pmol, respectively. Blank values in the absence of liposomes (2–5%) were subtracted. (G and H) Transfer at 4°C as a function of pH. The conditions for this experiment are the same as those in E and F except that the final volume of the reaction was 300 µl in buffer A, B, or E at the indicated pH, and the acceptor was 60 µg of PC liposomes in the absence or presence of 100 pmol of NPC2-His10 (G) or 100 pmol NPC1(NTD)-LVPRGS-His8-FLAG (H). The 100% values for transfer of [^{3}H]cholesterol from NPC1(NTD) and NPC2 were 0.8 and 0.5 pmol, respectively. Blank values in absence of liposomes (1–5%) were subtracted.

FIGURE 3-3

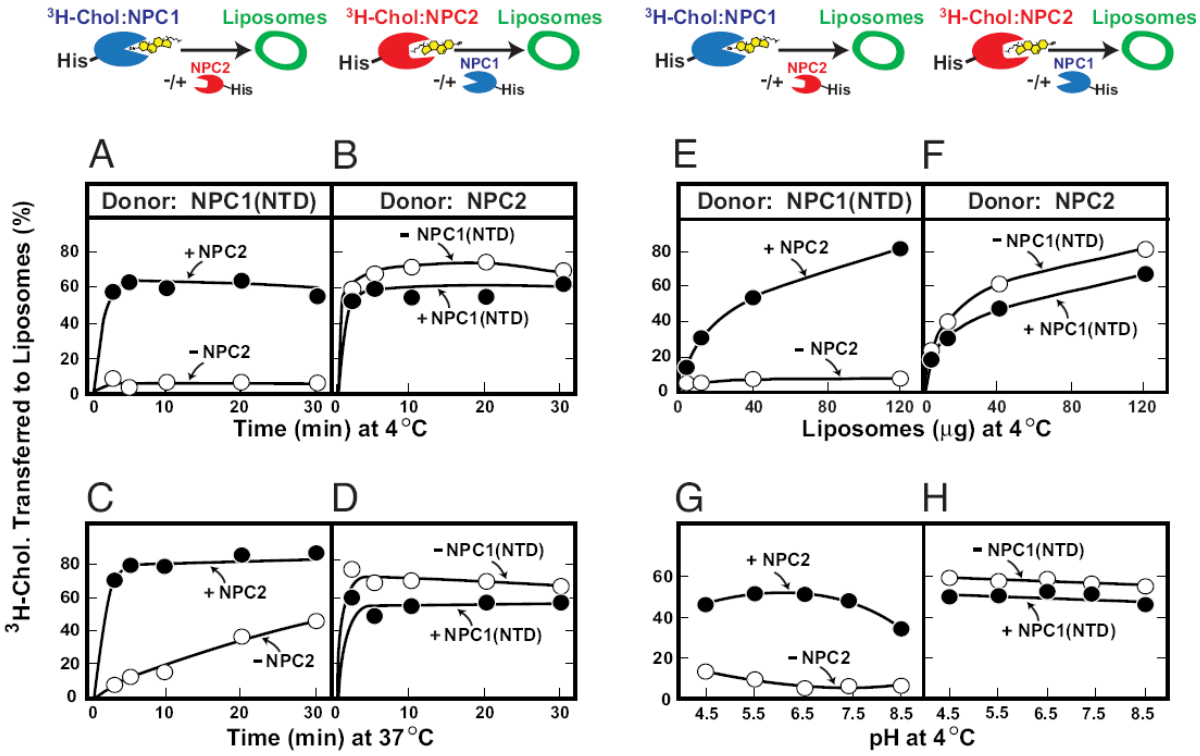
3H-Chol:NPC1
Liposomes
His
NPC2
-/+
His
3H-Chol:NPC2
Liposomes
His
NPC1
-/+
His
3H-Chol:NPC1
Liposomes
His
NPC2
-/+
His
3H-Chol:NPC2
Liposomes
His
NPC1
-/+
His
A
B
E
F
Donor: NPC1(NTD)
Donor: NPC2
Donor: NPC1(NTD)
Donor: NPC2
+ NPC2
- NPC2
- NPC1(NTD)
+ NPC1(NTD)
+ NPC2
- NPC2
- NPC1(NTD)
+ NPC1(NTD)
3H-Chol. Transferred to Liposomes (%)
Time (min) at 4 °C
Liposomes (μg) at 4 °C
C
D
G
H
+ NPC2
- NPC2
- NPC1(NTD)
+ NPC1(NTD)
+ NPC2
- NPC2
- NPC1(NTD)
+ NPC1(NTD)
Time (min) at 37 °C
pH at 4 °C

FIGURE 3-4. Mutant NPC2 Fails to Transfer [^{3}H]Cholesterol from NPC1(NTD) to Acceptor PC Liposomes.

(A) Saturation curves for equilibrium binding of [^{3}H]cholesterol for wild-type and mutant NPC2. Binding reactions were carried out as described in Fig. 3-1F except that each reaction was incubated for 2 h at 4°C and contained 8 pmol of wild-type or P120S mutant version of NPC2-His10. Each value is the average of duplicate assays and represents binding after subtraction of blank values (0.01–0.11 pmol). (*Inset*) Coomassie stain of wild-type and mutant NPC2 proteins after electrophoresis on 13% SDS-PAGE (3 μg of each protein loaded on gel). (B) Transfer of [^{3}H]cholesterol from donor NPC1(NTD) to acceptor liposomes as a function of varying concentrations of wild-type or mutant NPC2. Assays were carried out as in Fig. 3-3 except that each reaction was carried out for 10 min at 4°C and contained ~50 pmol of NPC1(NTD)-LVPRGS-His-8-FLAG complexed to [^{3}H]cholesterol (1.2 pmol; 132 x 10^3 dpm/pmol), 60 μg of PC liposomes, and the indicated concentration of wild-type or P120S mutant version of NPC2-His10. Each value is the average of duplicate assays and represents the percentage of [^{3}H]cholesterol transferred to liposomes. The 100% value for transfer from NPC1(NTD) was 1.2 pmol. Blank values in the absence of NPC2 protein (8%) were subtracted.

FIGURE 3-4

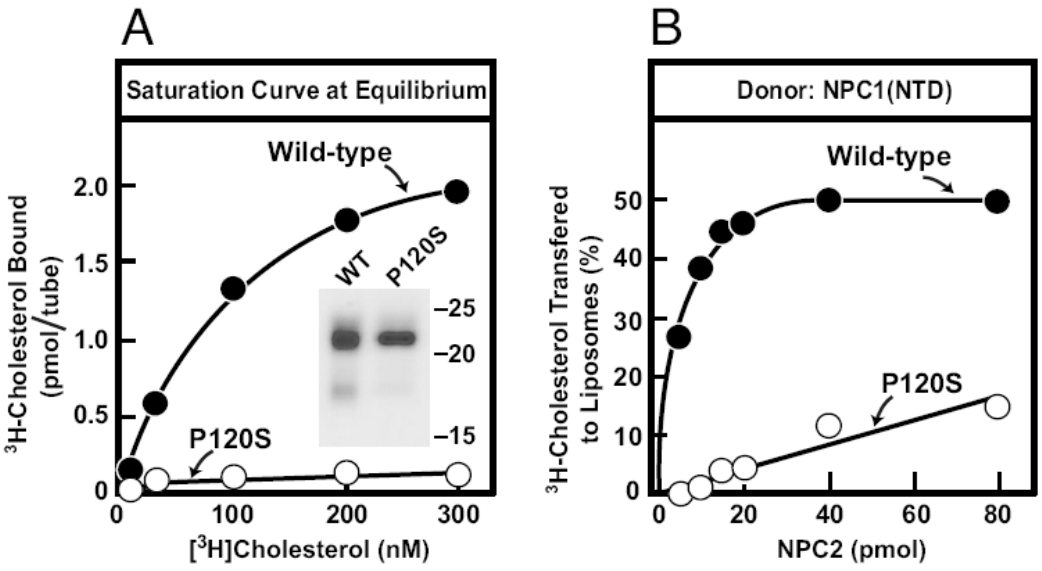
A
Saturation Curve at Equilibrium
Wild-type
P120S
WT
P120S
–25
–20
–15
^{3}H-Cholesterol Bound (pmol/tube)
2.0
1.5
1.0
0.5
0
0
100
200
300
[^{3}H]Cholesterol (nM)
B
Donor: NPC1(NTD)
Wild-type
P120S
^{3}H-Cholesterol Transfered to Liposomes (%)
50
40
30
20
10
0
0
20
40
60
80
NPC2 (pmol)

FIGURE 3-5. Transfer of [^{3}H]Cholesterol from Donor PC Liposomes to Acceptor NPC Protein.

Schematic diagrams of the two transfer assays are shown at the top of each column. (A–D) Time course at different temperatures. Each reaction, in a final volume of 200 µl of buffer B (pH 5.5), contained 17 µg of PC liposomes containing 540 pmol of [^{3}H]cholesterol (930 dpm/pmol) labeled with Texas Red dye and 100 pmol of NPC1(NTD)-LVPRGS-His8-FLAG (A and C) or NPC2-His10 (B and D) in the presence or absence of 100 pmol of either NPC2-FLAG (A and C) or NPC1(NTD)-LVPR (B and D). After incubation for the indicated time at 4°C (A and B) or 37°C (C and D), the amount of [^{3}H]cholesterol transferred to acceptor His-tagged NPC protein was measured in the Ni-NTA-agarose cholesterol transfer assay. Each value is the average of duplicate assays and represents the amount of [^{3}H]cholesterol transferred from liposomes to the indicated acceptor His-tagged NPC protein. Blank values in the absence of His-tagged NPC protein (0.2– 0.3 pmol) were subtracted. (E and F) Transfer at 4°C as a function of the concentration of NPC protein. This experiment was carried out as in A–D except that the amount of acceptor NPC1(NTD)-LVPRGS-His8-FLAG (E) or acceptor NPC2-FLAG (F) varied as indicated, and the time of incubation at 4°C was 30 min. Each value is the average of duplicate assays and represents the amount of [^{3}H]cholesterol transferred from liposomes to the indicated acceptor NPC protein. Blank values in the absence of His-tagged NPC protein (0.2–0.4pmol) were subtracted. (G and H) Transfer at 4°C as a function of pH. The conditions for this experiment are the same as those in Fig. 3-3 G and H except that the donor was 17 µg of PC:[^{3}H]cholesterol liposomes (930 dpm/fmol), and the acceptor was 100 pmol of NPC1(NTD)-LVPRGS-His8-FLAG (G) or NPC2-His10 (H) in the absence or presence of 100 pmol of either NPC2-FLAG (G) or NPC1(NTD)-LVPR (H). Each value is the average of duplicate assays and

represents the amount of [^{3}H]cholesterol transferred from liposomes to the indicated His-tagged NPC protein. Blank values in the absence of His-tagged NPC protein (0.2–0.3 pmol) were subtracted.

FIGURE 3-5

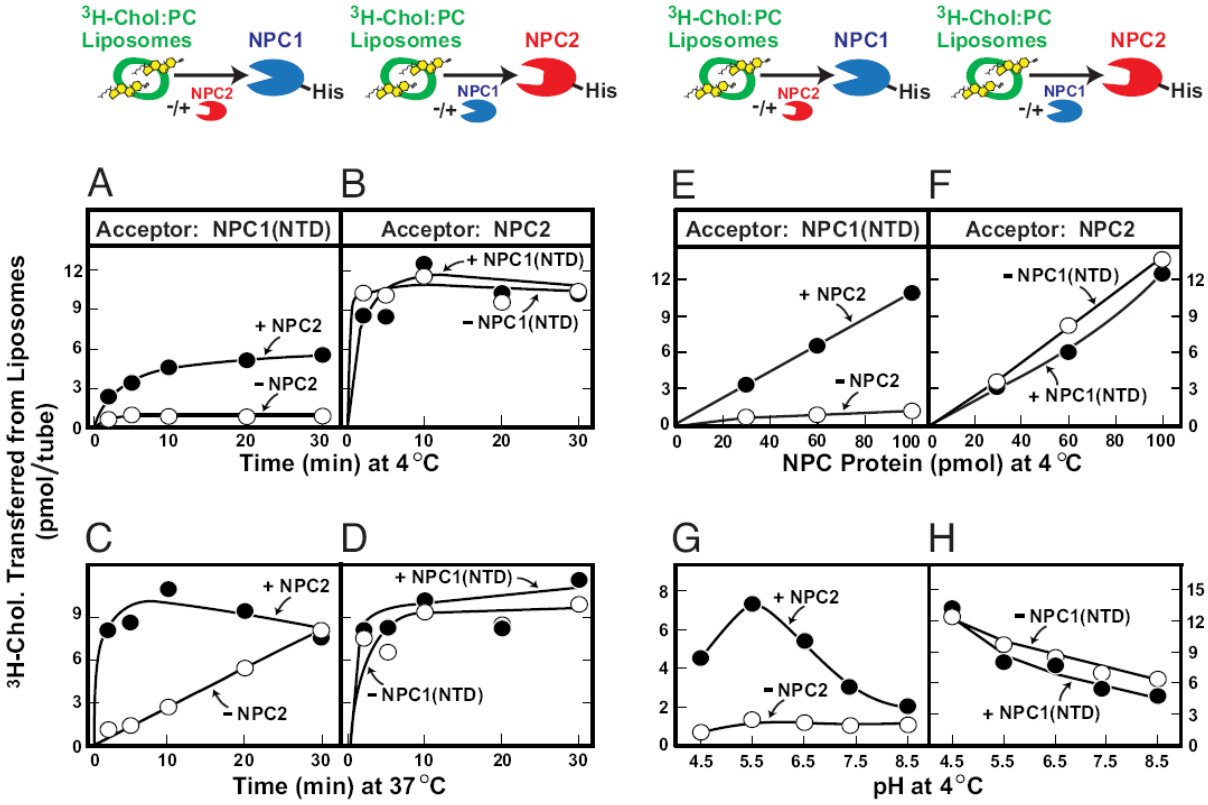

FIGURE 3-6. Alternative Models for the Transfer of Cholesterol from LDL to Lysosomal Membranes.

The interpretations of Model A and Model B are explained in *Discussion*.

FIGURE 3-6

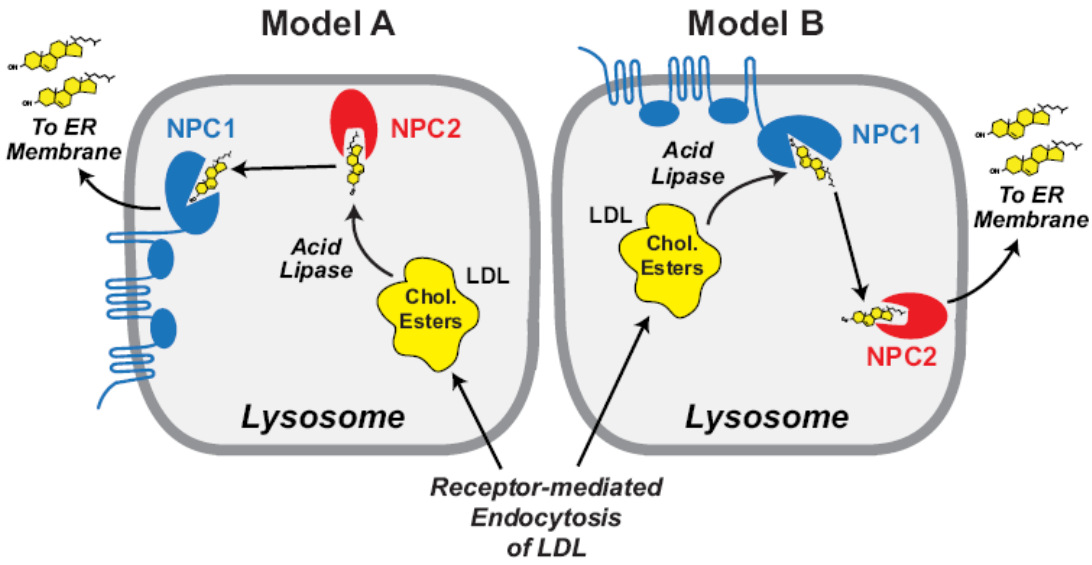

DISCUSSION

The present studies establish conditions for study of the transfer of cholesterol between the water-soluble NTD of NPC1 and water-soluble NPC2 and between both proteins and liposomes. NPC1 and NPC2 are both required in order for lipoprotein-derived cholesterol to exit from endosomes and lysosomes. Consistent with this common function, NPC2 and NPC1 can both bind cholesterol, the latter in the luminal NTD (Infante et al., 2008a; Infante et al., 2008b).

Despite these similarities, the cholesterol binding reactions exhibit major differences, as shown in Fig. 3-1. NPC2 behaves like a typical receptor. Binding is rapid and reversible at both 4°C and 37°C. NPC1(NTD) behaves quite differently. The protein binds cholesterol extremely slowly at 4°C. The rate of binding is accelerated at least 140-fold at 37°C. Once bound to NPC1(NTD), cholesterol does not dissociate from NPC1(NTD) at 4°C over at least 2 h. At 37°C the dissociation is much faster.

Because of these reciprocal changes, the equilibrium dissociation constant for NPC1(NTD) is similar at the two temperatures (50 nM and 90 nM at 4°C and 37°C, respectively). The above data suggest that the binding site on NPC1(NTD) exists in a relatively closed conformation, although less so at 37°C than at 4°C. Remarkably, this site on NPC1(NTD) can be opened by NPC2. When NPC2 is used as a donor to transfer cholesterol to NPC1(NTD), the transfer is rapid both at 4°C and 37°C (Fig. 3-2B). Indeed, NPC2 transfers cholesterol to NPC1(NTD) as rapidly as it transfers cholesterol to unoccupied NPC2 molecules. NPC2 can also rapidly remove cholesterol from NPC1(NTD) (Fig. 3-2, A and C) even under conditions where cholesterol has not dissociated from NPC1(NTD) (Fig. 3-1C). Although the physical basis for the temperature effect on NPC1(NTD) is not yet known, the ability to slow the reaction at 4°C experimentally permits detailed study of the kinetics using the relatively slow bead-trapping

assay. In the cell, NPC1 operates at 37°C where it has an intrinsic ability to bind and release cholesterol. However, even at 37°C, the binding and release reactions are markedly accelerated by NPC2, suggesting that NPC2 performs this function in the living cell. Because of its ability to open the binding site on NPC1(NTD), NPC2 facilitates the transfer of cholesterol from NPC1(NTD) to PC liposomes (Fig. 3-3) and from liposomes to NPC1(NTD) (Fig. 3-5).

Genetic evidence for this function of NPC2 was provided by the studies in Fig. 3-4 in which a naturally occurring NPC2 mutant (P120S) failed both to bind [^{3}H]cholesterol and to facilitate its transfer from NPC1(NTD) to lysosomes. The precise mechanism for the facilitated transfer reaction cannot be ascertained with the relatively slow bead-trapping assay, which requires several minutes of adherence and washing before the bound [^{3}H]cholesterol can be quantified. It seems likely that the process is catalytic, i.e., NPC2 accepts or donates a cholesterol molecule in a hit-and-run fashion.

Consistent with this hypothesis, we were unable to isolate a stable complex between untagged versions of NPC1(NTD) and NPC2 and His-tagged versions of these proteins as determined by nickel agarose chromatography (data not shown).

Within cells, cholesterol egress from lysosomes is unidirectional, i.e., from LDL to lysosomal membranes to ER. To establish this unidirectional flux, NPC1 and NPC2 could act in one of two possible orders, as illustrated in Fig. 3-6. In both models, NPC2 performs a shuttling function with respect to NPC1. In Model B, acid lipase interacts with the membranous domain of NPC1 and releases cholesterol directly to the NTD of NPC1, which then transfers it to NPC2. Given the relative simplicity of NPC2's structure, insertion of cholesterol into the lysosomal membrane, from which it travels to the ER, would likely require NPC2 to interact with a lysosomal cholesterol transporter, as yet unidentified. In Model A, acid lipase liberates

cholesterol which is then bound by NPC2 and delivered to the NTD of NPC1. NPC1 then inserts the cholesterol into lysosomal membranes, from which it is transferred to the ER. In this case, membrane insertion is likely mediated by the complex membranous domain of NPC1. The current *in vitro* data do not permit an experimental distinction between these two models. Another important unanswered question concerns the role of the lysosomal anionic phospholipids such as bis(monooleoylglycerol) phosphate and phosphatidyl-inositol that have been reported to accelerate the transfer of cholesterol from NPC2 to liposomes (Babalola et al., 2007; Cheruku et al., 2006). Do either or both of these two lipids influence the rate and/or direction of transfer between the two NPC proteins? The answers to these questions may be forthcoming now that it is possible to study the cholesterol transfer reactions with soluble forms of both NPC proteins in a test tube.

Material from Chapter 3 was originally published in the Proceedings of the National Academy of Sciences. Infante RE, Wang ML, Radhakrishnan A, Kwon HJ, Brown MS, Goldstein JL. NPC2 facilitates bidirectional transfer of cholesterol between NPC1 and lipid bilayers, a step in cholesterol egress from lysosomes. *Proc Natl Acad Sci U S A.* 2008 Oct 7;105(40):15287-92.

CHAPTER FOUR

CHOLESTEROL BINDING AND TRANSFER BY THE N-TERMINAL DOMAIN OF NPC1 IS REQUIRED FOR CHOLESTEROL EXPORT FROM LYSOSOMES IN CELLS

SUMMARY

LDL delivers cholesterol to lysosomes by receptor-mediated endocytosis. Exit of cholesterol from lysosomes requires two cholesterol-binding proteins, membrane-bound Niemann-Pick C1 (NPC1) and soluble NPC2. The cholesterol-binding site of NPC1 has been localized to a 240-amino acid N-terminal domain of NPC1, designated the NPC1(NTD). In addition to binding cholesterol, NPC1(NTD) can engage in a transfer of cholesterol with NPC2. Here we describe two mutants of NPC1(NTD): 1) a mutant that does not bind cholesterol, and 2) a mutant that binds cholesterol with similar affinity and kinetics as WT protein but cannot engage in transfer of cholesterol with NPC2. Both the binding and transfer mutant cannot restore cholesterol exit from lysosomes in NPC1-deficient cells, demonstrating the requirement of NPC1(NTD)'s abilities to bind cholesterol as well as to transfer cholesterol with NPC2 for egress of LDL-derived cholesterol from lysosomes.

INTRODUCTION

Over the last 30 years, much has been learned about the receptor-mediated endocytosis of plasma low-density lipoprotein (LDL) in coated pits and its subsequent delivery to endosomes and lysosomes (Brown and Goldstein, 1986; Roth, 2006). Each LDL particle contains ~500 molecules of free cholesterol and ~1,500 molecules of esterified cholesterol that are hydrolyzed by acid lipase in the lumen of the lysosome (Goldstein et al., 1975). The liberated cholesterol must then exit the lysosomal compartment in order to reach the plasma membrane and the endoplasmic reticulum (ER) where it performs structural and regulatory roles, respectively (Demel and De Kruyff, 1976; Goldstein et al., 2006; Simons and Ikonen, 2000). A major unanswered question is how this exit process is accomplished.

Insight into two proteins required for cholesterol exit from lysosomes comes from Niemann-Pick Type C (NPC) disease (Pentchev, 2004), a fatal hereditary disorder characterized by the accumulation of cholesterol, sphingomyelin, and other lipids in endosomes and lysosomes. Evidence indicates that the primary cause is a failure of LDL-derived cholesterol to exit the lysosomes, which secondarily causes the buildup of other lipids. Mutations in either of two genes underlie NPC disease. Both genes encode lysosomal cholesterol-binding proteins. One gene encodes NPC1, a large 1278-amino acid polytopic membrane protein that is localized to the membranes of endosomes and lysosomes (Carstea et al., 1997; Davies and Ioannou, 2000). The other gene encodes NPC2, a small soluble protein of 132 amino acids that resides in endosomes and lysosomes and is also secreted from the cell (Naureckiene et al., 2000). Homozygous mutations in either gene produce the same pattern of lysosomal lipid accumulation and the same clinical phenotype, providing strong genetic evidence that both proteins are required for cholesterol egress (Sleat et al., 2004).

NPC2 was shown previously to bind with high affinity to cholesterol, but not to cholesterol derivatives with hydrophilic substitutions on the iso-octyl side chain, such as 25-hydroxycholesterol (25-HC) and 27-HC [32, 34, 83, 84]. Xu *et al.* (2007) (Xu et al., 2007) used X-ray crystallography to reveal the structure of bovine NPC2 in complex with cholesterol sulfate, which contains a sulfate in place of the 3β-hydroxyl group. Their data explained why hydrophilic substitutions on the iso-octyl side chain prevent binding (Infante et al., 2008b). When cholesterol binds to NPC2, its iso-octyl side chain is buried deep within a hydrophobic pocket. In contrast, the 3β-hydroxyl group is exposed on the surface. This exposure explains why a sulfate substitution (as in cholesterol sulfate) or a reversal of the orientation of the hydroxyl from 3β to 3α (as in epicholesterol) does not prevent binding. On the other hand, hydrophilic additions to the side chain, as in 25-HC, prevent burial of the side chain in the deep hydrophobic pocket.

NPC1 is much more complex than NPC2. NPC1 contains 13 predicted membrane-spanning helices and 3 large luminal domains (Davies and Ioannou, 2000). The first luminal domain is designated the N-terminal domain (NTD). It consists of ~240 amino acids, which project into the lumen. This domain is hereafter designated NPC1(NTD). The other two large luminal domains are loops that span between transmembrane helices 2/3 and 8/9. We previously showed that full-length NPC1 binds [^{3}H]cholesterol with nanomolar affinity (Infante et al., 2008a). Surprisingly, the binding site is localized to the soluble NTD [34]. In sharp contrast to NPC2, NPC1(NTD) binds not only cholesterol, but also its oxygenated derivatives, 25-HC and 27-HC. On the other hand, NPC1(NTD) does not bind sterols with modifications at the 3β-hydroxyl position such as cholesterol sulfate or epicholesterol. These data led to the suggestion that NPC1(NTD) binds cholesterol in an orientation opposite to that of NPC2 with the 3β-

hydroxyl of cholesterol facing the interior of NPC1(NTD) and the iso-octyl side chain exposed (Infante et al., 2008b).

In a subsequent study, we provided evidence that cholesterol could transfer between purified NPC1(NTD) and NPC2 in a bidirectional fashion (Infante et al., 2008c). When [^{3}H]cholesterol was bound to NPC1 at 4°C, the dissociation rate into detergents was extremely slow, but the [^{3}H]cholesterol transferred rapidly to NPC2. The transfer could also proceed in the opposite direction: NPC2 transferred its bound [^{3}H]cholesterol to NPC1(NTD) two orders of magnitude faster than when [^{3}H]cholesterol was delivered to NPC1(NTD) in detergent solution (Infante et al., 2008c). NPC2 can deliver bound cholesterol directly to liposomes even in the absence of NPC1 (Babalola et al., 2007; Cheruku et al., 2006; Infante et al., 2008c; Xu et al., 2008). However, NPC1(NTD) could not deliver its bound cholesterol to liposomes unless NPC2 was present as an intermediate carrier. Although these studies showed a unique ability of NPC2 to facilitate entry and exit of cholesterol from NPC1(NTD), they did not indicate which direction this transfer took within lysosomes, i.e., LDL to NPC2 to NPC1 vs. LDL to NPC1 to NPC2. Although the NPC2-to-NPC1 model seems more logical (Infante et al., 2008c; Schulze et al., 2009; Subramanian and Balch, 2008), direct data in support of this model are lacking.

In a recent study, we used X-ray crystallography to determine a high resolution structure of NPC1(NTD) in the apoprotein (apo) form and in complex with cholesterol or 25-HC (Kwon et al., 2009). The protein contains a deep pocket that surrounds the sterol, burying the 3ß-hydroxyl group and the tetracyclic ring, but leaving the iso-octyl side chain partially exposed. This orientation is opposite to the orientation of cholesterol bound to NPC2 in which the side chain is buried and the 3ß-hydroxyl exposed (Kwon et al., 2009). In the current study, we identified two functional subdomains of NPC1(NTD) through mutational analysis – one for sterol binding and

the other for NPC2-mediated transfer. The crystal structure of NPC1(NTD) (Kwon et al., 2009) reveals that mutations that inhibit binding to cholesterol (e.g. P202A/F203A), are located deep in the binding pocket; whereas mutations in NPC1(NTD) that disrupt the transfer of cholesterol with NPC2 (e.g. L175A/L76A) are located on the surface adjacent to the opening of the sterol binding pocket (Figure 4-3B and C). When these mutations were made in the full-length protein and transfected into mutant CHO cells that lack a functional NPC1 protein, they could not rescue the NPC1 phenotype. This study provides the first evidence that NPC1's binding of cholesterol as well as transfer of cholesterol with NPC2 are required for lysosomal cholesterol export.

EXPERIMENTAL PROCEDURES

Materials - We obtained [1,2,6,7-^{3}H]cholesterol (60 Ci/mmol) and [26,27-^{3}H]25-HC (75 Ci/mmol) from American Radiolabeled Chemicals; all other sterols from Steraloids; anti-FLAG M2-Agarose affinity beads, FLAG peptide, and anti-FLAG M2 antibody from Sigma; FuGENE6 and NP-40 from Roche Applied Sciences; Ni-NTA agarose from Qiagen; egg yolk L-α-phosphatidylcholine (PC) and bis(monooleoylglycero)phosphate (BMP) from Avanti Polar Lipids; glycosidase Endo H from New England Biolabs; Hybond C Extra nitrocellulose filters and all chromatography products (unless otherwise stated) from GE Healthcare Biosciences. Reagents and lipoproteins for assays of cholesterol esterification and SREBP-2 processing were previously described (Goldstein et al., 1983; Infante et al., 2008a).

Buffers and Medium - Buffer A contained 25 mM Tris-chloride (pH 7.5), 150 mM NaCl, and 0.01% (w/v) NaN_3. Buffer B contained 25 mM Tris-chloride (pH 7.5), 50 mM NaCl, and 0.01% NaN_3. Buffer C contained 50 mM Tris-chloride (pH 7.4) and 150 mM NaCl. Buffer D contained 50 mM MES-chloride (pH 5.5) and 150 mM NaCl. Medium A contained a 1:1

mixture of Ham's F12 medium and Dulbecco's modified Eagle's medium, 100 units/ml penicillin, and 100 μg/ml streptomycin sulfate.

Plasmid Constructions - Under control of the cytomegalovirus (CMV) promoter, pCMV-NPC1-His8-FLAG encodes WT human NPC1 followed sequentially by 8 histidines and a FLAG tag (Infante et al., 2008a). pCMV-NPC1(1-264)-His8-FLAG encodes (after signal peptide cleavage) the N-terminal domain of WT human NPC1 (amino acids 23-264) followed sequentially by 8 histidines and a FLAG tag (Infante et al., 2008b). pCMV-NPC1(1-264)-LVPRGS-His8-FLAG encodes the same protein except that a thrombin cleavage site (LVPRGS) is inserted between the C-terminus of NPC1(NTD) and the His8 epitope tag (Infante et al., 2008c). pCMV-NPC2-His10 encodes (after signal peptide cleavage) WT human NPC2 (amino acids 20-151) followed sequentially by 10 histidines under the control of the CMV promoter (Infante et al., 2008c). pTK-HSV-BP2 encodes WT herpes simplex virus (HSV)-tagged human SREBP-2 under control of the thymidine kinase promoter (Hua et al., 1996a).

Under control of the Herpes Simplex virus thymidine kinase promoter, pTK-NPC1-His8-FLAG3 encodes WT human NPC1 followed sequentially by 8 histidines and 3 FLAG tags was constructed as described in (Infante et al., 2008b). The coding regions of all plasmids were sequenced to ensure the integrity of each construct.

Alanine Scan Mutagenesis of NPC1(NTD) - A panel of 84 mutant plasmids in which 1, 2, or 3 contiguous amino acids in NPC1(NTD) were changed to alanines was constructed by site-directed mutagenesis (Stratagene). To evaluate these NPC1(NTD) proteins encoded by these plasmids, we transfected the plasmids into CHO-K1 cells, after which assays for ^{3}H-sterol binding and transfer were performed on the secreted proteins.

CHO-K1 cells were grown in monolayer at 37°C in 8-9% CO_2. On day 0, cells were plated at a density of 6 x 10^6 cells per 100-mm dish in medium A containing 5% (v/v) fetal calf serum. On day 2, each dish was transfected with 5 μg pcDNA3.1 or pCMV-NPC1(1-264)-His8-FLAG (WT or mutant versions) using FuGENE 6 as previously described (Rawson et al., 1999). On day 3, each dish was washed twice with 5 ml of Dulbecco's Phosphate-Buffered Saline and then switched to 7 ml of medium A containing 1% (v/v) Cellgro ITS (Fisher Scientific). On day 6, the medium from each dish (7 ml) was collected and concentrated to 1 ml using a 30-kDa Amicon Ultracel filter module (Millipore). Aliquots of the concentrated media were used for the three assays described below. The amount of secreted NPC1(NTD) was estimated by SDS-PAGE (8%) and immunoblot analysis with monoclonal FLAG antibody as described (Infante et al., 2008c), followed by densitometric scanning of the immunoblots.

For the ^{3}H-sterol binding assays, each reaction contained, in a final volume of 160 μl, 76 μl buffer C, 80 μl of concentrated media (representing the media from 0.04-0.08 dish of transfected cells, 1.92 μg of BSA, 0.004% NP-40, and 200 nM [^{3}H]cholesterol (132 dpm/fmol) or 40 nM [^{3}H]25-HC (165 dpm/fmol). After incubation for 24 hr at 4°C, the amount of bound ^{3}H-sterol was measured with the ^{3}H-sterol binding assays (see Experimental Procedures). An aliquot of the eluate was also subjected to SDS-PAGE followed by immunoblot analysis with monoclonal FLAG antibody (see above).

For the [^{3}H]cholesterol transfer assay, aliquots of concentrated media from each transfected dish of cells were first incubated with [^{3}H]cholesterol to form a [^{3}H]cholesterol:NPC1(NTD) complex that was isolated by FLAG chromatography. Each reaction, in a final volume of 200 μl, contained 44 μl of buffer C, 150 μl of concentrated media (representing 0.15 dish of cells and containing WT or mutant NPC1(NTD)-His8-FLAG), 2.4 μg

BSA, 0.004% NP-40, and 300 nM [^{3}H]cholesterol (132 dpm/fmol). After incubation for 24 hr at 4°C, the mixture was passed through a 2-ml gravity column containing 200 μl of anti-FLAG M2-agarose beads preequilibrated with buffer C. Each column was washed first with 4 ml of buffer C containing 0.004% NP-40, then with 2 ml of buffer D, and eluted with 750 μl of buffer D containing 0.1 mg/ml of FLAG peptide. An aliquot of the eluate (0.1 ml) was subjected to scintillation counting to determine the amount of [^{3}H]cholesterol bound to each mutant protein.

The eluate from each column was then subjected to the [^{3}H]cholesterol:NPC1(NTD)-to-liposome transfer assay. Each reaction, in a final volume of 207 μl, contained 200 μl of the FLAG column eluate (in buffer D) containing the indicated version of NPC1(NTD) complexed to [^{3}H]cholesterol (264 fmol, average for WT in 3 experiments; 214 fmol, average for 71 mutants in 3 experiments; specific activity, 132 dpm/fmol) and 20 μg liposomes containing PC and BMP (9:1) in the absence or presence of 0.8 μg NPC2-His10. After incubation for 15 min at 4°C, the reaction was diluted with 800 μl of buffer C and loaded onto a Ni-NTA-agarose column as previously described (Infante et al., 2008c). The flow-through fraction, representing the amount of [^{3}H]cholesterol transferred to liposomes, was quantified by scintillation counting. Liposomes were prepared as previously described (Infante et al., 2008c) except for the addition of BMP to the PC mixture.

Purification of Epitope-Tagged NPC1(NTD) and NPC2 from Medium of Transfected CHO Cells - WT NPC1(NTD) was purified by Ni-NTA-agarose and gel filtration chromatography of the media from CHO-K1 cells stably transfected with pCMV-NPC1(1-264)-LVPRGS-His8-FLAG as previously described (Infante et al., 2008c). NPC2 and mutant versions of NPC1(NTD) were purified by Ni-NTA-agarose and gel filtration chromatography of the

media from CHO-K1 cells that had been transiently transfected with pCMV-NPC2-His10 or pCMV-NPC1(1-264)-LVPRGS-His8-FLAG as previously described (Infante et al., 2008b).

^{3}H-Sterol Binding Assays for Purified NPC1(NTD) - The assays for binding of [^{3}H]cholesterol and [^{3}H]25-HC to purified NPC1(NTD) were previously described in (Infante et al., 2008b). In brief, each reaction contained, in a final volume of 80 μl of the indicated buffer, varying concentrations of [^{3}H]cholesterol or [^{3}H]25-HC (132 and 165 dpm/fmol, respectively; delivered in ethanol), 1 μg bovine serum albumin (BSA), and varying amounts of NPC1(NTD). After incubation for 24 hr at 4°C, each assay mixture was loaded onto a 2-ml column packed with 0.3 ml of Ni-NTA-agarose beads that had been preequilibrated with buffer C containing 0.004% (w/v) NP-40 and then washed with 5 ml of buffer C with 1% NP-40. Protein-bound [^{3}H]cholesterol was eluted with 1 ml of buffer C containing 250 mM imidazole and 1% NP-40 and quantified by scintillation counting.

[^{3}H]Cholesterol Transfer Assays for Purified NPC Proteins - The transfer assays, including methods for isolation of complexes of [^{3}H]cholesterol bound to NPC1(NTD) or NPC2 and for preparation of liposomes, have been described (Infante et al., 2008c). For transfer assays of NPC1(NTD) to liposomes, incubation conditions are described in Figure 4-5E. After incubation, the 200-μl mixture was diluted with 750 μl of buffer C and loaded onto a 2-ml column packed with 0.3 ml of Ni-NTA-agarose beads preequilibrated with buffer C. Each column was washed with 1 ml of buffer C. The amount of [^{3}H]cholesterol transferred to liposomes was quantified by scintillation counting of the combined flow-through and wash fractions. For transfer assays of NPC2 to NPC1(NTD), incubation conditions are described in Figure 4-5D. After incubation, each mixture was processed as above except that the column was

washed with 3 ml of buffer C and eluted with 250 mM imidazole, after which the eluate was subjected to scintillation counting.

Assays for Cholesterol Esterification and SREBP-2 Processing in Cultured Cells - Mutant CHO 4-4-19 cells, defective in NPC1 function (Dahl et al., 1992), were transfected and tested for incorporation of [^{14}C]oleate into cholesteryl [^{14}C]oleate and proteolytic processing of SREBP-2 as described in (Infante et al., 2008a). For assays of cholesterol esterification, cells were transfected with 2 μg pcDNA3.1 or pCMV-NPC1-His$_8$-FLAG (wild-type or mutant versions). For assays of SREBP-2 processing, cells were co-transfected with 0.5 μg pcDNA3.1 or pTK-NPC1-His$_8$-FLAG$_3$ (wild-type or mutant versions) plus 3 μg pTK-HSV-BP2. Incubation conditions are described in the legend to Figure 4-5.

RESULTS

Alanine Scan Mutagenesis to Identify Residues of NPC1(NTD) Required for Sterol Binding - To determine key residues in NPC1(NTD) that are important for sterol binding, we performed an alanine scan mutagenesis across the protein (amino acids 23-264) and assayed each mutant for binding to [^{3}H]cholesterol and [^{3}H]25-HC (Figure 4-1). We generated a panel of 84 mutant plasmids in which 1, 2, or 3 contiguous amino acids were changed to alanines. This panel included all 242 residues in NPC1(NTD) except for the following: 4 conserved residues previously shown (Infante et al., 2008b) to have normal binding activity when replaced with alanine (Asn103, Gln117, Phe120, Tyr157) [34]; 1 conserved residue that when mutated to alanine (Gln79) showed reduced cholesterol binding (60% of normal) and virtually no 25-HC binding (Infante et al., 2008b); 6 naturally-occurring mutations that were shown previously to have normal binding activity (Gln92, Thr137, Pro166, Asn222, Asp242, Gly248) (Infante et al.,

2008b); 18 cysteines; and the C-terminal 32 residues (amino acids 233-264), which when deleted do not decrease binding of [^{3}H]cholesterol or [^{3}H]25-HC (data not shown).

As described in Experimental Procedures, we developed a rapid assay that allowed measurement of ^{3}H-sterol binding to aliquots of concentrated media from CHO-K1 cells that had been transfected with plasmids encoding epitope-tagged WT or mutant versions of NPC1(NTD). The amount of secreted protein was determined by immunoblotting with an antibody directed against the FLAG epitope tag. Of the 84 mutants, 5 did not produce secreted protein (Y28-E30, L80/Q81, W189/I190, M193/F194, and V208/F209). Binding assays were performed by trapping the His-tagged proteins with bound ^{3}H-sterol on nickel columns as described in Experimental Procedures. Media from cells transfected with mock vector showed no binding of [^{3}H]cholesterol or [^{3}H]25-HC (<20 fmol/tube), whereas media from cells transfected with WT NPC1(NTD) showed 860-1500 fmol/tube and 780-1000 fmol/tube for [^{3}H]cholesterol and [^{3}H]25-HC, respectively (Figure 4-1B). Six of the 84 NPC1(NTD) mutant proteins showed binding that was less than 25% of WT (Figure 4-1B, blue). All of these mutations (R39-N41, T82/L83, N106-F108, D197/N198, P202/F203, and T204/I205) replace residues that map to the binding pocket (Figure 4-3, B and C, blue). These residues include the majority of the hydrophobic amino acids that line the binding pocket around the tetracyclic ring except for Trp27, whose replacement reduced [^{3}H]cholesterol binding to a level slightly above the 25% threshold (Figure 4-1B). Of the two hydrophilic residues that form direct hydrogen bonds with the 3β-hydroxy group, the replacement of Asn41 with alanine disrupted [^{3}H]cholesterol binding by 90% (Figure 4-1B). The other hydrophilic residue (Gln79) was previously shown to produce a 40% reduction in cholesterol binding when replaced with alanine (Infante et al., 2008b). The only amino acid in the sterol binding domain that could not be evaluated in the alanine scan was Glu30; which

forms a water-mediated bond with the 3ß-hydroxyl. This mutant protein was not secreted into the media. We identified 7 mutant NPC1(NTD) proteins that exhibited a preferential reduction of binding of [^{3}H]25-HC as compared with [^{3}H]cholesterol (Figure 4-1B, pink). All 7 of these mutations replaced amino acids that mapped either to the binding pocket (V26/W27 and G199/Q200) or to adjacent amino acids (F101/Y102, L144/Q145, Y146/Y147, T187/N188, and N195/K196) (data not shown).

To validate the major findings from the assays with unfractionated culture media, we purified the mutant protein with the least amount of cholesterol binding (P202A/F203A) and analyzed it in detail. As shown in Figures 4-4A and 4-4B, the purified protein showed no detectable binding of either [^{3}H]cholesterol or [^{3}H]25-HC.

Alanine Scan Mutagenesis to Identify Residues Required for NPC2-mediated Transfer - Previously, we showed that NPC2 catalyzes the bidirectional transfer of cholesterol between NPC1(NTD) and liposomes *in vitro* (Infante et al., 2008c). To test the amino acids in NPC1(NTD) that are important for this action, we performed a transfer assay with all of the alanine scan mutants except for the 8 mutants whose [^{3}H]cholesterol binding activity was less than 50% of the WT. For this assay, we prepared stable complexes of [^{3}H]cholesterol:NPC1(NTD) and purified them by immunoaffinity chromatography as described in Experimental Procedures. We then measured the transfer of the bound [^{3}H]cholesterol to liposomes in the presence and absence of purified NPC2. In the absence of NPC2, less than 8% of bound [^{3}H]cholesterol from WT NPC1(NTD) was transferred to liposomes. In the presence of NPC2, WT NPC1(NTD) transferred an additional 54-90% of bound [^{3}H]cholesterol in 3 experiments (Figure 4-2B, shaded region) with an average of 80%. Six mutant NPC1(NTD) proteins transferred less than 25% of their bound [^{3}H]cholesterol to liposomes in an NPC2-

dependent manner (Figures 4-2B, red). These mutations replaced residues L175/L176, D180/D182, N185, T187/N188, E191/Y192, and G199/Q200, all of which map to a surface of a subdomain of NPC1(NTD) spanning amino acids 162-200. This region includes helices 7 and 8 and the intervening loop (Figure 4-3, B and C, red). Of the 6 mutants in this region, the two most deficient in transfer are L175A/L176A and E191A/Y192A. Two of these 4 WT residues (L176 and Y192) are identical in 12 out of 12 mammalian species, and the other two (L175 and E191) are identical in 11 of the 12 species (Infante et al., 2008b).

To validate the findings from the above transfer assays done with culture media, we purified one of the mutants, L175A/L176A, that showed a marked decrease in the amount of NPC2-dependent [^{3}H]cholesterol transfer from NPC1(NTD) to liposomes. When incubated with [^{3}H]cholesterol for 24 hr at 4°C, a time necessary to achieve equilibrium binding in the absence of NPC2 (Infante et al., 2008c), the mutant protein bound cholesterol with similar affinity to that of the WT protein (Figure 4-4C). Moreover, its rates of association and dissociation of [^{3}H]cholesterol at 4°C and 37°C were virtually identical to those of WT NPC1(NTD) (data not shown). Equilibrium binding for both WT and mutant proteins was achieved within 30 min at 37°C, and dissociation of previously bound [^{3}H]cholesterol for both proteins occurred rapidly at 37°C and extremely slowly at 4°C (data not shown).

Despite its normal binding kinetics, the mutant protein showed a marked defect in NPC2-stimulated transfer of cholesterol to liposomes (Figure 4-4E). As compared to WT NPC1(NTD), the mutant protein required 5 times more NPC2 to transfer an equivalent amount of [^{3}H]cholesterol to liposomes. To show that this transfer defect is the result of defective interaction with NPC2 and not with liposomes, we tested the ability of NPC2 to transfer its

cholesterol to WT NPC1(NTD) and to this mutant. Within 15 min, NPC2 transferred 4-fold more [^{3}H]cholesterol to WT NPC1(NTD) as compared to the L175A/L176A mutant (Figure 4-4D).

Cholesterol Binding and Transfer Mutants Fail to Restore Function to NPC1-deficient Cells - To assay the function of mutant NPC1 proteins, we measured the two reactions that occur when cholesterol or oxysterols reach the ER: 1) activation of acyl-CoA:cholesterol acyltransferase (ACAT), thereby increasing incorporation of radiolabeled fatty acids into cholesteryl esters (Liscum and Faust, 1987); and 2) inhibition of the proteolytic processing of sterol regulatory element-binding proteins (SREBPs), thereby inactivating transcription of genes for cholesterol synthesis and uptake (Brown and Goldstein, 1997; Infante et al., 2008a). Figures 4-5A and B show an experiment in which we transfected plasmids encoding full-length WT and mutant NPC1 into CHO 4-4-19 cells. These cells lack NPC1 function as a result of a point mutation (G660R) in transmembrane helix 3 (Dahl et al., 1992; Infante et al., 2008b). 48 hr after transfection, the cells were incubated for 5 hr with varying concentrations of β-VLDL, a cholesterol-rich lipoprotein that binds LDL receptors and delivers cholesterol to lysosomes. (Because of its high affinity for the LDL receptor, ß-VLDL is frequently used as a ligand in cell culture studies (van Driel et al., 1987)). After incubation with ß-VLDL, the cells then received [^{14}C]oleate and the incorporation into cholesteryl [^{14}C]oleate was measured. When transfected with a control (mock) plasmid, the CHO 4-4-19 cells showed little cholesteryl [^{14}C]oleate formation. Expression of WT NPC1 allowed β-VLDL to stimulate cholesteryl oleate formation by 20-fold (Figure 4-4A). Full-length NPC1 harboring the P202A/F203A mutation in the NTD was markedly defective in restoring sensitivity to β-VLDL (Figure 4-4A, red triangles). Similar defects were seen when full-length NPC1 contained the L175A/L176A mutation (blue triangles).

None of the mutant proteins interfered with the ability of 25-HC to stimulate cholesteryl ester formation, a response that is normal in the NPC1 mutant cells (Figure 4-4B).

Immunoblotting revealed that the mutant proteins were expressed at the same level as WT (Figure 4-4A, *inset*). Both mutant and WT proteins showed a diffuse band characteristic of fully glycosylated lysosomal proteins that have left the ER (Watari et al., 1999). Moreover, treatment of the mutant proteins with the glycosidase Endo H (which removes only high mannose chains) did not alter their migration pattern on SDS-PAGE, providing further evidence that the mutant proteins had folded properly and left the ER (data not shown). In the same experiment, Endo H treatment of a control protein containing a high mannose chain (Site-1 protease) (DeBose-Boyd et al., 1999) showed the expected increase in electrophoretic mobility.

To study the inhibition of SREBP processing, we employed a standard protocol in which CHO 4-4-19 cells that are deficient in NPC1 function were deprived of sterols and then incubated with β-VLDL for 5 hr after which membrane and nuclear extracts were subjected to immunoblotting to detect the full-length precursor and the processed nuclear form of SREBP-2. Mock-transfected CHO 4-4-19 cells failed to suppress SREBP-2 cleavage when incubated with β-VLDL (Figure 4-4C; lanes 2 and 3). Suppression was restored by transfection with a plasmid encoding WT NPC1 (lanes 4-7), but not with plasmids encoding the binding-defective mutant (lanes 8-11) or transfer-defective mutant (lanes 12-15). None of these plasmids affected suppression by 25-HC, which is normal in NPC1 deficient cells (Figure 4-4D).

FIGURE 4-1. Alanine Scan of NPC1(NTD): ^{3}H-Sterol Binding Activity.

(A) Sequence of human NPC1(NTD), amino acids 22-264. Black boxes denote residues invariant in 12 vertebrate species (Infante et al., 2008b). Blue ovals denote residues that when mutated to alanine decrease binding of both [^{3}H]cholesterol and [^{3}H]25-HC by > 75%. Pink ovals denote residues that when mutated to alanine preferentially decrease by >2.5-fold the binding of [^{3}H]25-HC relative to [^{3}H]cholesterol, as determined in 2 independent experiments. (B) Alanine scan for binding activity of [^{3}H]cholesterol (top panel) and [^{3}H]25-HC (bottom panel). Each reaction, in a final volume of 160 μl, contained 76 μl buffer C, 80 μl of concentrated media (representing 0.04-0.08 dish of cells and containing the indicated WT or mutant version of NPC1(NTD)-His_8-FLAG), 1.92 μg of BSA, 0.004% NP-40, and either 200 nM [^{3}H]cholesterol (132 dpm/fmol; top panel) or 40 nM [^{3}H]25-HC (165 dpm/fmol; bottom panel). After incubation for 24 hr at 4°C, the amount of bound ^{3}H-sterol was measured as described in Experimental Procedures. Each bar is the average of duplicate assays and represents the amount of binding relative to that of WT NPC1(NTD) studied in the same experiment. All data were adjusted for variations (typically <2-fold) in the amount of secreted NPC1(NTD) protein as determined by densitometric scanning of immunoblots of the assayed protein. The data in the graph were obtained in three separate experiments. The "100% of control" values for WT NPC1(NTD) in the three experiments ranged from 0.86-1.5 pmol for [^{3}H]cholesterol and 0.78-1.0 pmol for [^{3}H]25-HC. All mutants giving transfer values of <50% were repeated with similar results. Color coding is same as in A.

FIGURE 4-1

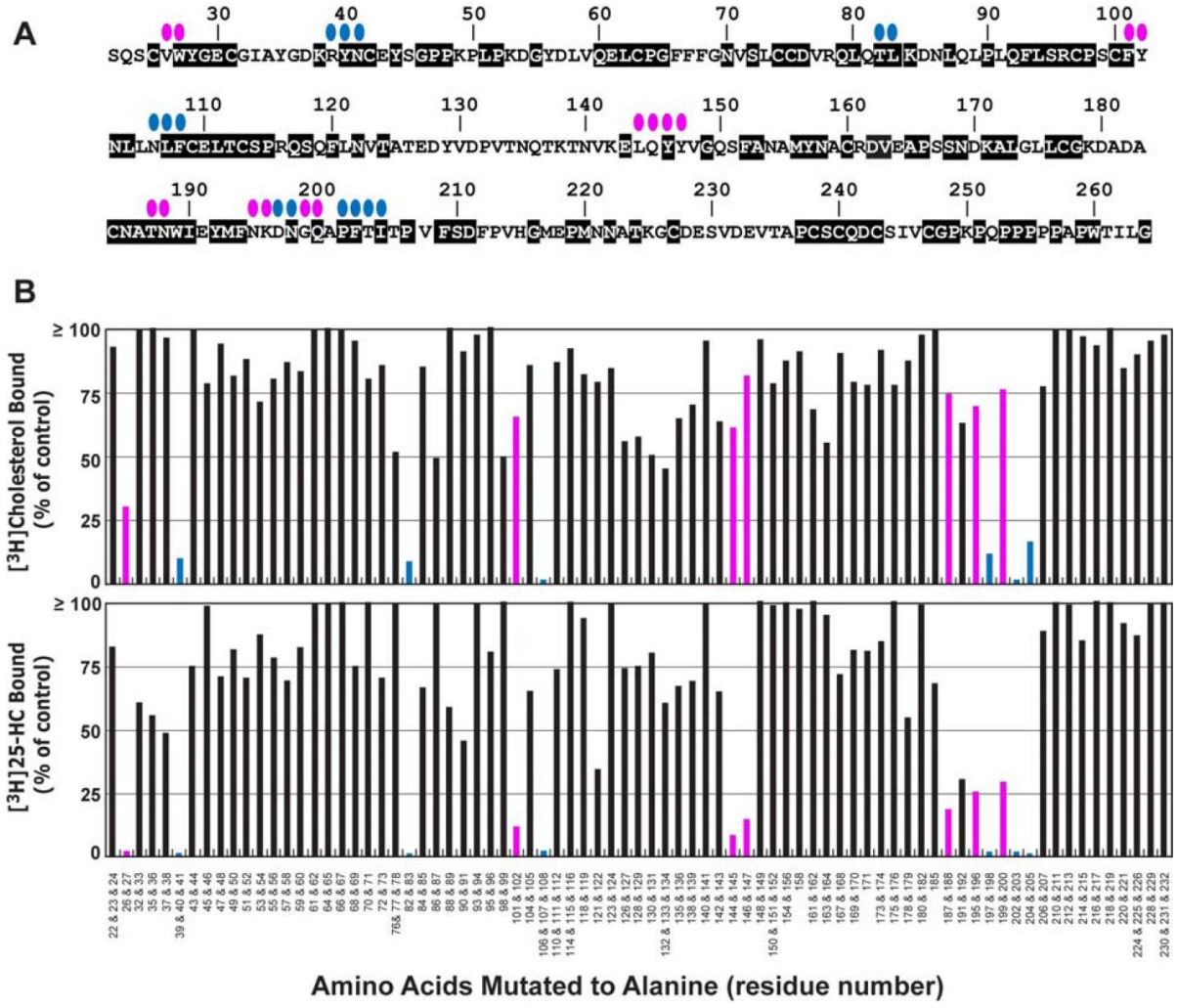
A
30
40
50
60
70
80
90
100
SQSCVWYGECGIAYGDKRYNCEYSGPPKPLPKDGYDLVQELCPGFFFGNVSLCCDVRQLQTLKDNLQLPLQFLSRCPSCFY
110
120
130
140
150
160
170
180
NLLNLFCELTCSPRQSQFLNVTATEDYVDPVTNQTKTNVKELQYYVGQSFANAMYNACRDVEAPSSNDKALGLLCGKDADA
190
200
210
220
230
240
250
260
CNATNWIEYMFNKDNGQAPFTITPVFSDFPVHGMEPMNNATKGCDESVDEVTAPCSCQDCSIVCGPKPQPPFPPAPWTILG
B
[3H]Cholesterol Bound (% of control)
[3H]25-HC Bound (% of control)
≥ 100
75
50
25
0
Amino Acids Mutated to Alanine (residue number)

FIGURE 4-2. Alanine Scan of NPC1(NTD): [^{3}H]Cholesterol Transfer Activity.

(A) Sequence of human NPC1(NTD), amino acids 22-264. Black boxes denote residues invariant in 12 vertebrate species (Infante et al., 2008b). Red ovals denote residues that when mutated to alanine decrease the amount of [^{3}H]cholesterol transferred from NPC1(NTD) to liposomes by > 70%. (B) Alanine scan for [^{3}H]cholesterol transfer from NPC1(NTD) to liposomes. WT and mutant [^{3}H]cholesterol:NPC1(NTD) complexes were isolated by FLAG chromatography as described in Experimental Procedures. Each reaction, in a final volume of 207 μl, contained 200 μl of the indicated [^{3}H]cholesterol:NPC1(NTD)-His8-FLAG complex and 20 μg PC:BMP (9:1) liposomes in the presence or absence of 0.8 μg NPC2-His10. After incubation for 15 min at 4°C, the amount of [^{3}H]cholesterol transferred to liposomes was measured as described in Supplemental Experimental Procedures. Each value represents the percentage of [^{3}H]cholesterol transferred to liposomes in the presence of NPC2 after subtraction of the percentage in the absence of NPC2. The data in the graph were obtained in 3 separate experiments. The shaded region denotes the range of WT values obtained in the 3 experiments. The entire experiment was repeated with similar results. Color coding is the same as in A.

FIGURE 4-2

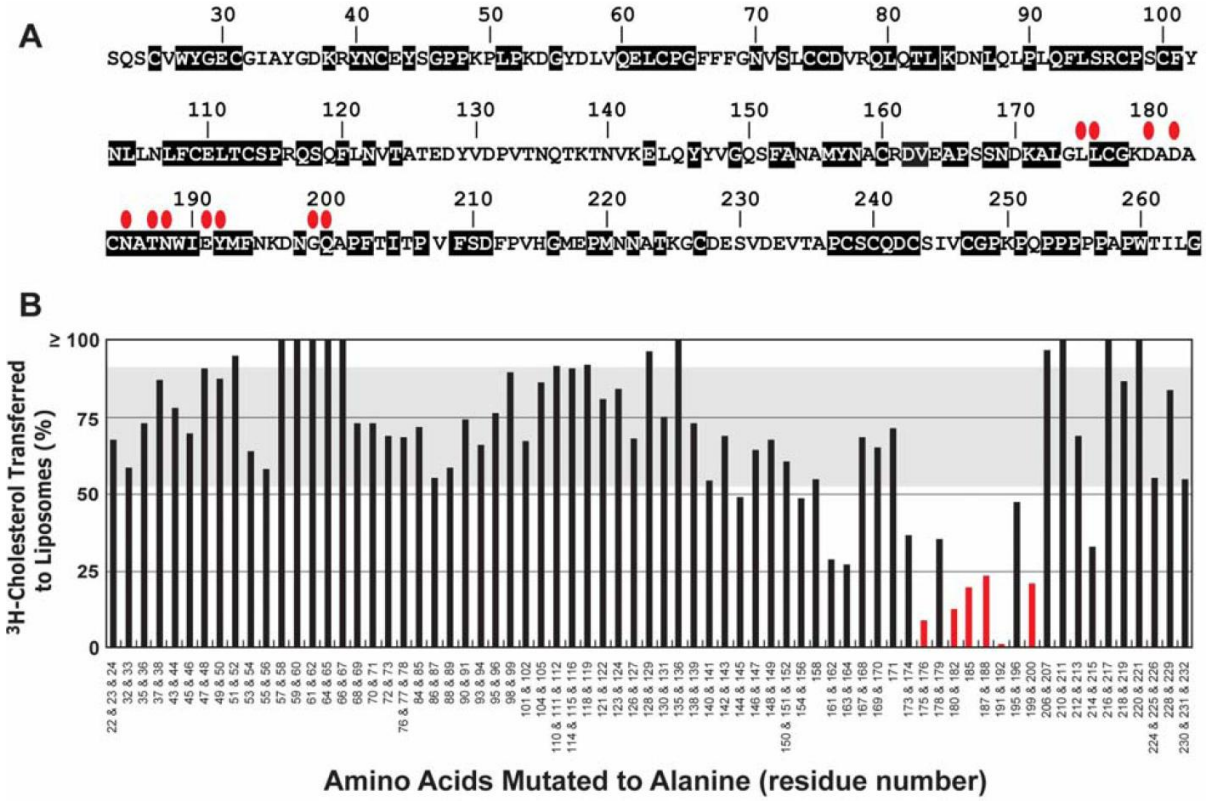
A
30 40 50 60 70 80 90 100
SQSCVWYGECGIAYGDKRYNCEYSGPPKPLPKDGYDLVQELCPGFFFGNVSLCCDVRQLQTLKDNLQLPLQFLSRCPSCFY
110 120 130 140 150 160 170 180
NLLNLFCELTCSPRQSQFLNVTATEDYVDPVTNQTKTNVKELQYYVGQSFANAMYNACRDVEAPSSNDKALGLLCGKDADA
190 200 210 220 230 240 250 260
CNATNWIEYMFNKDNGQAPFTITPVFSDFPVHGMEPMNNATKGCDESVDEVTAPCSCQDCSIVCGPKPQPPPPPAPWTILG
B
3H-Cholesterol Transferred to Liposomes (%)
≥ 100
75
50
25
0
22 & 23 & 24
32 & 33
35 & 36
37 & 38
43 & 44
45 & 46
47 & 48
49 & 50
51 & 52
53 & 54
55 & 56
57 & 58
59 & 60
61 & 62
64 & 65
66 & 67
68 & 69
70 & 71
72 & 73
76 & 77 & 78
84 & 85
86 & 87
88 & 89
90 & 91
93 & 94
95 & 96
98 & 99
101 & 102
104 & 105
110 & 111 & 112
114 & 115 & 116
118 & 119
121 & 122
123 & 124
126 & 127
128 & 129
130 & 131
135 & 136
138 & 139
140 & 141
142 & 143
144 & 145
146 & 147
148 & 149
150 & 151 & 152
154 & 156
158
161 & 162
163 & 164
167 & 168
169 & 170
171
173 & 174
175 & 176
178 & 179
180 & 182
185
187 & 188
191 & 192
195 & 196
199 & 200
206 & 207
210 & 211
212 & 213
214 & 215
216 & 217
218 & 219
220 & 221
224 & 225 & 226
228 & 229
230 & 231 & 232
Amino Acids Mutated to Alanine (residue number)

FIGURE 4-3. Location of Residues Important for Sterol Binding and Transfer in NPC1(NTD).

(A) Amino acid sequence of NPC1(NTD) with functionally important residues highlighted. Blue ovals denote residues that exhibit decreased binding of cholesterol and 25-HC by >75% when mutated to alanine. Red ovals denote residues that exhibit decreased transfer of cholesterol to liposomes by >70% when mutated to alanine. Cyan ovals denote naturally-occurring mutations in patients with NPC1 disease. Residues that line the binding pocket are shaded yellow. N-linked glycosylation sites that were eliminated are shaded green. The secondary structure of NPC1(NTD) is indicated below the sequence. (B and C) Ribbon diagram (B) and surface representation (C) of NPC1(NTD), showing the positions of functionally important residues. Bound 25-HC is shown as a stick model in green. Color coding is the same as in (A). The location of the L175, L176, P202, and F203 residues are denoted by arrows.

FIGURE 4-3

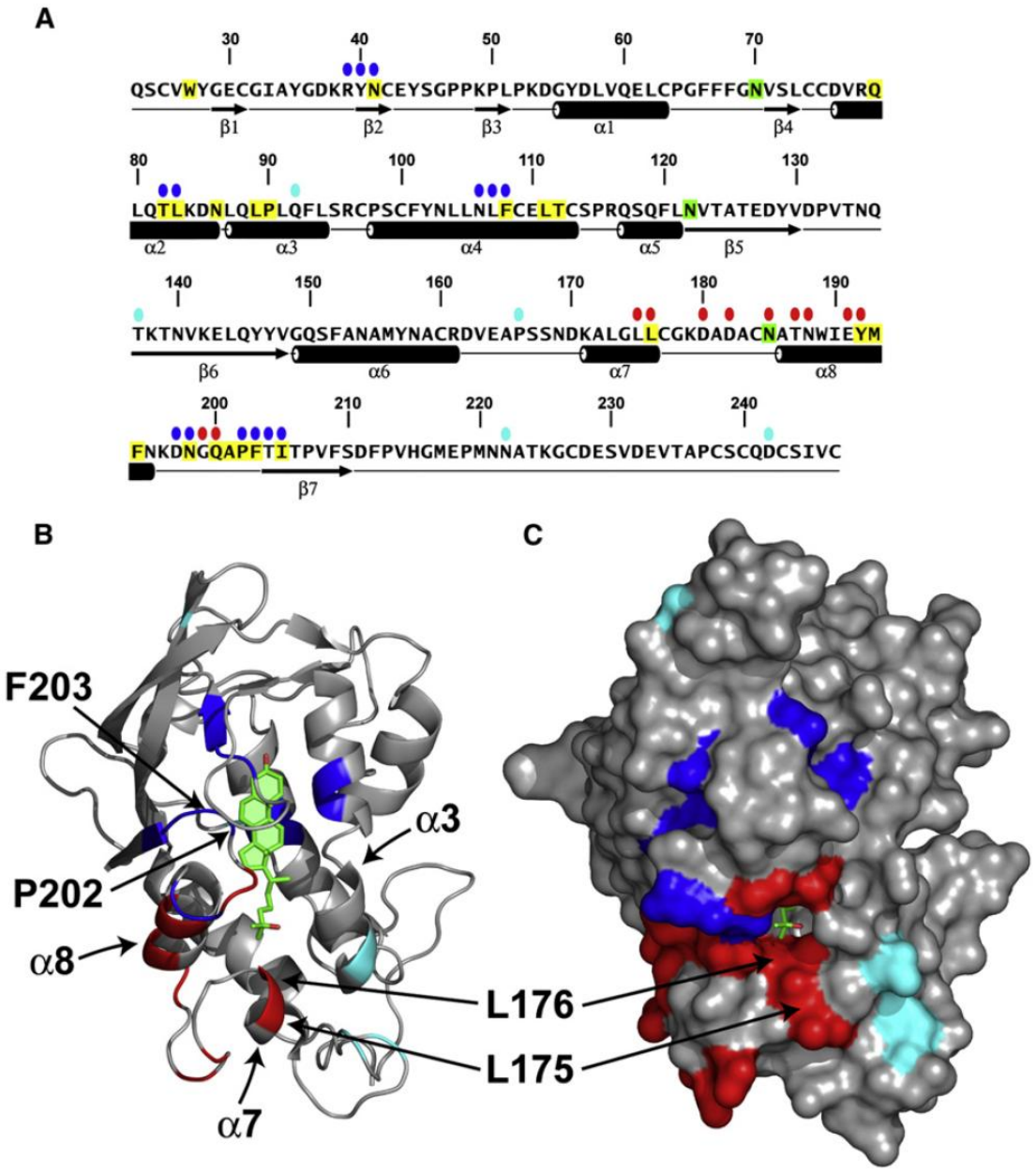

(Crystal structure in B and C from Hyock Kwon)

FIGURE 4-4. Biochemical Analysis of Sterol Binding and Transfer Mutants.

(A-C**)** ^{3}H-Sterol binding. Each reaction, in a final volume of 80 μl buffer C with 0.004% NP-40, contained 220 ng purified WT or mutant NPC1(NTD)-LVPRGS-His8-FLAG, 1 μg BSA, and indicated concentration of [^{3}H]cholesterol (132 dpm/fmol) (A,C) or [^{3}H]25-HC (165 dpm/fmol) (B). After incubation for 24 hr at 4°C, the amount of bound ^{3}H-sterol was measured as described in Supplemental Experimental Procedures. Each value is the average of duplicate assays and represents total binding after subtraction of a blank value (10-70 fmol/tube). Mean variation for each of the duplicate assays in A, B, and C were 6.1%, 5.0%, and 5.0%, respectively. (D) [^{3}H]Cholesterol transfer from NPC2 to NPC1(NTD). Each reaction, in a final volume of 200 μl buffer D (pH 5.5) without detergent, contained ~40 pmol of donor protein NPC2-FLAG complexed to [^{3}H]cholesterol (830 fmol, 132 dpm/fmol) and increasing concentrations of purified WT or mutant NPC1(NTD)-LVPRGS-His8-FLAG acceptor protein. After incubation for 15 min at 4°C, the amount of [^{3}H]cholesterol transferred to NPC1(NTD) was measured by Ni-NTA-agarose chromatography as described in the [^{3}H]cholesterol transfer assay in Experimental Procedures. Each value is the average of duplicate assays and represents percentage of [^{3}H]cholesterol transferred to NPC1(NTD). The 100% value for transfer from NPC2 was 830 fmol/tube. Mean variation for each of the duplicate assays for WT and mutant were 7.9% and 8.2%, respectively (E) [^{3}H]Cholesterol transfer from NPC1(NTD) to liposomes as a function of NPC2. Each reaction, in final a volume of 200 μl buffer D (pH 5.5) without detergent, contained ~50 pmol of WT or L175A/L176A versions of NPC1(NTD)-LVPRGS-His8-FLAG, each complexed to [^{3}H]cholesterol (950 and 660 fmol, respectively; 132 dpm/fmol); 20 μg PC liposomes labeled with Texas Red dye; and increasing concentrations of NPC2-His10. After incubation for 10 min at 4°C, the amount of [^{3}H]cholesterol transferred to

liposomes was measured in the flow-through of the nickel column as described for the [^{3}H]cholesterol transfer assay in Experimental Procedures. Each value is the average of duplicate assays and represents the percentage of [^{3}H]cholesterol transferred to liposomes. Blank values in the absence of NPC2 (5-6% transfer) were subtracted. The 100% values for transfer from WT and L175A/176A versions of NPC1(NTD) were 950 and 660 fmol/tube, respectively. Mean variation for each of the duplicate assays for WT and mutant were 8.8% and 9.3%, respectively.

FIGURE 4-4

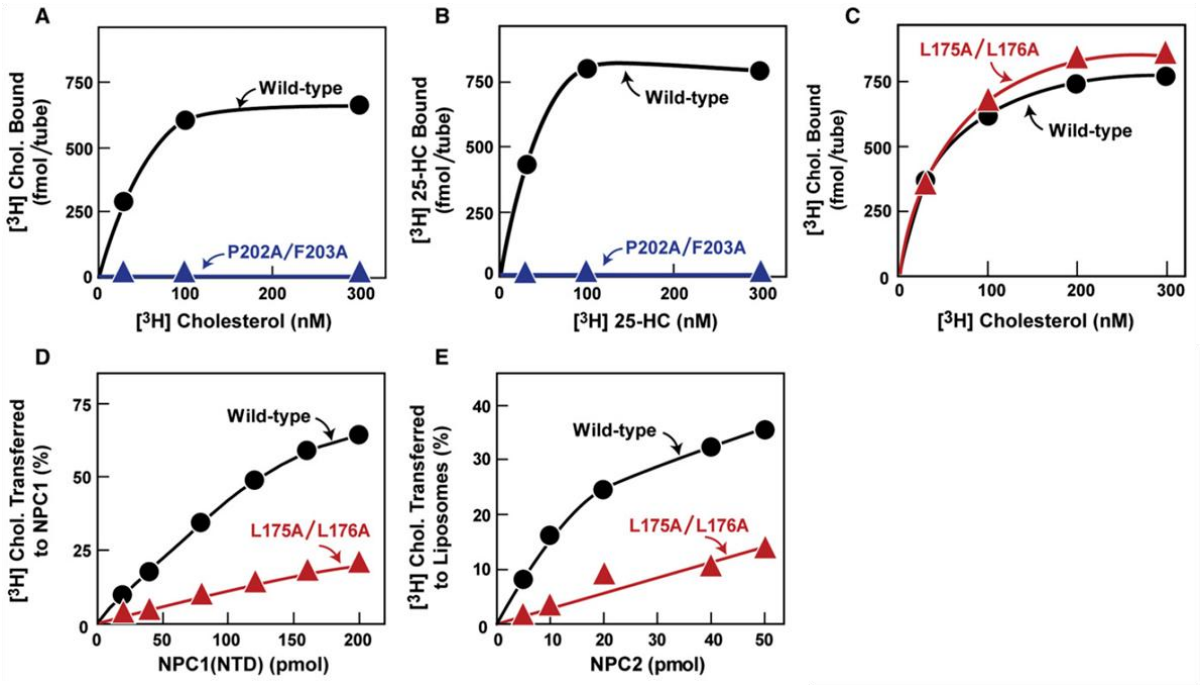

FIGURE 4-5. Functional Analysis of Sterol Binding and Transfer Mutants.

(A-D**)** Cholesterol esterification and SREBP-2 processing in mutant CHO cells lacking NPC1 function transfected with NPC1 cDNAs. Mutant CHO 4-4-19 cells were set up for experiments and transfected with 2 μg pcDNA3.1 or with WT or mutant versions of pCMV-NPC1-His_8-FLAG (A and B); or co-transfected with 0.4 μg pcDNA3.1 or with WT or mutant versions of pTK-NPC1-His8-$FLAG_3$ plus 3 μg pTK-HSV-BP2 (C and D) as described in Experimental Procedures. 24 hr after transfection, the medium was switched to medium A containing 5% newborn calf lipoprotein-deficient serum, 5 μM compactin, and 50 μM sodium mevalonate. After incubation for 24 hr, the medium was switched to the same medium containing 50 μM compactin and various concentrations of ß-VLDL (A and C) or 25-HC (B and D) as indicated. (A and B) Cholesterol esterification. After incubation for 5 hr at 37°C, each cell monolayer was pulse-labeled for 1 hr with 0.2 mM sodium [^{14}C]oleate (6301 dpm/pmol). The cells were then harvested for measurement of their content of cholesteryl [^{14}C]oleate and [^{14}C]triglycerides. Each value is the average of duplicate incubations. Mean variation for each of the duplicate incubations for WT, P202A/F203A, and L175A/L176A were 9.6%, 14.5%, and 4.3%, respectively. The rate of synthesis of [^{14}C]triglycerides for mock, NPC1 WT, NPC1(P202A/F203A), and NPC1(L175A/L176A) transfected cells incubated with 5 μg/ml ß-VLDL was 340, 396, 352, and 365 nmol/hr per mg protein, respectively. The rate of synthesis of [^{14}C]triglycerides incubated with 25-HC was 347, 496, 304, and 434 nmol/hr per mg protein, respectively. (C and D) SREBP-2 processing. After incubation for 4 hr at 37°C, cells received a direct addition of 25 μg/ml of N-acetyl-leucinal-leucinal norleucinal. After 1 hr, triplicate dishes were harvested and pooled for preparation of nuclear extracts and 100,000 g membrane fractions, which were analyzed by immunoblotting for the indicated protein. The concentrations of

antibodies were 0.2 and 4 μg/ml for SREBP-2 (anti-HSV) and NPC1 (anti-FLAG), respectively. All filters were exposed on x-ray film for 2-10 s.

FIGURE 4-5

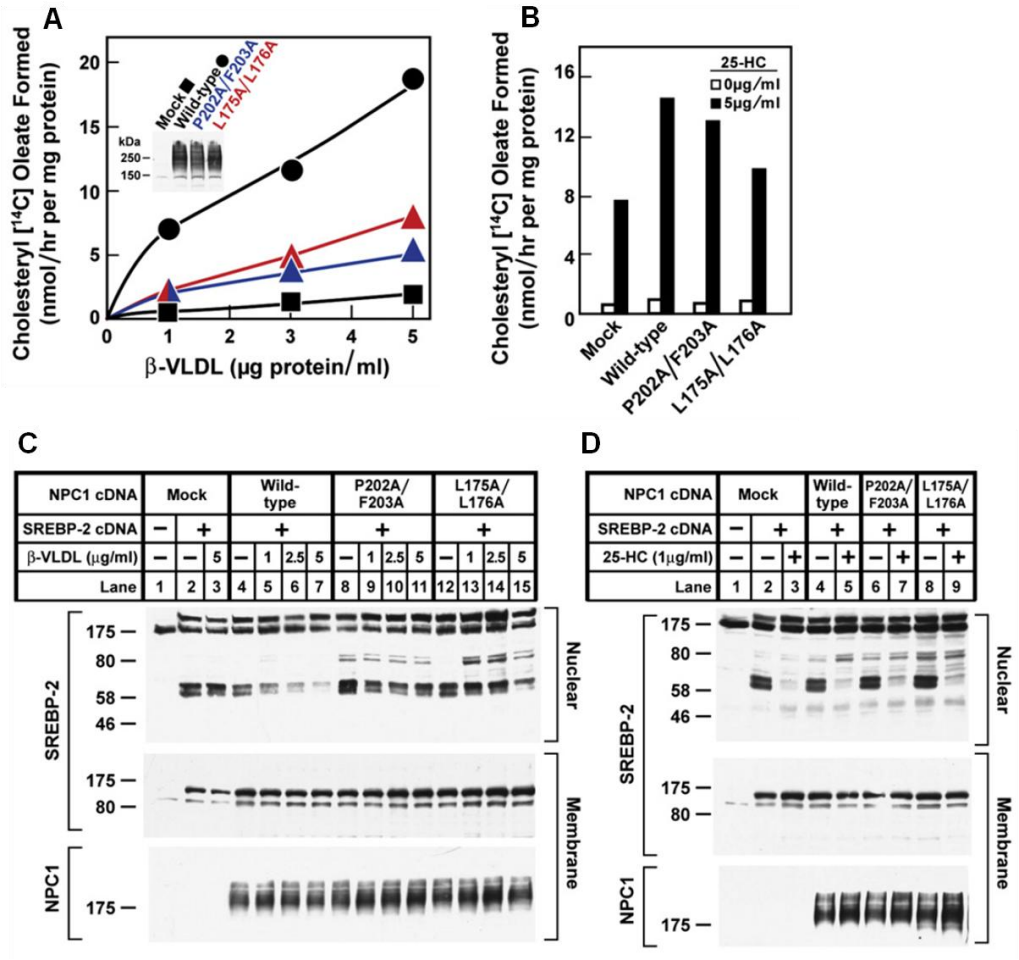

(Data for this figure from Lina Abi-Mosleh)

DISCUSSION

Egress of lipoprotein-derived cholesterol from lysosomes requires two lysosomal proteins, polytopic membrane-bound Niemann–Pick C1 (NPC1) and soluble Niemann–Pick C2 (NPC2). Both proteins bind cholesterol (Infante et al., 2008a; Xu et al., 2007), and the cholesterol binding site of NPC1 is located in its N-terminal domain (Infante et al., 2008b), designated NPC1(NTD). In addition, NPC1(NTD) can engage in a transfer of bound cholesterol with NPC2 (Infante et al., 2008c). Through mutational analysis, we identified the amino acid residues important for cholesterol binding or transfer in NPC1(NTD). At the same time, the crystallographic structure of NPC1(NTD) was solved through collaboration (Kwon et al., 2009), and allowed us to map the results of the mutagenesis study onto the structure. This led to the identification of two functional subdomains in NPC1(NTD): residues surrounding the cholesterol binding pocket form the sterol binding domain, while a patch of residues adjacent to the opening of the binding pocket on helices 7 and 8 form the transfer subdomain. The cell culture data of Figure 4-5 support the notion that both the binding of cholesterol by NPC1(NTD) and the transfer of cholesterol between NPC1 and NPC2 are required for exit of lipoprotein-derived cholesterol from lysosomes. When the P202A/F203A (binding mutant) or the L175A/L176A (transfer mutant) mutation was introduced into full-length NPC1, the protein could not restore egress of cholesterol from lysosomes to a normal degree as judged by a failure of normal cholesterol esterification (Fig. 4-5A) and suppression of SREBP-2 cleavage (Fig. 4-5C) in the presence of β-VLDL. These data provide strong support for the notion that cholesterol must be transferred between NPC2 and NPC1(NTD) in order to exit the lysosome.

This study provides the first evidence that the cholesterol binding of NPC1 is important for the transport of the lipoprotein-derived cholesterol out of lysosomes to the ER. Importantly,

it also provides the first insight into the dual requirement of NPC1 and NPC2 in the export of lipoprotein-derived cholesterol. The failure of NPC1 to transfer cholesterol with NPC2, despite the ability to bind cholesterol similarly to WT NPC1 when the sterol is delivered in solution, also resulted in the failure to export lysosomal cholesterol in cells.

Material from Chapter 4 was originally published in Cell. Kwon HJ , Abi-Mosleh L ,Wang ML, Deisenhofer J, Goldstein JL, Brown MS, Goldstein JL, Infante RE. Structure of the N-terminal domain of NPC1 suggests transfer mechanism for exit of LDL-Cholesterol from lysosomes. *Cell*. 2009 Jun 26;137(7):1213-24.

CHAPTER FIVE

CHOLESTEROL BINDING AND TRANSFER BY NPC2 IS REQUIRED FOR CHOLESTEROL EXPORT FROM LYSOSOMES IN CELLS

SUMMARY

Water-soluble Niemann-Pick C2 (NPC2) and membrane-bound NPC1 are cholesterol-binding lysosomal proteins required for export of lipoprotein-derived cholesterol from lysosomes. The binding site in NPC1 is located in its N-terminal domain (NTD), which projects into the lysosomal lumen. Here, we perform alanine-scanning mutagenesis to identify residues in NPC2 that are essential for transfer of cholesterol to NPC1(NTD). Transfer requires three residues that form a patch on the surface of NPC2. We previously identified a patch of residues on the surface of NPC1(NTD) that are required for transfer. We present a model in which these two surface patches on NPC2 and NPC1(NTD) interact, thereby opening an entry pore on NPC1(NTD) and allowing cholesterol to transfer without passing through the water phase. We refer to this transfer as a hydrophobic handoff and hypothesize that this handoff is essential for cholesterol export from lysosomes.

INTRODUCTION

Low density lipoproteins (LDL) and related plasma lipoproteins deliver cholesterol to cells by receptor-mediated endocytosis. The lipoprotein is degraded in late endosomes and lysosomes where its cholesterol is released (Brown and Goldstein, 1986). Egress of cholesterol from late endosomes and lysosomes (hereafter referred to as lysosomes) requires two proteins: Niemann-Pick C2 (NPC2), a soluble protein of 132 amino acids (Naureckiene et al., 2000); and NPC1, an intrinsic membrane protein of 1278 amino acids and 13 postulated membrane-spanning helices that span the lysosomal membrane (Carstea et al., 1997; Pentchev, 1995). Recessive loss-of-function mutations in either NPC2 or NPC1 produce NPC disease, which causes death in childhood owing to cholesterol accumulation in lysosomes of liver, brain, and lung (Pentchev, 1995).

In keeping with their cholesterol export role, NPC2 and NPC1 both bind cholesterol (Infante et al., 2008a; Xu et al., 2007). Competitive binding studies (Infante et al., 2008b) and crystal structures (Kwon et al., 2009; Xu et al., 2007) indicate that the two proteins bind cholesterol in opposite orientations. NPC2 binds the iso-octyl side chain, leaving the 3ß-hydroxyl exposed, whereas NPC1 binds the 3ß-hydroxyl, leaving the side chain partially exposed. The cholesterol binding site on NPC1 is located in the NH_2-terminal domain (NTD), which projects into the lysosomal lumen. This domain, designated NPC1(NTD), can be expressed *in vitro* as a soluble protein of 240 amino acids that retains cholesterol binding activity (Infante et al., 2008b).

An important difference between NPC2 and NPC1(NTD) lies in the kinetics of sterol binding. When incubated at 4°C, NPC2 binds and releases cholesterol rapidly (half-time < 2 min) (Infante et al., 2008c). This rapid binding allows NPC2 to transfer cholesterol from one

liposome to another (Babalola et al., 2007). In contrast, at 4°C NPC1(NTD) binds cholesterol very slowly (half-time > 2 hr) (Infante et al., 2008c). Cholesterol binding to NPC1(NTD) is accelerated by >15-fold when the sterol is first bound to NPC2 and then transferred to NPC1(NTD). Unlike NPC2, NPC1(NTD) cannot rapidly transfer its bound cholesterol to liposomes (Infante et al., 2008c). However, NPC1(NTD) can accomplish this delivery when NPC2 is present (Infante et al., 2008c). These data led us to advance a model in which NPC2 can mediate bi-directional transfer of cholesterol to or from NPC1(NTD). In cells, we envision that NPC2 accepts cholesterol in the lysosomal lumen and transports it to membrane-bound NPC1, thus accounting for the requirement for both proteins for lysosomal cholesterol export (Infante et al., 2008c; Kwon et al., 2009).

The crystallographic structure of NPC1(NTD) with bound sterol gave a clue as to the possible requirement for NPC2. In NPC1(NTD), entrance into the cholesterol binding pocket is obstructed by α-helices that must move aside to permit entry or exit, thus explaining the slow binding of cholesterol when delivered in solution (Kwon et al., 2009). We envision that NPC2 binds to NPC1(NTD), displacing the helices and allowing direct transfer of cholesterol into the binding pocket of NPC1(NTD). This direct transfer avoids the necessity for insoluble cholesterol to transit the water phase. In the current study, we test this transfer hypothesis by producing mutant forms of NPC2 and NPC1(NTD) that can bind cholesterol but cannot engage in transfer from one protein to the other. These transfer mutants map to discrete regions on the surface of the two proteins that may be sites where the two proteins interact.

EXPERIMENTAL PROCEDURES

Materials – We obtained [1,2,6,7-^{3}H]cholesterol (60 or 100 Ci/mmol) from American Radiolabeled Chemicals; anti-FLAG M2-Agarose affinity beads, FLAG peptide, and anti-FLAG M2 antibody from Sigma; Nonidet P-40 from Roche Applied Sciences; Ni-NTA-agarose beads from Qiagen; egg yolk L-α-phosphatidylcholine (PC) and Texas Red dye from Avanti Polar Lipids; Cellgro ITS (insulin, transferrin, selenium) from Mediatech, Inc.; glycosidase Endo H and PNGase F from New England Biolabs; Superdex 200 10/300 GL columns from GE Healthcare Biosciences; and Bovine Serum Albumin Standard (2 mg/ml) from Thermo Scientific. Reagents and lipoproteins for assays of cholesterol esterification were as previously described (Goldstein et al., 1983; Infante et al., 2008a).

Buffers and Media – Buffer A contained 50 mM MES (pH 5.5 or 6.5) and 150 mM NaCl. Buffer B contained 50 mM Tris-chloride (pH 7.4) and 150 mM NaCl. Buffer C contained 10 mM HEPES (pH 7.6), 1.5 mM $MgCl_2$, 10 mM KCl, 5 mM sodium EDTA, 5 mM sodium EGTA, and 250 mM sucrose. Buffer D contained 10 mM Tris-chloride (pH 6.8), 100 mM NaCl, and 0.5% (w/v) SDS. Buffer E contained 62.5 mM Tris-chloride (pH 6.8), 15% SDS, 8 M urea, 10% (v/v) glycerol, and 100 mM DTT. Medium A contained a 1:1 mixture of Ham's F12 medium and DMEM, 100 units/ml penicillin, and 100 μg/ml streptomycin sulfate. Medium B contained DMEM, 100 units/ml penicillin, and 100 μg/ml streptomycin sulfate.

Plasmid Construction – Four previously described plasmids were used in these studies. All 4 are under the control of the CMV promoter. pCMV-NPC1-His8-FLAG encodes wild type (WT) human NPC1 followed sequentially by 8 histidines and a FLAG tag (Infante et al., 2008a). pCMV-NPC1(1-264)-LVPRGS-His8-FLAG encodes the N-terminal domain of WT human NPC1 (amino acids 1-264) followed sequentially by a thrombin cleavage site (LVPRGS), 8

histidines, and a FLAG tag (Infante et al., 2008c). pCMV-NPC2-His10 encodes WT human NPC2 (amino acids 1-151) followed sequentially by 10 histidines (Infante et al., 2008b). pCMV-NPC2-FLAG encodes WT human NPC2 (amino acids 1-151) followed sequentially by a FLAG tag (Infante et al., 2008c).

Mutations in the above plasmid constructs were generated by site-directed mutagenesis (Stratagene QuikChange kit). The coding regions of all plasmids were sequenced to ensure integrity of each construct.

Purification of Epitope-Tagged NPC1(NTD) and NPC2 from Medium of Transfected CHO Cells – NPC proteins were purified from the media of stably or transiently transfected CHO-K1 cells (Infante et al., 2008c). NPC proteins containing a histidine tag (with or without a FLAG tag) were purified by Ni-NTA-agarose and gel filtration chromatography; NPC proteins with only a FLAG tag were purified by anti-FLAG M2 agarose and gel filtration chromatography. Plasmids used in the stably transfected cells were WT versions of pCMV-NPC1(1-264)-LVPRGS-His8-FLAG and pCMV-NPC2-FLAG. Plasmids used for transient transfections were mutant versions of pCMV-NPC1(1-264)-LVPRGS-His8-FLAG, mutant versions of pCMV-NPC2-FLAG, and WT and mutant versions of pCMV-NPC2-His10. The concentration of purified protein was determined with the BCA assay (Smith et al., 1985).

[^{3}H]Cholesterol Binding Assay – This assay was previously described (Infante et al., 2008b). Incubation conditions are detailed in figure legends. After incubation for the indicated time at 4°C, each reaction was diluted 5-fold with ice-cold buffer B containing 0.004% (v/v) NP-40, loaded onto a 2-ml Bio-Spin column (Bio-Rad) packed with 0.3 ml of Ni-NTA-agarose beads that had been preequilibrated with buffer B containing 0.004% NP-40. The beads were washed with either 5 ml buffer B with 1% NP-40 for NPC1(NTD) or 6 ml buffer B with 0.004% NP-40

for NPC2. Protein-bound [^{3}H]cholesterol was eluted with 1 ml buffer B containing 250 mM imidazole and 1 or 0.5% NP-40 for NPC1(NTD) and NPC2, respectively, and quantified by scintillation counting.

Preparation of Complexes of [^{3}H]Cholesterol:NPC1(NTD) and [^{3}H]Cholesterol:NPC2 – To prepare material for the [^{3}H]cholesterol dissociation assays, we incubated 500 nM [^{3}H]cholesterol (132 x 10^3 dpm/pmol) and 30 μg NPC2-His10 in a final volume of 300 μl of buffer A (pH 5.5). To prepare material for the [^{3}H]cholesterol transfer assays, we incubated 500 nM [^{3}H]cholesterol (132 x 10^3 or 222 x 10^3 dpm/pmol) in a final volume of 500 μl buffer A (pH 5.5) with one of the following proteins: 20 μg NPC2-His10, 30 μg NPC2-FLAG, or 100 μg NPC1(NTD)-LVPRGS-His8-FLAG. After incubation for 10 min at 37°C and then 30 min at 4°C, the solution was passed at 4°C through a 24-ml Superdex-200 column that had been preequilibrated with buffer A (pH 5.5). Protein-bound [^{3}H]cholesterol emerged between 15.5 and 18.5 ml for NPC2 and between 13.5 and 16.5 ml for NPC1(NTD). The respective pooled fractions were used for the [^{3}H]cholesterol dissociation and transfer assays described below.

[^{3}H]Cholesterol Dissociation Assay – [^{3}H]Cholesterol:NPC2-His10 was isolated at 4°C (3 ml), diluted 9-fold with ice-cold buffer A (pH 6.5) containing 0.004% NP-40 and 11.25 μM unlabeled cholesterol and then incubated at 4 or 37°C. At the indicated time, a 1-ml aliquot of the pooled 27-ml sample was transferred to a tube containing 600 μl of Ni-NTA-agarose beads. After incubation for 3 min at 4°C, the beads were centrifuged at 800 x *g* for 1 min at room temperature, after which the supernatant was assayed for radioactivity.

[^{3}H]Cholesterol Transfer Assays – Three types of transfer assays were performed. Incubation conditions for the assays are detailed in figure legends. Assay A involves the transfer of [^{3}H]cholesterol from donor NPC2-FLAG to acceptor NPC1(NTD)-LVPRGS-His8-FLAG.

After incubation for 10 min at 4°C, each 100 μl reaction mixture was diluted with 500 μl of ice-cold buffer B and loaded onto a 2-ml column packed with 0.3 ml Ni-NTA-agarose beads that had been preequilibrated with buffer B. Each column was washed with 3 ml buffer B, after which NPC1(NTD)-LVPRGS-His8-FLAG was eluted with 1 ml buffer B containing 250 mM imidazole. The amount of [^{3}H]cholesterol transferred to NPC1(NTD)-LVPRGS-His8-FLAG was quantified by scintillation counting of the eluate.

Assay B involves the transfer of [^{3}H]cholesterol from donor NPC2-His10 to acceptor NPC1(NTD)-LVPRGS-His8-FLAG. After incubation for 10 min at 4°C, each 200-μl reaction mixture was diluted with 500 μl of ice-cold buffer B and loaded onto a 2-ml column packed with 0.2 ml of anti-FLAG M2-agarose beads that had been preequilibrated with buffer B. Each column was washed with 3 ml buffer B, after which NPC1(NTD)-LVPRGS-His8-FLAG was eluted with 1 ml buffer B containing 0.1 mg/ml FLAG peptide. The amount of [^{3}H]cholesterol transferred to NPC1(NTD)-LVPRGS-His8-FLAG was quantified by scintillation counting of the eluate.

Assay C involves the transfer of [^{3}H]cholesterol from donor NPC1(NTD) to acceptor PC liposomes. PC liposomes labeled with Texas Red dye were prepared as described (Infante et al., 2008c). After incubation for 10 min at 4°C, each reaction was diluted with 750 μl ice-cold buffer B, loaded onto a 2-ml column packed with 0.3 ml Ni-NTA-agarose beads that had been preequilibrated with buffer B, and then washed with 1 ml buffer B. The amount of [^{3}H]cholesterol transferred to liposomes was quantified by scintillation counting of the flow-through plus 1 ml buffer B wash.

Alanine Scan Mutagenesis of NPC2 – We prepared 57 plasmids encoding mutant forms of NPC2 in which 1, 2, or 3 sequential amino acids were changed to alanine by site-directed

mutagenesis (Stratagene QuikChange kit). (Amino acid residues are numbered starting at the initiator methionine, which is designated no. 1.) To evaluate the NPC2 proteins encoded by these plasmids, the plasmids were transfected into CHO-K1 cells, after which assays for [^{3}H]cholesterol binding and transfer were performed with the secreted proteins. CHO-K1 cells were grown in monolayer at 37°C in 8-9% CO_2. On day 0, cells were plated at a density of 6 x 10^6 cells per 100-mm dish in medium A containing 5% (v/v) FCS. On day 2, dishes were transfected with 5 μg pcDNA3.1 or pCMV-NPC2-His10 (WT or mutant versions) as described (Rawson et al., 1999). On day 3, each dish was washed once with 10 ml Dulbecco's PBS and then switched to 7 ml medium A containing 1% (v/v) ITS. On day 6, the media from 5 dishes (35 ml) was collected and concentrated to 0.5 ml using a 10-kDa Amicon Ultra-15 Centrifugal Filter Unit (Millipore). The amount of secreted NPC2 in the concentrated media was estimated by densitometric scanning of immunoblots with anti-NPC2 antibody. Aliquots of the concentrated media containing either WT or mutant version of NPC2-His10 were used for the [^{3}H]cholesterol binding and transfer assays.

Cholesterol Esterification Assay in Intact Cells – Cholesterol esterification assays were done with human fibroblasts as described (Goldstein et al., 1983). On day 0, control and NPC2-deficient fibroblasts (GM 18455; compound heterozygote with mutant alleles E20X and C47F; obtained from Coriell Institute for Medical Research) were set up in medium B containing 10% FCS at 25 x 10^3 and 100 x 10^3 cells/60-mm dish, respectively, and grown in monolayer at 37°C in 5% CO_2. On day 3, cells were refed with the same medium. On day 5, cells were washed once with PBS and switched to medium B containing 10% human lipoprotein-deficient serum and 1% ITS. On day 7, cells were used for experiments. After incubation for 5 hr at 37°C with various additions as described in figure legends, each cell monolayer was pulse-labeled for 1 hr

with 0.2 mM sodium [^{14}C]oleate. The rate of incorporation of [^{14}C]oleate into cholesteryl [^{14}C]oleate and [^{14}C]triglycerides by intact cell monolayers was measured as described (Goldstein et al., 1983; Kwon et al., 2009).

Cholesterol esterification assays were also done in mutant CHO 4-4-19 cells defective in NPC1 function (Dahl et al., 1992). Cells were set up for experiments at 400 x 10^3 cells/60-mm dish in medium A with 5% FCS, transfected with 2-2.5 μg of the indicated plasmid on day 1 as described (Infante et al., 2008b), and incubated with various additions as described in figure legends, after which the incorporation of [^{14}C]oleate into cellular cholesteryl [^{14}C]oleate and [^{14}C]triglycerides was determined.

Glycosidase Treatment – 48 hr after transfection, NPC1 deficient CHO 4-4-19 cells were harvested, washed with PBS, and lysed in 200 μl buffer C containing 5 μg/ml pepstatin, 10 μg/ml leupeptin, and 1.9 μg/ml aprotinin by passing through a 22 gauge needle 30 times. The lysate was centrifuged at 2200 rpm for 5 min at 4°C. The supernatant was then centrifuged at 100,000 x *g* for 30 min at 4°C. The pellet was then resuspended in 100 μl buffer D and shaken for 30 min at room temperature. Reactions, in a final volume of 100 μl buffer D, contained 40 μl of solubilized membranes, 0.16 mM dithiothreitol in the absence or presence of 5000 U Endo H or 2500 U PNGase F. After incubation at 37°C for 3 hr, an equal volume of buffer E was added to each reaction and incubated at 37°C for 30 min. Samples were then subjected to 8% SDS-PAGE and immunoblotted with monoclonal anti-FLAG antibody.

Immunoblot Analysis – Samples for immunoblotting were subjected to 8% or 13% SDS-PAGE, after which the proteins were transferred to nitrocellulose filters. The immunoblots were performed at room temperature using the following primary antibodies: 1 μg/ml mouse monoclonal anti-FLAG M2 (Sigma) and 1:3000 dilution of a rabbit antiserum directed against

human NPC2. The latter antibody was raised by injecting rabbits with a His10-tagged recombinant version of the antigen. Bound antibodies were visualized by chemiluminescence (SuperSignal West Pico Chemiluminescent Substrate, Thermo Scientific) using a 1:5000 dilution of anti-mouse IgG (Jackson ImmunoResearch Laboratories, Inc.) or anti-rabbit IgG (GE Healthcare) conjugated to horseradish peroxidase. The filters were exposed to Phenix Research Products Blue X-ray Film (F-BX810) at room temperature.

RESULTS

Alanine Scan Mutagenesis to Identify Residues of NPC2 Required for Cholesterol Binding and Transfer – To establish an assay to screen for residues in NPC2 that are essential for cholesterol binding or transfer to NPC1(NTD), we transfected CHO-K1 cells with plasmids encoding histidine-tagged wild-type or mutant NPC2. Like other lysosomal proteins (Kornfeld, 1987), a portion of NPC2 was secreted into the culture medium. To measure binding ability, aliquots of media were incubated with [^{3}H]cholesterol and the NPC2-bound sterol was isolated by nickel chromatography. When cells expressed wild-type NPC2, the His-tagged NPC2 in the medium bound [^{3}H]cholesterol, whereas medium from mock-transfected cells showed no binding (Figure 5-1A). To measure cholesterol transfer, we used a previously described liposome transfer assay (Infante et al., 2008c). First, purified NPC1(NTD) was incubated with [^{3}H]cholesterol and the bound sterol was separated from free [^{3}H]cholesterol by gel filtration chromatography as described in Experimental Procedures. The isolated [^{3}H]cholesterol:NPC1(NTD) complex was then incubated with phosphatidylcholine (PC) liposomes, and the amount of [^{3}H]cholesterol transferred to liposomes was measured. In the presence of culture medium from mock-transfected cells, NPC1(NTD) failed to transfer its

bound [^{3}H]cholesterol to liposomes (Figure 5-1B). Transfer was stimulated markedly in the presence of culture medium containing WT NPC2.

We next prepared 57 plasmids encoding mutant forms of NPC2 in which 1, 2, or 3 sequential amino acids were changed to alanine. (Amino acid residues are numbered starting at the initiator methionine, which is designated no. 1; the first residue after signal peptide cleavage is no. 20.) Our mutant panel included all residues in NPC2 that are exposed to the surface (Xu et al., 2007). We did not mutate any of the 6 cysteines or the single residue that was already alanine. We also did not mutate P120. When P120 is changed to serine, as in certain patients with NPC2 disease (Verot et al., 2007), binding of [^{3}H]cholesterol is abolished (Infante et al., 2008c). The mutant plasmids were introduced into CHO-K1 cells by transfection. We assayed aliquots of culture media that contained equivalent amounts of NPC2 as determined by immunoblotting. Thirteen of the 57 NPC2 mutant proteins showed binding that was less than 15% of the WT value determined in the same experiment (Figure 5-1C, blue). As shown in blue (with the exception of P100, which is remote), these mutations replaced residues that surround the sterol-binding pocket as delineated in the crystal structure of Xu, et al. (Xu et al., 2007) (Figure 5-1E). Moreover, the results of our mutant screen are consistent with the three binding mutants identified by Ko, et al. (2003), who used a different screening assay based on complementation by endocytosis of heterologously expressed mutant NPC2 proteins (Ko et al., 2003). Their binding mutants (F66, V96, and Y100) correspond in our numbering scheme to residues F85, V115, and Y119. In our screen, F85A and Y119A gave binding values of 3% and 8% of WT. Amino acid V115 was not included in our alanine scan, but the two adjacent residues, P114 and K116, when mutated to alanine, gave binding values of 15% and 5% as compared to WT (Figure 5-1C).

We used the liposome transfer assay to analyze transfer activity in culture media from all of the alanine scan mutants whose [^{3}H]cholesterol binding activity exceeded 50% of WT (Figure 5-1D). Three of these mutants exhibited transfer activity that was less than 40% of WT (Figure 5-1D, red). All three of these closely spaced residues map to a surface patch on NPC2 that is adjacent to the opening of the cholesterol binding pocket (Figure 5-1E, red). When the alanine scan was repeated in its entirety in an independent experiment, the same three mutants were identified and none of the other tested mutants showed defective transfer activity.

Biochemical Characterization of NPC2 Cholesterol Transfer Mutant – To further explore the transfer defect detected in the mutant screen, we studied additional amino acid substitutions at the valine-81 position. We used nickel affinity and gel filtration chromatography to purify His-tagged WT and mutant NPC2 proteins from culture media. Increasing amounts of purified WT NPC2 stimulated transfer of [^{3}H]cholesterol from NPC1(NTD) to liposomes, whereas the V81A mutant was less effective (Figure 5-2A). When valine-81 was changed to aspartic acid (V81D), the transfer defect was even greater (Figure 5-2A). Figure 5-2B shows the results of a 2-hr equilibrium binding assay at 4°C, indicating that the V81A and V81D mutants both bound cholesterol with affinities indistinguishable from WT. The calculated K_d values were 81, 80, and 72 nM for WT, V81A, and V81D, respectively. The V81D mutant and the WT protein showed identical rates of association with [^{3}H]cholesterol at 4°C (Figure 5-2C). To measure dissociation rates, we first isolated a [^{3}H]cholesterol:NPC2 complex by gel filtration, then diluted the complex, and then measured the rate of dissociation of bound [^{3}H]cholesterol. Both proteins exhibited identical dissociation rates at 4°C, and both were markedly accelerated at 37°C (Figure 5-2D). We used the isolated [^{3}H]cholesterol:NPC2 complexes as donors to measure the direct

transfer of [^{3}H]cholesterol to NPC1(NTD) (Figure 5-2E). The V81A mutant was partially defective in this transfer and the V81D mutant was severely defective.

NPC2 Cholesterol Binding and Transfer Mutants Fail to Restore Function to NPC2-Deficient Cells – To confirm that the transfer mutants are defective in living cells, we measured the ability of WT and mutant NPC2 proteins to restore egress of LDL-derived cholesterol in fibroblasts from a patient with two defective NPC2 alleles. We incubated the cells with [^{14}C]oleate and measured the rate of its incorporation into cholesteryl [^{14}C]oleate, a reaction that requires movement of LDL-derived cholesterol from lysosomes to ER (Goldstein et al., 1983). In WT cells, LDL caused a marked increase in cholesteryl [^{14}C]oleate formation (Figure 5-3A), whereas the mutant NPC2 cells showed no response. Both cells responded to 25-hydroxycholesterol, which enhances cholesteryl [^{14}C]oleate synthesis in a fashion that does not require the lysosome. To correct the NPC2 phenotype in the mutant cells, we took advantage of the fact that NPC2 is a lysosomal protein that contains mannose-6-phosphate residues that mediate its cellular uptake and delivery to lysosomes (Chikh et al., 2004; Naureckiene et al., 2000). In the presence of LDL, addition of purified WT NPC2 protein to the culture medium led to a marked increase in cholesteryl [^{14}C]oleate synthesis in the mutant NPC2 cells (Figure 5-3B). There was little stimulation when we added the previously described cholesterol-binding mutant of NPC2 (P120S) (Infante et al., 2008c). We also found little stimulation with the cholesterol transfer mutant (V81D). None of these proteins influenced cholesteryl [^{14}C]oleate synthesis in control fibroblasts (Figure 5-3C). We repeated these experiments with NPC2 proteins that contained a FLAG epitope tag and observed identical results (data not shown). Immunoblotting of cell extracts with anti-NPC2 confirmed that both control and mutant fibroblasts took up all three proteins (data not shown).

Biochemical Characterization of NPC1(NTD) Cholesterol Transfer Mutant – Previously, we described a mutation in NPC1(NTD) that did not alter cholesterol binding but partially reduced the ability of the NPC1(NTD) to transfer cholesterol to or from NPC2 (Kwon et al., 2009). This mutation converted two adjacent leucines to alanine (L175A/L176A). To increase this transfer defect, we changed the two leucines to glutamines (L175Q/L176Q). When incubated with [^{3}H]cholesterol in solution for 24 hr at 4°C, this mutant protein bound [^{3}H]cholesterol indistinguishably from WT (Figure 5-4A). However, when incubated with NPC2-bound [^{3}H]cholesterol for 10 min, WT NPC1(NTD) accepted the [^{3}H]cholesterol, whereas the L175Q/L176Q mutant was nearly devoid of acceptor activity (Figure 5-4B). Thus, the L175Q/L176Q mutant of NPC1(NTD) is analogous to the V81D mutant of NPC2. Both mutant proteins can bind cholesterol, but cannot transfer it to the other protein.

NPC1 Cholesterol Transfer Mutant Fails to Restore Function to NPC1-Deficient Cells – To confirm that the L175Q/L176Q mutation disrupted the function of NPC1 in living cells, we introduced this mutation into a plasmid encoding full-length NPC1. Plasmids encoding WT or L175Q/L176Q mutant NPC1 were transfected into CHO 4-4-19 cells, which are deficient in NPC1 (Dahl et al., 1992). To test for NPC1 function, we measured synthesis of cholesteryl [^{14}C]oleate after administration of ß-VLDL, a cholesterol-rich lipoprotein that binds to hamster LDL receptors more avidly than does human LDL. In mock-transfected CHO 4-4-19 cells, ß-VLDL did not stimulate cholesteryl ester synthesis (Figure 5-5A). Expression of WT NPC1 permitted a marked stimulation, whereas the L175Q/L176Q mutant was much less effective. The transfected cells expressed similar amounts of WT and L175Q/L176Q NPC1 as determined by immunoblotting (Figure 5-5A, inset). In both proteins, the *N*-linked carbohydrate chains were partially resistant to treatment with Endo H, indicating that the proteins had folded properly and

reached the Golgi apparatus. Treatment with PNGase F lowered the apparent molecular mass of both proteins as a result of removal of all *N*-linked carbohydrates (Figure 5-5B).

FIGURE 5-1. Alanine Scan Mutagenesis of NPC2: [^{3}H]Cholesterol Binding and Transfer Activities.

(A and C) [^{3}H]Cholesterol binding to NPC2 in culture medium from transfected cells. Each reaction, in final volume of 160 μl, contained 110 μl buffer B, 50 μl concentrated medium as described in Experimental Procedures, 1.9 μg BSA, 0.004% NP-40, and [^{3}H]cholesterol (A, indicated concentration at 222 x 10^3 dpm/pmol; C, 200 nM at 132 x 10^3 dpm/pmol). After 2 hr at 4°C, the amount of bound [^{3}H]cholesterol was measured as described in Experimental Procedures except reactions were not diluted before loading onto Ni-NTA columns. (A) Each value represents total binding after subtraction of blank value (<0.03 pmol/tube). (C) Each bar (average of duplicate assays; mean variation ± SEM for all duplicate values, 9.6 ± 1.2%) represents binding relative to WT NPC2 studied in same experiment. All binding data were adjusted for variations (typically <2-fold) in the amount of secreted NPC2 protein as determined by densitometric scanning of immunoblots of the assayed protein in the eluate. The data in the graph were obtained in 5 separate experiments. The "100% of control" values (WT NPC2) averaged 1.5 pmol/tube (average value for mock-transfected cells in same 5 experiments was <0.1 pmol/tube). The entire alanine scan was repeated in an independent experiment with similar results. Blue bars denote residues that when mutated to alanine decrease binding by >85%. (B and D) [^{3}H]Cholesterol transfer from NPC1(NTD) to liposomes in presence of NPC2 contained in culture medium from transfected cells. Each reaction, in a final volume of 200 μl, contained 130 μl buffer A (pH 5.5), ~40 pmol of WT NPC1(NTD)-LVPRGS-His8-FLAG complexed to [^{3}H]cholesterol (132 x 10^3 dpm/pmol), 20 μg PC liposomes, and concentrated medium (B, 0-10 μl; D, 30 μl). After 10 min at 4°C, [^{3}H]cholesterol transferred to liposomes was measured as described in Experimental Procedures (assay *C*). (B*)* Each value

represents percentage of [^{3}H]cholesterol transferred after subtraction of percentage in absence of medium (11% transfer). The 100% value for transfer was 0.14 pmol/tube. (D) Each bar (average of duplicate assays; mean variation ± SEM for all duplicate values, 8.8 ± 1.1%) denotes percentage of [^{3}H]cholesterol transferred in presence of NPC2 after subtraction of percentage in absence of NPC2. The data in the graph were obtained in 5 separate experiments. The "100% of control" values (WT NPC2) averaged 38% transfer of total input (average value for mock-transfected cells in same 5 experiments was 1.8%). The entire alanine scan was repeated in an independent experiment with similar results. Red bars denote residues that when mutated to alanine decrease NPC2-mediated [^{3}H]cholesterol transfer by >60%. (E) Ribbon diagram of bovine NPC2 (Xu et al., 2007), showing positions of residues crucial for cholesterol binding (blue) and transfer (red). Residue P100 is only one of 14 residues important for binding [^{3}H]cholesterol that does not map to sterol-binding pocket. Residue 81 (Ile bovine sequence; Val in human) was identified in above alanine scan as essential for [^{3}H]cholesterol transfer, but not binding. Residue P120 was previously identified as essential for both binding and transfer (Infante et al., 2008c). Bound cholesterol sulfate is shown in green.

FIGURE 5-1

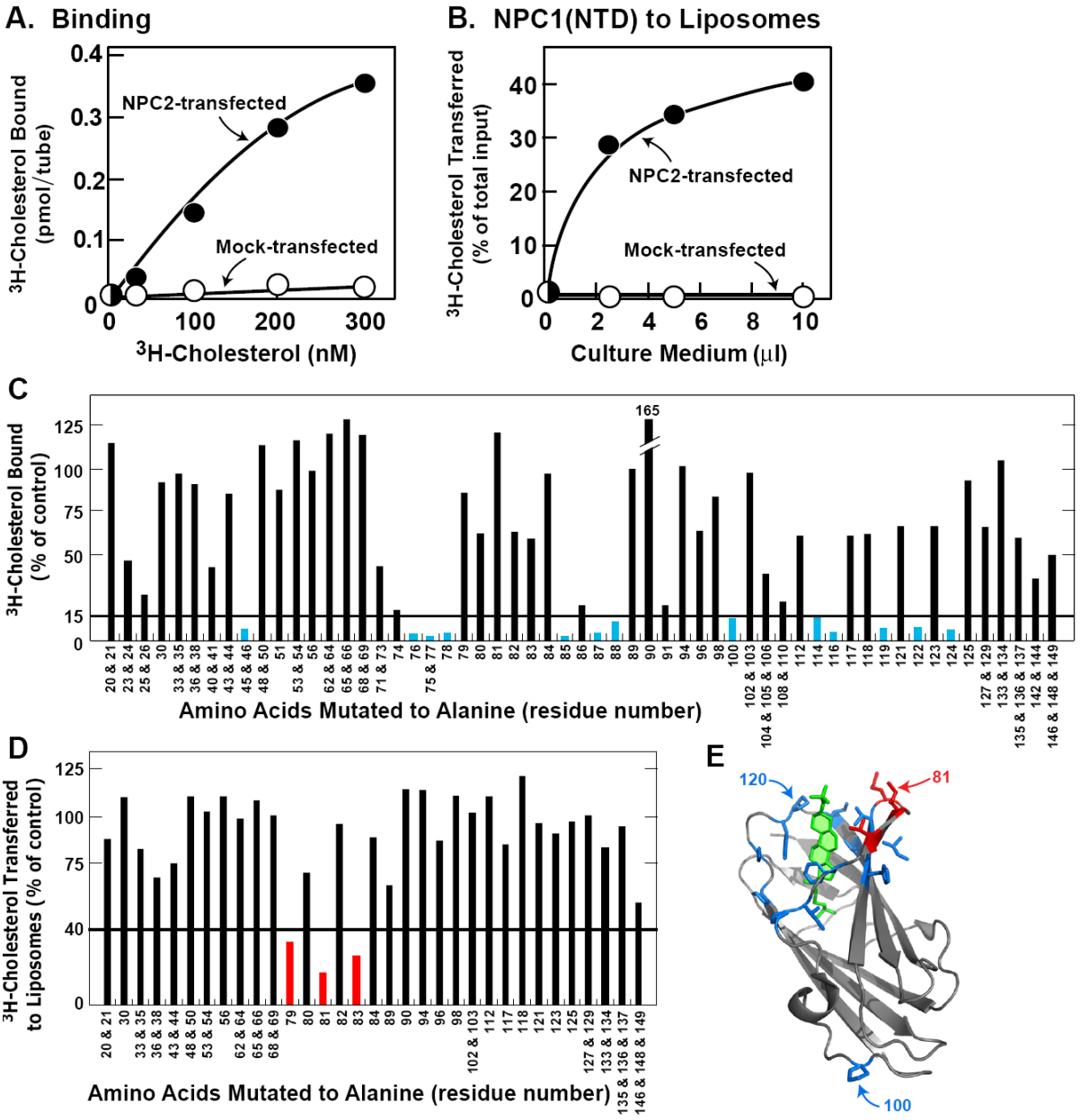
A. Binding
^{3}H-Cholesterol Bound (pmol/tube)
NPC2-transfected
Mock-transfected
^{3}H-Cholesterol (nM)
B. NPC1(NTD) to Liposomes
^{3}H-Cholesterol Transferred (% of total input)
NPC2-transfected
Mock-transfected
Culture Medium (μl)
C
^{3}H-Cholesterol Bound (% of control)
165
Amino Acids Mutated to Alanine (residue number)
D
^{3}H-Cholesterol Transferred to Liposomes (% of control)
Amino Acids Mutated to Alanine (residue number)
E
120
81
100

FIGURE 5-2. Biochemical Analysis of NPC2 Transfer-defective Mutants.

(A) [^{3}H]Cholesterol transfer from NPC1(NTD) to liposomes as a function of NPC2. Each reaction, in a final volume of 200 μl buffer A (pH 5.5), contained ~50 pmol of WT NPC1(NTD)-LVPRGS-His8-FLAG complexed to [^{3}H]cholesterol (222 x 10^3 dpm/pmol), 20 μg PC liposomes, and the indicated concentration of WT or mutant NPC2-His10. After 10 min at 4°C, [^{3}H]cholesterol transferred to liposomes was measured as described in Experimental Procedures (assay C). Each value represents percentage of [^{3}H]cholesterol transferred. A blank value in the absence of NPC2 (7% transfer) was subtracted. The 100% value for transfer was 1.9 pmol/tube. (B) [^{3}H]Cholesterol binding. Each reaction, in a final volume of 80 μl buffer A (pH 5.5) with 0.004% NP-40, contained 8 pmol of purified WT or mutant NPC2-His10, 1 μg BSA, and the indicated concentration of [^{3}H]cholesterol (222x10^3 dpm/pmol). After 2 hr at 4°C, bound [^{3}H]cholesterol was measured. Each value represents total binding after subtraction of blank value (<0.1 pmol/tube). (C) Time course of association of [^{3}H]cholesterol to NPC2. Each reaction, in a final volume of 80 μl of buffer A (pH 5.5) with 0.004% NP-40, contained 8 pmol of WT or mutant NPC2-His10 and 200 nM [^{3}H]cholesterol (132 x 10^3 dpm/pmol). After incubation for indicated time at 4°C, bound [^{3}H]cholesterol was determined. Each value represents total binding after subtraction of a blank value (<0.03 pmol/tube). (D) Dissociation of previously bound [^{3}H]cholesterol from NPC2 at different temperatures. Dissociation of [^{3}H]cholesterol from [^{3}H]cholesterol:NPC2-His10 (WT or mutant) was measured as described in Experimental Procedures. Each value represents the percentage of [^{3}H]cholesterol remaining bound to WT or mutant NPC2 relative to zero-time value. The ‘‘100% initial binding’’ values at zero time for NPC2 was 0.48 (WT) and 0.26 (mutant) pmol/tube. (E) [^{3}H]Cholesterol transfer from NPC2 to NPC1(NTD). Each reaction, in a final volume of 200 μl buffer A (pH 5.5),

contained ~40 pmol of WT or mutant NPC2-His10 complexed to [^{3}H]cholesterol (222 x 10^3 dpm/pmol) and the indicated concentration of WT NPC1(NTD)-LVPRGS-His8-FLAG. After 10 min at 4°C, [^{3}H]cholesterol transferred was measured as described in Experimental Procedures (assay *B*). Each value represents percentage of [^{3}H]cholesterol transferred to NPC1(NTD). Blank values in the absence of NPC1(NTD) (0.1-0.5% transfer) were subtracted. The 100% values for transfer from WT, V81A, and V81D NPC2 were 0.24, 0.78, and 0.29 pmol/tube, respectively. (A-E) Each value is the average of duplicate assays.

FIGURE 5-2

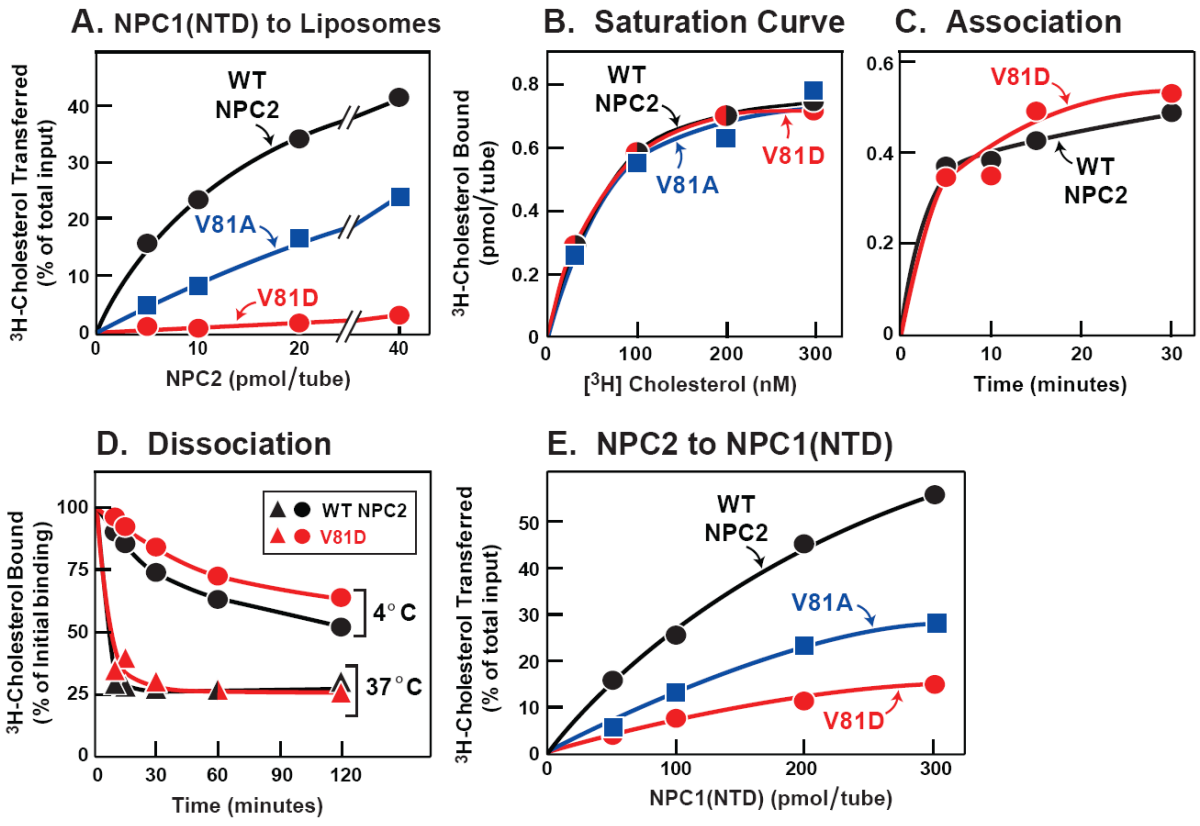

FIGURE 5-3. Ability of WT NPC2, but not Mutant NPC2, to Rescue LDL-stimulated Cholesteryl Ester Formation in NPC2-deficient Human Fibroblasts.

(A) Control and NPC2-deficient cells were set up for experiments as described in Experimental Procedures. On day 7, cells were switched to medium B containing 5% lipoprotein-deficient serum, 50 μM compactin, and 50 μM sodium mevalonate in the absence or presence of 10 μg/ml 25-hydroxycholesterol (25-HC) or 60 μg protein/ml LDL as indicated. (B and C) On day 7, cells were switched to above medium supplemented with 60 μg protein/ml LDL and indicated concentration of purified WT or mutant NPC2-His10. (A-C) After 5 hr at 37°C, each cell monolayer was pulse-labeled for 1 h with 0.2 mM sodium [^{14}C]oleate (3480 dpm/nmol), and cellular content of cholesteryl [^{14}C]oleate and [^{14}C]triglycerides were determined. Each value is the average of duplicate incubations. Content of [^{14}C]triglycerides in NPC2-deficient fibroblasts treated with 60 μg/ml LDL and 3 μg/ml of WT, V81D, or P120S NPC2-His10 proteins was 3.1, 3.0, and 4.0 nmol/hr per mg protein, respectively.

FIGURE 5-3

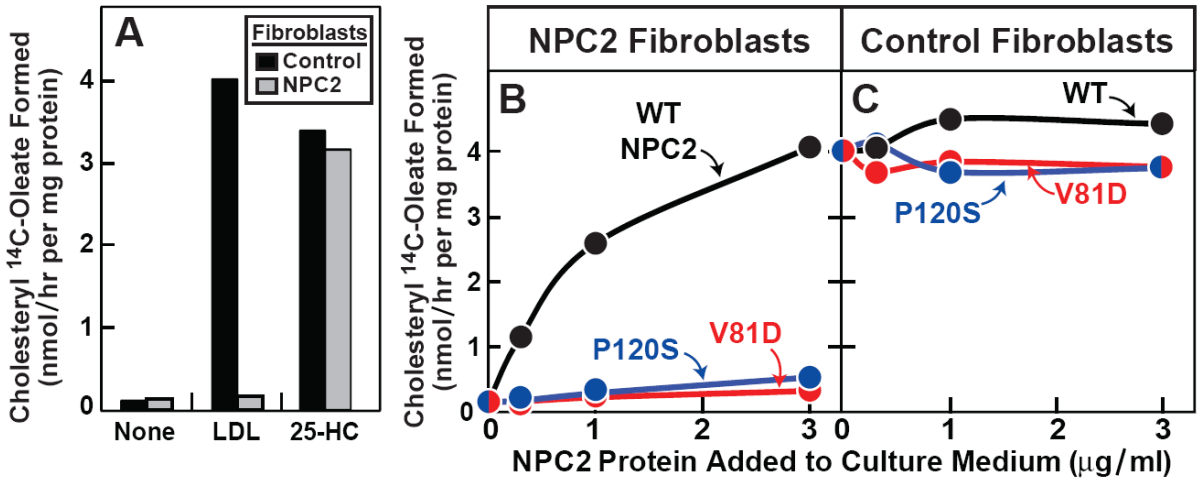

FIGURE 5-4. Biochemical Analysis of NPC1(NTD) Transfer-defective Mutant.

(A) [^{3}H]Cholesterol binding. Each reaction, in a final volume of 80 µl buffer A (pH 5.5) with 0.004% NP-40, contained 4 pmol purified WT or mutant NPC1(NTD)-LVPRGS-His8-FLAG, 1 µg BSA, and indicated concentration of [^{3}H]cholesterol (132 x 10^3 dpm/pmol). After 24 hr at 4°C, bound [^{3}H]cholesterol was measured. Each value represents total binding after subtraction of a blank value (<0.06 pmol/tube). (B) [^{3}H]Cholesterol transfer from NPC2 to NPC1(NTD). Each reaction, in a final volume of 100 µl buffer A (pH 5.5), contained ~24 pmol of NPC2-FLAG complexed to [^{3}H]cholesterol (132 x 10^3 dpm/pmol) and indicated concentration of WT or mutant NPC1(NTD)-LVPRGS-His8-FLAG. After 10 min at 4°C, [^{3}H]cholesterol transferred was measured as described in Experimental Procedures (assay A). Each value represents percentage of [^{3}H]cholesterol transferred to NPC1(NTD). A blank value in the absence of NPC1(NTD) (0.3% transfer) was not subtracted. The 100% value for transfer from NPC2 was 0.85 pmol/tube. (A and B) Each value is the average of duplicate assays.

FIGURE 5-4

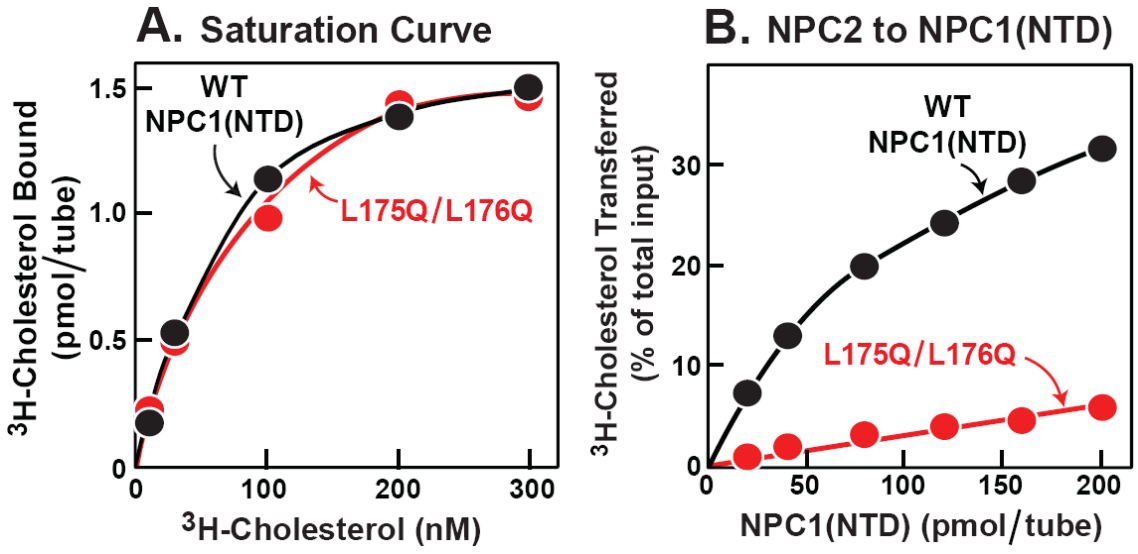

FIGURE 5-5. Failure of Mutant L175Q/L176Q Version of Full-length NPC1 to Rescue Cholesteryl Ester Formation in NPC1-defective Hamster Cells.

(A) Cholesterol esterification in response to ß-VLDL. NPC1-deficient CHO 4-4-19 cells were transfected on day 1 with 2 μg pcDNA3.1 (mock), WT pCMV-NPC1-His8-FLAG, or its mutant version (L175Q/L176Q) as described in Experimental Procedures. Five hr after transfection, the medium was switched to medium A containing 5% newborn calf lipoprotein-deficient serum. On day 2, the medium was switched to same medium containing 5 μM compactin and 50 μM sodium mevalonate. After 16 hr, fresh medium containing 50 μM compactin, 50 μM sodium mevalonate, and the indicated concentration of ß-VLDL was added. After 5 hr at 37°C, each monolayer was pulse-labeled for 1 hr with 0.2 mM sodium [^{14}C]oleate (7433 dpm/nmol). The cells were then harvested for measurement of their content of cholesteryl [^{14}C]oleate and [^{14}C]triglycerides as described in Experimental Procedures. Each value is the average of duplicate incubations. The content of [^{14}C]triglycerides for mock, WT, and mutant NPC1 transfected cells incubated with 10 μg/ml ß-VLDL was 201, 222, and 129 nmol/hr per mg protein, respectively. Inset shows an immunoblot of whole cell extracts from the various transfected cells probed with anti-FLAG antibody as described in Experimental Procedures. (B) Deglycosidase treatment. NPC1-deficient CHO cells were transfected with the indicated plasmid as in (A). Five hr after transfection, the medium was switched to medium A with 5% FCS. Two days later, cells were harvested, and their solubilized membranes were treated with glycosidase Endo H or PNGase F and then subjected to immunoblot analysis with anti-FLAG antibody as described in Experimental Procedures. (A and B) Filters were exposed to film for ~10 sec at room temperature.

FIGURE 5-5

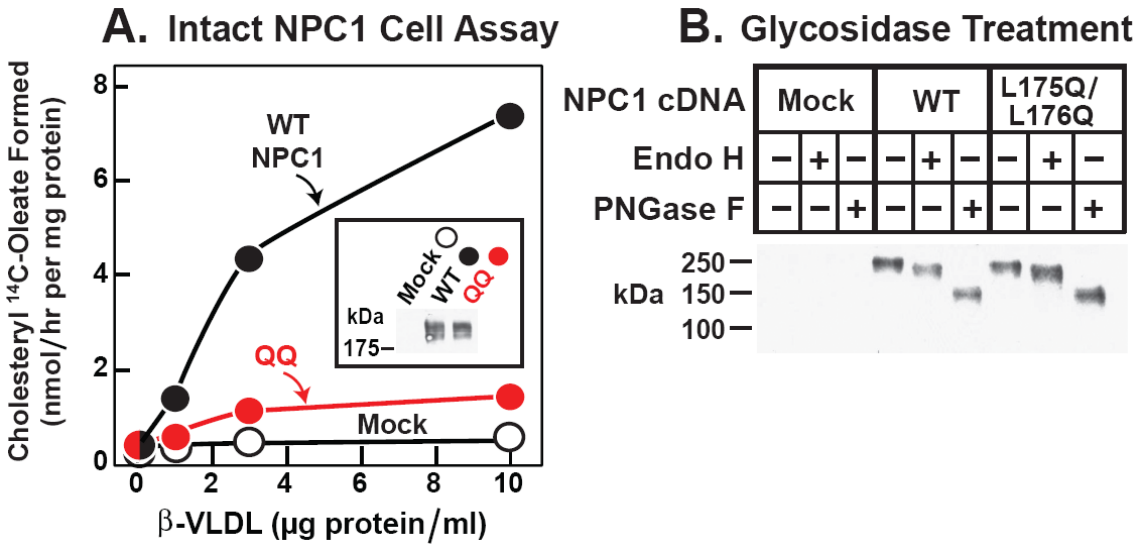

(Data for A from Lina Abi-Mosleh)

FIGURE 5-6. Conceptual Model Illustrating One Possible Mechanism of Interaction Between NPC2 and NPC1(NTD).

This model is based on the published structures of sterol-bound NPC2 (Xu et al., 2007) and sterol-bound NPC1(NTD) in the putative open conformation (Kwon et al., 2009). A stable complex between NPC2 and NPC1(NTD) has not been demonstrated experimentally, and the interaction models in A and B are hypothetical. (A) Surface representation showing residues in NPC2 (purple) and NPC1(NTD) (green) that are crucial for transfer of cholesterol (red) between NPC2 and NPC1(NTD). The cholesterol molecule is shown after its transfer to NPC1(NTD). The two proteins are positioned so that the openings in their respective sterol-binding pockets are juxtaposed and the planes of the cholesterol-binding pockets in NPC2 and NPC1(NTD) are aligned. (B) Cutaway view of the NPC2:NPC1(NTD) complex shown in A, revealing alignment of the cholesterol-binding pockets and juxtaposition of the surface patches on both proteins postulated to be crucial for protein-protein interaction.

FIGURE 5-6

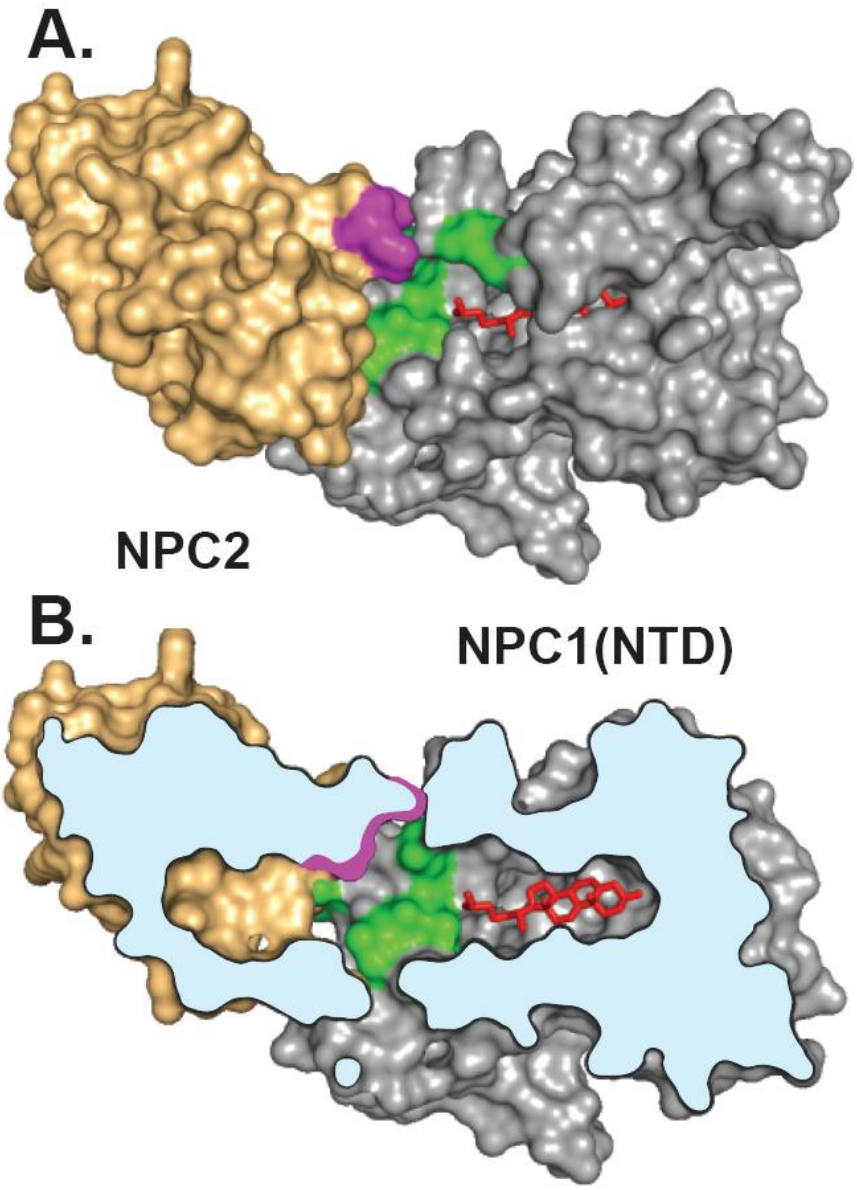

(Spatial alignment of NPC2 and NPC1(NTD) by Hyock Kwon)

DISCUSSION

In the current studies, we used alanine-scanning mutagenesis to identify residues in NPC2 that are important for cholesterol binding and for cholesterol transfer to or from NPC1(NTD). When the crucial residues are mapped to the published structure of NPC2 (Xu et al., 2007), they reveal that the binding-defective mutations cluster around the sterol-binding pocket. Three of the mutant proteins bound cholesterol normally, but failed to catalyze the transfer of cholesterol from NPC1(NTD) to PC liposomes. These three sites were all on the surface of the protein in a patch that is adjacent to the opening of the sterol-binding pocket.

We previously performed a similar alanine-scanning mutagenesis study of NPC1(NTD) (Kwon et al., 2009). In that study, we identified 11 amino acids whose replacement disrupted transfer without disrupting cholesterol binding. These residues clustered in a surface patch of NPC1(NTD) that surrounds the helices that must be moved aside in order for cholesterol to enter the binding pocket. The finding that transfer mutants in both proteins cluster in surface patches raises the possibility that these two patches must interact in order for NPC2 to open the binding pocket of NPC1(NTD) so that cholesterol can move between the two proteins. Figure 5-6 shows a model illustrating one way in which these two proteins could interact. The hypothesis of direct interaction between NPC2 and NPC1(NTD) is by no means proven. So far we have been unable to demonstrate a stable physical complex between these two proteins with or without cholesterol in the binding pockets.

The model for direct cholesterol transfer between NPC2 and NPC1(NTD) is formally analogous to the proposed model for substrate channeling between two sequential enzymes in a biochemical pathway (Anderson, 1999). A well studied example of substrate channeling is the transfer of ß-aspartyl phosphate between aspartokinase-homoserine dehydrogenase I and aspartate semialdehyde dehydrogenase (James and Viola, 2002). So far, the evidence for such

channeling is kinetic, much like the current evidence for cholesterol transfer in the NPC2/NPC1(NTD) system. To our knowledge, direct complexes between two different enzymes in substrate channeling have not been demonstrated. On the other hand, in the case of tryptophan synthase in which two sequential enzymes are linked together in a $\alpha_2ß_2$ tetrameric complex, crystallographic studies document intersections between the two active sites (Anderson, 1999).

In the case of channeling systems not involving stable heterodimeric complexes, it is likely that the interactions are transient, and additional methods, such as chemical crosslinking, may be necessary to freeze the contacts so as to permit a direct demonstration of relevant interactions. Initial efforts to use nonspecific crosslinkers to detect interaction between NPC2 and NPC1(NTD) have so far been unsuccessful. We have also been unsuccessful in using several detection methods such as gel filtration, Biacore, and AlphaScreen. Transfer-defective mutants like NPC2(V81D) provide negative controls that allow us to study only the physiologically relevant interactions.

The transfer of cholesterol from NPC2 to NPC1(NTD) has a special functional relevance in light of the near-absolute insolubility of cholesterol in water. Our model envisions that NPC2 binds cholesterol the instant that it is released from LDL, either as the free sterol or after cleavage of cholesteryl esters by lysosomal acid lipase. This binding would prevent cholesterol from crystallizing in the lysosomal lumen. According to the model, NPC2 can transfer its bound cholesterol to NPC1(NTD) directly, thus avoiding the necessity for the insoluble cholesterol to transit the water phase. We have named this process a "hydrophobic handoff." Additional studies will be needed to test and validate this model. The transfer mutants described in this chapter should facilitate this validation.

Material from Chapter 5 was originally published in Cell Metabolism. Wang ML, Motamed M, Infante RE, Abi-Mosleh L, Kwon HJ, Brown MS, Goldstein JL. Identification of Surface Residues on Niemann-Pick C2 (NPC2) Essential for Hydrophobic Handoff of Cholesterol to NPC1 in Lysosomes. *Cell Metab.* 2010 Aug 4;12(2):166-73.

CHAPTER 6

CONCLUSION AND PERSEPECTIVE

Maintenance of cellular cholesterol homeostasis is important, as evidenced by diseases that arise when homeostasis is disrupted (Ikonen, 2006). Familial hypercholesterolemia occurs when cells are unable to uptake LDL particles due to defects in the LDL receptor (Brown and Goldstein, 1986); Wohlmann's disease occurs when cells are unable to hydrolyze cholesteryl esters to fatty acids and cholesterol in the lysosomes (Pentchev et al., 1987); and NPC disease occurs when cells are unable to transport LDL-derived cholesterol out of lysosomes (Blanchette-Mackie et al., 1988; Pentchev et al., 1987). However, studying these diseases have allowed us to understand cellular cholesterol transport in more detail. It was through the study of NPC patients that identified NPC1 and NPC2 as important players in the egress of LDL-derived cholesterol from lysosomes (Carstea et al., 1997; Carstea et al., 1993; Naureckiene et al., 2000). NPC1 is a membrane bound protein of ~1300 amino acids located in the lysosomal membrane; while NPC2 is a soluble protein of ~130 amino acids located in the lysosomal lumen. Both proteins bind cholesterol (Infante et al., 2008a; Xu et al., 2007), and the cholesterol binding site of NPC1 is located in its N-terminal domain (Infante et al., 2008b), designated NPC1(NTD). As defects in either protein result in near identical clinical phenotype, the two likely function in the same pathway to export cholesterol. It is then the goal of the experiments in this thesis to decipher how these two proteins function, and more importantly how they function together.

Comparing the cholesterol binding of NPC2 and NPC1(NTD) revealed two contrasting characteristics between the proteins. First, the two proteins bound cholesterol in opposite orientations (Infante et al., 2008b; Kwon et al., 2009; Xu et al., 2007). NPC2 binds the iso-octyl

side chain, leaving the 3ß-hydroxyl exposed, while NPC1 binds the 3ß-hydroxyl, leaving the side chain partially exposed. This was shown through competitive binding studies, and confirmed by crystal structures with bound sterols. Second, NPC2 binds cholesterol with a relatively fast on- and off-rates in comparison to NPC1(NTD) (Infante et al., 2008c). When incubated at 4°C, NPC2 binds and releases cholesterol rapidly (half-time <2 min). In contrast, at 4°C NPC1(NTD) binds cholesterol very slowly (half-time >2 hr).

The striking contrasts in these cholesterol binding proteins that function in the same cholesterol transport pathway led to the hypothesis that NPC2 and NPC1(NTD) can transfer bound cholesterol to one another. To test this we established an *in vitro* assay to measure the transfer of cholesterol between these two proteins and phosphatidylcholine liposomes (Infante et al., 2008c). Despite the slow on- and off-rates of cholesterol binding to NPC1(NTD), it could both accept NPC2-bound cholesterol and deliver bound cholesterol to NPC2 rapidly (both with half-times <3min). In agreement with the kinetics of cholesterol binding to NPC2 and NPC1(NTD), NPC2 can readily deliver or accept cholesterol from liposomes, while NPC1(NTD) cannot. However, rapid transfer of cholesterol between NPC1(NTD) and liposomes can be achieved in the presence of NPC2.

To understand the binding and transfer of cholesterol by NPC2 and NPC1(NTD) in more detail, we determined the amino acid residues important for binding or transfer in both proteins through alanine scan mutagenesis (Kwon et al., 2009; Wang et al., 2010). At the same time, the crystal structure of NPC1(NTD) was solved through collaboration (Kwon et al., 2009), which allowed us to map the results of the alanine scan mutagenesis experiments onto the crystal structures of both NPC1(NTD) and NPC2 (Xu et al., 2007). For both proteins, residues that decreased binding mapped to areas surrounding the binding pockets on the crystal structures;

residues that decreased transfer, but not binding, mapped to discrete surface patches near the opening of the binding pockets.

The crystal structure of NPC1(NTD) not only provided a means to visualize our mutagenesis data, but revealed another important insight into the kinetics of NPC1(NTD)'s binding of cholesterol. Entrance into the cholesterol binding pocket is obstructed by α-helices that must move aside to permit entry or exit (Kwon et al., 2009), thus explaining the slow binding of cholesterol when delivered in solution as seen in earlier studies (Infante et al., 2008c). We envision that NPC2 binds to NPC1(NTD), displacing the helices and allowing direct transfer of cholesterol into or out of the binding pocket of NPC1(NTD).

Using binding- and transfer-defective mutants of NPC2 and NPC1(NTD) (identified above through alanine scan mutagenesis) in cell culture rescue assays, we established the functional significance of the cholesterol binding and transfer seen *in vitro* in the transport of cholesterol in cells. The binding or transfer mutants in NPC2 and NPC1 failed to restore the egress of LDL-derived cholesterol from lysosomes as seen by their inability to rescue LDL-stimulated cholesteryl ester synthesis in NPC2- or NPC1-deficient cells, respectively, in contrast to wild-type NPC2 and NPC1 (Kwon et al., 2009; Wang et al., 2010).

Taken together, these studies allow us to formulate a hypothetical working model to explain the requirement for these two proteins in the egress of lipoprotein-derived cholesterol from lysosomes (see Figure 6-1). A major consideration in formulating this model is how a hydrophobic molecule such as cholesterol can be transported safely and efficiently through the aqueous environment of the lysosomal lumen and into the lysosomal membranes.

As described previously, cholesterol binds to NPC2 with its 3β-hydroxyl group exposed to solvent (Figure 6-1A) (Infante et al., 2008b; Xu et al., 2007). The exposure of the 3ß-hydroxyl

allows NPC2 to bind lipoprotein-derived cholesterol either before or immediately after the fatty acid on the hydroxyl group is removed by acid lipase. Even though NPC2 can deliver cholesterol directly to liposomes *in vitro*, genetics reveals that NPC2 alone is not sufficient for cholesterol egress from lysosomes, and hence the requirement for NPC1 (Pentchev, 2004; Sleat et al., 2004). We hypothesize that the NPC1 requirement may be imposed to overcome either of two obstacles: 1) cholesterol should enter the hydrophobic lysosomal membrane most readily when its hydrophobic iso-octyl side chain leads the way. When cholesterol is bound to NPC2, the hydrophobic side chain is deeply buried in the protein and it cannot lead the way into the lysosomal membrane bilayer; and/or 2) the carbohydrate glycocalyx that lines the interior of the lysosomal membrane (Neiss, 1984) creates a diffusion barrier that would prevent NPC2 from interacting directly with the membrane (Kolter and Sandhoff, 2005; Schulze et al., 2009). Both of these impediments could be overcome if NPC2 transferred its cholesterol to NPC1(NTD). This would reverse the orientation of cholesterol so that its hydrophobic side chain could lead the way into the membrane, and it likely provides a mechanism for cholesterol to transit the glycocalyx. It is due to the above two considerations that the directionality of cholesterol transfer from NPC2 to NPC1 is hypothesized.

This transfer of cholesterol from NPC2 to NPC1(NTD) has a special functional relevance in light of the near-absolute insolubility of cholesterol in water. Our model envisions that NPC2 binds cholesterol the instant that it is released from LDL, either as the free sterol or after cleavage of cholesteryl esters by lysosomal acid lipase. This binding would prevent cholesterol from crystallizing in the lysosomal lumen. According to the model, NPC2 can transfer its bound cholesterol to NPC1(NTD) directly, thus avoiding the necessity for the insoluble cholesterol to transit the water phase. We have named this process a “hydrophobic

handoff," and it may have broader implications for transport of insoluble compounds around the cell. However, additional studies will be needed to test and validate this model. We have been unable to demonstrate a stable physical complex between NPC2 and NPC1(NTD) thus far through a variety of techniques, including gel-filtration, co-immunoprecipitation affinity chromatography, AlphaScreen, Surface Plasmon Resonance, and cross-linking. Therefore, we are led to believe that the postulated interaction underlying the transfer of cholesterol must be transient, analogous to the proposed model for substrate channeling between two sequential enzymes in a biochemical pathway. The transfer mutants described should facilitate this validation.

Once NPC1(NTD) has accepted cholesterol from NPC2, it has to deliver this cholesterol toward the lysosomal membrane for subsequent export from lysosomes. The NTD is separated from the membrane domain of NPC1 by a linker composed of ~20 amino acids, 8 of which are prolines (Figure 6-1D). It is likely that this sequence extends in such a way that the NTD domain can project through the glycocalyx, which has been measured at ~8 nm (Neiss, 1984). This glycocalyx is shown as stipples in Figure 6-1C. In order to deliver cholesterol to the membrane, the NTD would have to move toward the membrane. Moreover, another protein surface would have to enlarge the opening on NPC1(NTD) in order for cholesterol to leave the NTD and enter the membrane. It is likely that these processes are mediated by the remainder of NPC1 which contains 13 transmembrane helices and two large loops that project into the lysosomal lumen. Five of the 13 transmembrane helices (no. 3-7) bear sequence homology to the sterol-sensing domains of SCAP, a polytopic membrane protein in the SREBP pathway that has been shown to bind cholesterol with high affinity (Radhakrishnan et al., 2008). It seems likely that the sterol-sensing domain of NPC1 participates in cholesterol transfer. In Figure 6-1C, we

show the NPC1(NTD) domain interacting with the membrane domain of the same protein. However, we have not ruled out the possibility that the NPC1(NTD) transfers the cholesterol directly to the membrane.

In transferring its bound cholesterol to the lysosomal membrane, NPC1(NTD) could interact either with its own membrane domain (as shown in Figure 6-1C) in which case it might transfer the cholesterol to the putative sterol-sensing domain in transmembrane helices 3-7, or it could interact with the membrane domain of a neighboring NPC1 molecule. In this regard, Ohgami *et al.* (2004) reported they could crosslink photoactivated cholesterol to NPC1 when the photoactivated cholesterol was added to the culture medium of wild-type CHO cells. The reaction was reduced when the cells harbored mutant NPC1 with a point mutation in transmembrane helix3, which is part of the sterol-sensing domain. Once cholesterol is transferred to the membrane domain of NPC1, it could be flipped to the cytosolic leaflet from which it could then be picked up by cytosolic cholesterol-binding proteins. It seems likely that additional proteins would be required for the export process. Clues may come from study of patients with the NPC disease phenotype who do not have mutations in *NPC1* or *NPC2*.

Although the model of Figure 6-1 still remains to be proven, it offers a scheme that can be tested by further experiments using *in vitro* biochemistry and cell culture methodologies. It is hoped that testing of this model may lead to new insights into a fundamental biologic process - namely, how lipoprotein-derived cholesterol is transported out of the lysosomal compartment so that it can exert its structural and regulatory functions within the cell. Understanding this process hopefully will shed new light on a devastating disease.

FIGURE 6-1

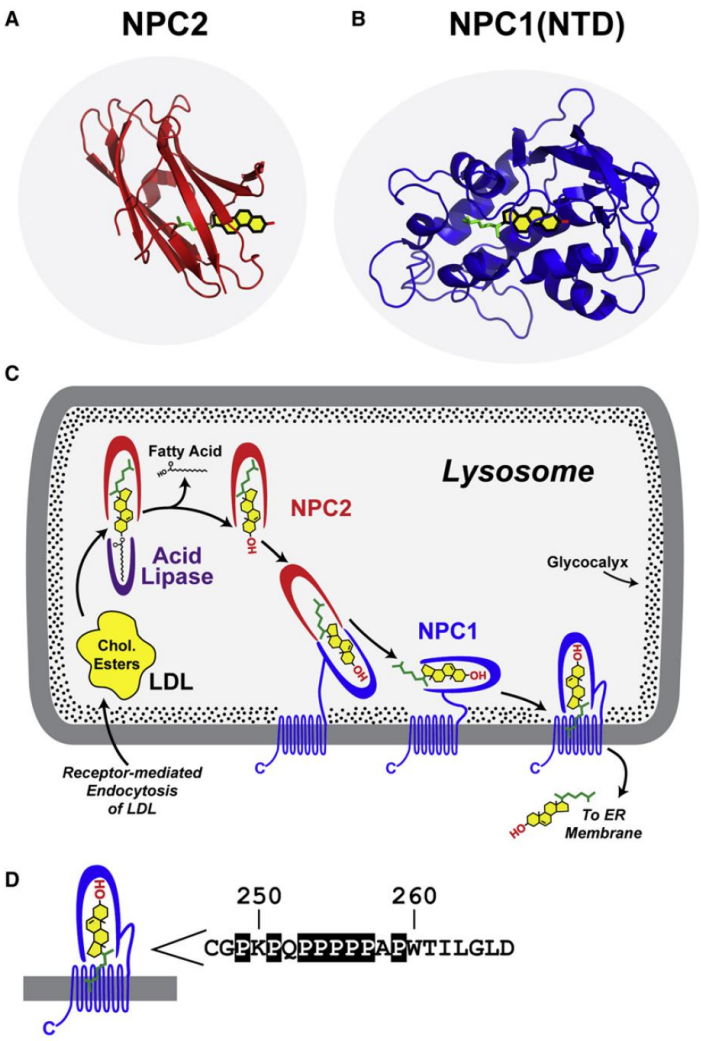

FIGURE 6-1. Model for Egress of Lipoprotein-derived Cholesterol from Lysosomes.

(A) Structure of NPC2 bound to cholesterol. Redrawn from Xu, et al. (2007) [35]. (B) Structure of NPC1(NTD) bound to cholesterol [90]. (C) Proposed pathway for transfer of cholesterol from LDL or ß-VLDL to NPC2 to NPC1 to membranes. See Discussion for explanation of this working model. (D) Sequence of amino acids 247-266 that link the NTD to the first transmembrane domain in NPC1 [21]. Prolines in this sequence are boxed. These prolines are invariant in 12 vertebrate species [34] except for P256, which is conserved in 8 of the 12 species.

Portions of the material from Chapter 6 were originally published in Cell or Cell Metabolism. Kwon HJ , Abi-Mosleh L ,Wang ML, Deisenhofer J, Goldstein JL, Brown MS, Goldstein JL, Infante RE. Structure of the N-terminal domain of NPC1 suggests transfer mechanism for exit of LDL-Cholesterol from lysosomes. *Cell*. 2009 Jun 26;137(7):1213-24. Wang ML, Motamed M, Infante RE, Abi-Mosleh L, Kwon HJ, Brown MS, Goldstein JL. Identification of Surface Residues on Niemann-Pick C2 (NPC2) Essential for Hydrophobic Handoff of Cholesterol to NPC1 in Lysosomes. *Cell Metab.* 2010 Aug 4;12(2):166-73.

BIBLIOGRAPHY

Adams, C.M., Reitz, J., De Brabander, J.K., Feramisco, J.D., Li, L., Brown, M.S., and Goldstein, J.L. (2004). Cholesterol and 25-hydroxycholesterol inhibit activation of SREBPs by different mechanisms, both involving SCAP and Insigs. J Biol Chem *279*, 52772-52780.

Anderson, K.S. (1999). Fundamental mechanisms of substrate channeling. Methods Enzymol *308*, 111-145.

Babalola, J.O., Wendeler, M., Breiden, B., Arenz, C., Schwarzmann, G., Locatelli-Hoops, S., and Sandhoff, K. (2007). Development of an assay for the intermembrane transfer of cholesterol by Niemann-Pick C2 protein. Biol Chem *388*, 617-626.

Blanchette-Mackie, E.J., Dwyer, N.K., Amende, L.M., Kruth, H.S., Butler, J.D., Sokol, J., Comly, M.E., Vanier, M.T., August, J.T., Brady, R.O., *et al.* (1988). Type-C Niemann-Pick disease: low density lipoprotein uptake is associated with premature cholesterol accumulation in the Golgi complex and excessive cholesterol storage in lysosomes. Proc Natl Acad Sci U S A *85*, 8022-8026.

Brady, R.O. (1978). Sphingolipidoses. Annu Rev Biochem *47*, 687-713.

Brown, M.S., and Goldstein, J.L. (1986). A receptor-mediated pathway for cholesterol homeostasis. Science *232*, 34-47.

Brown, M.S., and Goldstein, J.L. (1997). The SREBP pathway: regulation of cholesterol metabolism by proteolysis of a membrane-bound transcription factor. Cell *89*, 331-340.

Carstea, E.D., Morris, J.A., Coleman, K.G., Loftus, S.K., Zhang, D., Cummings, C., Gu, J., Rosenfeld, M.A., Pavan, W.J., Krizman, D.B., *et al.* (1997). Niemann-Pick C1 disease gene: homology to mediators of cholesterol homeostasis. Science *277*, 228-231.

Carstea, E.D., Polymeropoulos, M.H., Parker, C.C., Detera-Wadleigh, S.D., O'Neill, R.R., Patterson, M.C., Goldin, E., Xiao, H., Straub, R.E., Vanier, M.T., *et al.* (1993). Linkage of Niemann-Pick disease type C to human chromosome 18. Proc Natl Acad Sci U S A *90*, 2002-2004.

Chang, T.Y., Chang, C.C., and Cheng, D. (1997). Acyl-coenzyme A:cholesterol acyltransferase. Annu Rev Biochem *66*, 613-638.

Chang, T.Y., Chang, C.C., Ohgami, N., and Yamauchi, Y. (2006). Cholesterol sensing, trafficking, and esterification. Annu Rev Cell Dev Biol *22*, 129-157.

Chang, T.Y., Reid, P.C., Sugii, S., Ohgami, N., Cruz, J.C., and Chang, C.C. (2005). Niemann-Pick type C disease and intracellular cholesterol trafficking. J Biol Chem *280*, 20917-20920.

Chen, Y.H., Yang, J.T., and Chau, K.H. (1974). Determination of the helix and beta form of proteins in aqueous solution by circular dichroism. Biochemistry *13*, 3350-3359.

Cheruku, S.R., Xu, Z., Dutia, R., Lobel, P., and Storch, J. (2006). Mechanism of cholesterol transfer from the Niemann-Pick type C2 protein to model membranes supports a role in lysosomal cholesterol transport. J Biol Chem *281*, 31594-31604.

Chikh, K., Vey, S., Simonot, C., Vanier, M.T., and Millat, G. (2004). Niemann-Pick type C disease: importance of N-glycosylation sites for function and cellular location of the NPC2 protein. Mol Genet Metab *83*, 220-230.

Dahl, N.K., Reed, K.L., Daunais, M.A., Faust, J.R., and Liscum, L. (1992). Isolation and characterization of Chinese hamster ovary cells defective in the intracellular metabolism of low density lipoprotein-derived cholesterol. J Biol Chem *267*, 4889-4896.

Davies, J.P., and Ioannou, Y.A. (2000). Topological analysis of Niemann-Pick C1 protein reveals that the membrane orientation of the putative sterol-sensing domain is identical to those of 3-hydroxy-3-methylglutaryl-CoA reductase and sterol regulatory element binding protein cleavage-activating protein. J Biol Chem *275*, 24367-24374.

DeBose-Boyd, R.A., Brown, M.S., Li, W.P., Nohturfft, A., Goldstein, J.L., and Espenshade, P.J. (1999). Transport-dependent proteolysis of SREBP: relocation of site-1 protease from Golgi to ER obviates the need for SREBP transport to Golgi. Cell *99*, 703-712.

Demel, R.A., and De Kruyff, B. (1976). The function of sterols in membranes. Biochim Biophys Acta *457*, 109-132.

Friedland, N., Liou, H.L., Lobel, P., and Stock, A.M. (2003). Structure of a cholesterol-binding protein deficient in Niemann-Pick type C2 disease. Proc Natl Acad Sci U S A *100*, 2512-2517.

Frolov, A., Zielinski, S.E., Crowley, J.R., Dudley-Rucker, N., Schaffer, J.E., and Ory, D.S. (2003). NPC1 and NPC2 regulate cellular cholesterol homeostasis through generation of low density lipoprotein cholesterol-derived oxysterols. J Biol Chem *278*, 25517-25525.

Goldstein, J.L., Basu, S.K., and Brown, M.S. (1983). Receptor-mediated endocytosis of low-density lipoprotein in cultured cells. Methods Enzymol *98*, 241-260.

Goldstein, J.L., and Brown, M.S. (2001). Molecular medicine. The cholesterol quartet. Science *292*, 1310-1312.

Goldstein, J.L., Dana, S.E., Faust, J.R., Beaudet, A.L., and Brown, M.S. (1975). Role of lysosomal acid lipase in the metabolism of plasma low density lipoprotein. Observations in cultured fibroblasts from a patient with cholesteryl ester storage disease. J Biol Chem *250*, 8487-8495.

Goldstein, J.L., DeBose-Boyd, R.A., and Brown, M.S. (2006). Protein sensors for membrane sterols. Cell *124*, 35-46.

Greer, W.L., Dobson, M.J., Girouard, G.S., Byers, D.M., Riddell, D.C., and Neumann, P.E. (1999). Mutations in NPC1 highlight a conserved NPC1-specific cysteine-rich domain. Am J Hum Genet *65*, 1252-1260.

Hua, X., Nohturfft, A., Goldstein, J.L., and Brown, M.S. (1996a). Sterol resistance in CHO cells traced to point mutation in SREBP cleavage-activating protein. Cell *87*, 415-426.

Hua, X., Sakai, J., Brown, M.S., and Goldstein, J.L. (1996b). Regulated cleavage of sterol regulatory element binding proteins requires sequences on both sides of the endoplasmic reticulum membrane. J Biol Chem *271*, 10379-10384.

Ikonen, E. (2006). Mechanisms for cellular cholesterol transport: defects and human disease. Physiol Rev *86*, 1237-1261.

Infante, R.E., Abi-Mosleh, L., Radhakrishnan, A., Dale, J.D., Brown, M.S., and Goldstein, J.L. (2008a). Purified NPC1 protein. I. Binding of cholesterol and oxysterols to a 1278-amino acid membrane protein. J Biol Chem *283*, 1052-1063.

Infante, R.E., Radhakrishnan, A., Abi-Mosleh, L., Kinch, L.N., Wang, M.L., Grishin, N.V., Goldstein, J.L., and Brown, M.S. (2008b). Purified NPC1 protein: II. Localization of sterol binding to a 240-amino acid soluble luminal loop. J Biol Chem *283*, 1064-1075.

Infante, R.E., Wang, M.L., Radhakrishnan, A., Kwon, H.J., Brown, M.S., and Goldstein, J.L. (2008c). NPC2 facilitates bidirectional transfer of cholesterol between NPC1 and lipid bilayers, a step in cholesterol egress from lysosomes. Proc Natl Acad Sci U S A *105*, 15287-15292.

James, C.L., and Viola, R.E. (2002). Production and characterization of bifunctional enzymes. Substrate channeling in the aspartate pathway. Biochemistry *41*, 3726-3731.

Ko, D.C., Binkley, J., Sidow, A., and Scott, M.P. (2003). The integrity of a cholesterol-binding pocket in Niemann-Pick C2 protein is necessary to control lysosome cholesterol levels. Proc Natl Acad Sci U S A *100*, 2518-2525.

Kolter, T., and Sandhoff, K. (2005). Principles of lysosomal membrane digestion: stimulation of sphingolipid degradation by sphingolipid activator proteins and anionic lysosomal lipids. Annu Rev Cell Dev Biol *21*, 81-103.

Kolter, T., and Sandhoff, K. (2006). Sphingolipid metabolism diseases. Biochim Biophys Acta *1758*, 2057-2079.

Kornfeld, S. (1987). Trafficking of lysosomal enzymes. FASEB J *1*, 462-468.

Kwon, H.J., Abi-Mosleh, L., Wang, M.L., Deisenhofer, J., Goldstein, J.L., Brown, M.S., and Infante, R.E. (2009). Structure of N-terminal domain of NPC1 reveals distinct subdomains for binding and transfer of cholesterol. Cell *137*, 1213-1224.

Lasch, J., Weissig, V., Brandl, M. (2003). Liposomes: A Practical Approach (New York, Oxford Univ. Press).

Li, A.C., Tanaka, R.D., Callaway, K., Fogelman, A.M., and Edwards, P.A. (1988). Localization of 3-hydroxy-3-methylglutaryl CoA reductase and 3-hydroxy-3-methylglutaryl CoA synthase in the rat liver and intestine is affected by cholestyramine and mevinolin. J Lipid Res *29*, 781-796.

Liou, H.L., Dixit, S.S., Xu, S., Tint, G.S., Stock, A.M., and Lobel, P. (2006). NPC2, the protein deficient in Niemann-Pick C2 disease, consists of multiple glycoforms that bind a variety of sterols. J Biol Chem *281*, 36710-36723.

Liscum, L., and Faust, J.R. (1987). Low density lipoprotein (LDL)-mediated suppression of cholesterol synthesis and LDL uptake is defective in Niemann-Pick type C fibroblasts. J Biol Chem *262*, 17002-17008.

Loftus, S.K., Morris, J.A., Carstea, E.D., Gu, J.Z., Cummings, C., Brown, A., Ellison, J., Ohno, K., Rosenfeld, M.A., Tagle, D.A., *et al.* (1997). Murine model of Niemann-Pick C disease: mutation in a cholesterol homeostasis gene. Science *277*, 232-235.

Millard, E.E., Gale, S.E., Dudley, N., Zhang, J., Schaffer, J.E., and Ory, D.S. (2005). The sterol-sensing domain of the Niemann-Pick C1 (NPC1) protein regulates trafficking of low density lipoprotein cholesterol. J Biol Chem *280*, 28581-28590.

Millat, G., Chikh, K., Naureckiene, S., Sleat, D.E., Fensom, A.H., Higaki, K., Elleder, M., Lobel, P., and Vanier, M.T. (2001). Niemann-Pick disease type C: spectrum of HE1 mutations and genotype/phenotype correlations in the NPC2 group. Am J Hum Genet *69*, 1013-1021.

Naureckiene, S., Sleat, D.E., Lackland, H., Fensom, A., Vanier, M.T., Wattiaux, R., Jadot, M., and Lobel, P. (2000). Identification of HE1 as the second gene of Niemann-Pick C disease. Science *290*, 2298-2301.

Neiss, W.F. (1984). A coat of glycoconjugates on the inner surface of the lysosomal membrane in the rat kidney. Histochemistry *80*, 603-608.

Nohturfft, A., Brown, M.S., and Goldstein, J.L. (1998). Sterols regulate processing of carbohydrate chains of wild-type SREBP cleavage-activating protein (SCAP), but not sterol-resistant mutants Y298C or D443N. Proc Natl Acad Sci U S A *95*, 12848-12853.

Ohgami, N., Ko, D.C., Thomas, M., Scott, M.P., Chang, C.C., and Chang, T.Y. (2004). Binding between the Niemann-Pick C1 protein and a photoactivatable cholesterol analog requires a functional sterol-sensing domain. Proc Natl Acad Sci U S A *101*, 12473-12478.

Okamura, N., Kiuchi, S., Tamba, M., Kashima, T., Hiramoto, S., Baba, T., Dacheux, F., Dacheux, J.L., Sugita, Y., and Jin, Y.Z. (1999). A porcine homolog of the major secretory protein of human epididymis, HE1, specifically binds cholesterol. Biochim Biophys Acta *1438*, 377-387.

Park, W.D., O'Brien, J.F., Lundquist, P.A., Kraft, D.L., Vockley, C.W., Karnes, P.S., Patterson, M.C., and Snow, K. (2003). Identification of 58 novel mutations in Niemann-Pick disease type C: correlation with biochemical phenotype and importance of PTC1-like domains in NPC1. Hum Mutat *22*, 313-325.

Pentchev, P.G. (2004). Niemann-Pick C research from mouse to gene. Biochim Biophys Acta *1685*, 3-7.

Pentchev, P.G., Comly, M.E., Kruth, H.S., Tokoro, T., Butler, J., Sokol, J., Filling-Katz, M., Quirk, J.M., Marshall, D.C., Patel, S., *et al.* (1987). Group C Niemann-Pick disease: faulty regulation of low-density lipoprotein uptake and cholesterol storage in cultured fibroblasts. FASEB J *1*, 40-45.

Pentchev, P.G., Vanier, M.T., Suzuki, K., and Patterson, M.C. (1995). The Metabolic and Molecular Basis of Inherited Disease (New York, McGraw-Hill Inc.).

Radhakrishnan, A., Goldstein, J.L., McDonald, J.G., and Brown, M.S. (2008). Switch-like control of SREBP-2 transport triggered by small changes in ER cholesterol: a delicate balance. Cell Metab *8*, 512-521.

Radhakrishnan, A., Ikeda, Y., Kwon, H.J., Brown, M.S., and Goldstein, J.L. (2007). Sterol-regulated transport of SREBPs from endoplasmic reticulum to Golgi: oxysterols block transport by binding to Insig. Proc Natl Acad Sci U S A *104*, 6511-6518.

Rawson, R.B., DeBose-Boyd, R., Goldstein, J.L., and Brown, M.S. (1999). Failure to cleave sterol regulatory element-binding proteins (SREBPs) causes cholesterol auxotrophy in Chinese hamster ovary cells with genetic absence of SREBP cleavage-activating protein. J Biol Chem *274*, 28549-28556.

Roth, M.G. (2006). Clathrin-mediated endocytosis before fluorescent proteins. Nat Rev Mol Cell Biol *7*, 63-68.

Schulze, H., Kolter, T., and Sandhoff, K. (2009). Principles of lysosomal membrane degradation: Cellular topology and biochemistry of lysosomal lipid degradation. Biochim Biophys Acta *1793*, 674-683.

Scott, C., and Ioannou, Y.A. (2004). The NPC1 protein: structure implies function. Biochim Biophys Acta *1685*, 8-13.

Simons, K., and Ikonen, E. (2000). How cells handle cholesterol. Science *290*, 1721-1726.

Sleat, D.E., Wiseman, J.A., El-Banna, M., Price, S.M., Verot, L., Shen, M.M., Tint, G.S., Vanier, M.T., Walkley, S.U., and Lobel, P. (2004). Genetic evidence for nonredundant functional cooperativity between NPC1 and NPC2 in lipid transport. Proc Natl Acad Sci U S A *101*, 5886-5891.

Smith, P.K., Krohn, R.I., Hermanson, G.T., Mallia, A.K., Gartner, F.H., Provenzano, M.D., Fujimoto, E.K., Goeke, N.M., Olson, B.J., and Klenk, D.C. (1985). Measurement of protein using bicinchoninic acid. Anal Biochem *150*, 76-85.

Subramanian, K., and Balch, W.E. (2008). NPC1/NPC2 function as a tag team duo to mobilize cholesterol. Proc Natl Acad Sci U S A *105*, 15223-15224.

van Driel, I.R., Goldstein, J.L., Sudhof, T.C., and Brown, M.S. (1987). First cysteine-rich repeat in ligand-binding domain of low density lipoprotein receptor binds Ca2+ and monoclonal antibodies, but not lipoproteins. J Biol Chem *262*, 17443-17449.

Vanier, M.T., Duthel, S., Rodriguez-Lafrasse, C., Pentchev, P., and Carstea, E.D. (1996). Genetic heterogeneity in Niemann-Pick C disease: a study using somatic cell hybridization and linkage analysis. Am J Hum Genet *58*, 118-125.

Vanier, M.T., and Millat, G. (2003). Niemann-Pick disease type C. Clin Genet *64*, 269-281.

Verot, L., Chikh, K., Freydiere, E., Honore, R., Vanier, M.T., and Millat, G. (2007). Niemann-Pick C disease: functional characterization of three NPC2 mutations and clinical and molecular update on patients with NPC2. Clin Genet *71*, 320-330.

Wang, M.L., Motamed, M., Infante, R.E., Abi-Mosleh, L., Kwon, H.J., Brown, M.S., and Goldstein, J.L. (2010). Identification of surface residues on niemann-pick C2 essential for hydrophobic Handoff of cholesterol to NPC1 in lysosomes. Cell Metab *12*, 166-173.

Watari, H., Blanchette-Mackie, E.J., Dwyer, N.K., Watari, M., Neufeld, E.B., Patel, S., Pentchev, P.G., and Strauss, J.F., 3rd (1999). Mutations in the leucine zipper motif and sterol-sensing domain inactivate the Niemann-Pick C1 glycoprotein. J Biol Chem *274*, 21861-21866.

Xu, S., Benoff, B., Liou, H.L., Lobel, P., and Stock, A.M. (2007). Structural basis of sterol binding by NPC2, a lysosomal protein deficient in Niemann-Pick type C2 disease. J Biol Chem *282*, 23525-23531.

Xu, Z., Farver, W., Kodukula, S., and Storch, J. (2008). Regulation of sterol transport between membranes and NPC2. Biochemistry *47*, 11134-11143.